การจัดสรรกำลังสูญเสียและการจัดการความคับคั่งในสายส่งของตลาดแบบคู่สัญญา

นายคมสันติ์ ดาโรจน์

สถาบันวิทยบริการ
จุฬาลงกรณ์มหาวิทยาลัย

วิทยานิพนธ์นี้เป็นส่วนหนึ่งของการศึกษาตามหลักสูตรปริญญาดุษฎีบัณฑิต
สาขาวิชาวิศวกรรมไฟฟ้า ภาควิชาวิศวกรรมไฟฟ้า
คณะวิศวกรรมศาสตร์ จุฬาลงกรณ์มหาวิทยาลัย
ปีการศึกษา 2549

ลิขสิทธิ์ของจุฬาลงกรณ์มหาวิทยาลัย

LOSS ALLOCATION AND CONGESTION MANAGEMENT
IN BILATERAL MARKETS

Mr. Komson Daroj

สถาบันวิทยบริการ
จุฬาลงกรณ์มหาวิทยาลัย

A Dissertation Submitted in Partial Fulfillment of the Requirements
for the Degree of Doctor of Philosophy Program in Electrical Engineering
Department of Electrical Engineering
Faculty of Engineering
Chulalongkorn University
Academic Year 2006
Copyright of Chulalongkorn University

Thesis Title	LOSS ALLOCATION AND CONGESTION MANAGEMENT IN BILATERAL MARKETS
By	Mr. Komson Daroj
Field of Study	Electrical Engineering
Thesis Advisor	Associate Professor Bundhit Eua-arporn, Ph. D.

Accepted by the Faculty of Engineering, Chulalongkorn University in Partial Fulfillment of the Requirements for the Doctoral Degree

.... Dean of the Faculty of Engineering
(Professor Direk Lavansiri, Ph. D.)

THESIS COMMITTEE

.... Chairman
(Associate Professor Sukumvit Phoomvuthisarn, Ph. D.)

.... Thesis Advisor
(Associate Professor Bundhit Eua-arporn, Ph. D.)

.... Member
(Associate Professor Somchat Jiriwibhakorn, Ph. D.)

.... Member
(Naebboon Hoonchareon, Ph. D.)

.... Member
(Songsak Chusanapiputt, Ph. D.)

สถาบันวิทยบริการ
จุฬาลงกรณ์มหาวิทยาลัย

คมสันติ์ ดาโรจน์ : การจัดสรรกำลังสูญเสียและการจัดการความคับคั่งในสายส่งของตลาดแบบคู่สัญญา (LOSS ALLOCATION AND CONGESTION MANAGEMENT IN BILATERAL MARKETS) อ. ที่ปรึกษา : รองศาสตราจารย์ ดร. บัณฑิต เอื้ออาภรณ์, 175 หน้า.

อุตสาหกรรมผลิตและจำหน่ายไฟฟ้าทั่วโลกในปัจจุบันอยู่ในระหว่างการแปรรูป จากระบบใหญ่ที่ดำเนินงานโดยหน่วยงานเดียวมาเป็นระบบตลาดซื้อขายพลังงานไฟฟ้าที่มีการแข่งขันมากขึ้น โครงสร้างการจัดการตลาดซื้อขายพลังงานไฟฟ้าได้มีการพัฒนาเพื่อให้เหมาะสมในแต่ละประเทศอย่างต่อเนื่อง

ในวิทยานิพนธ์ฉบับนี้จะศึกษาและนำเสนอวิธีการจัดการซื้อขายพลังงานไฟฟ้า ในระบบตลาดแบบคู่สัญญาทั้งในสภาวะปกติและในสภาวะที่มีปัญหาความคับคั่งของสายส่งเกิดขึ้น โดยวิธีที่นำเสนอจะใช้กำลังไฟฟ้าที่แต่ละคู่สัญญามีต่อกันเป็นดัชนีเบื้องต้น เพื่อใช้ในการจัดสรรกำลังสูญเสียในสภาวะซื้อขายปกติและเพื่อแบ่งเบาภาระราคาพลังงานไฟฟ้าที่เพิ่มขึ้นในกรณีที่มีปัญหาความคับคั่งของสายส่ง นอกจาก นั้นยังจะได้นำเสนอวิธีการประเมินสมรรถนะของสายส่ง ซึ่งสามารถที่จะใช้ในการวางแผนปรับปรุงระบบสายส่งรวมทั้งยังสามารถประยุกต์ใช้ในการประเมินเสถียรภาพแรงดันไฟฟ้าของระบบในเวลาจริงได้อีกด้วย นอกเหนือ จากที่ได้กล่าวมาแล้ว วิทยานิพนธ์ฉบับนี้ได้นำเสนอการจัดการปัญหาความคับคั่งของสายส่งในระบบตลาดแบบคู่สัญญา โดยแบ่งเป็น 2 ขั้นตอนดังนี้ ขั้นแรกจะนำเสนอวิธีการบรรเทาปัญหาความคับคั่งในสายส่งแบบที่มีต้นทุนต่ำที่สุด และในขั้นที่สองจะนำเสนอวิธีการกระจายต้นทุนที่เพิ่มขึ้นนี้ไปยังแต่ละคู่สัญญา ตามค่าของผลกระทบที่แต่ละคู่สัญญามีต่อสายส่งเส้นที่เกิดปัญหาความคับคั่ง

วิธีการที่พัฒนาขึ้นสามารถประยุกต์ใช้ได้จริงกับระบบตลาดแบบคู่สัญญา โดยในวิทยานิพนธ์ฉบับนี้ได้มีการทดสอบกับระบบไฟฟ้า 3 ระบบ ได้แก่ ระบบไฟฟ้า 6 บัส ระบบทดสอบ IEEE 30 บัส และระบบไฟฟ้าภาคใต้ของประเทศไทยขนาด 28 บัส

สถาบันวิทยบริการ
จุฬาลงกรณ์มหาวิทยาลัย

ภาควิชา......วิศวกรรมไฟฟ้า............ ลายมือชื่อนิสิต....................................

สาขาวิชา.....วิศวกรรมไฟฟ้า............ ลายมือชื่ออาจารย์ที่ปรึกษา.........................

ปีการศึกษา.....2549...........................

4571805121 : MAJOR ELECTRICAL ENGINEERING
KEY WORD: LOSS ALLOCATION / CONGESTION MANAGEMENT / BILATERAL MARKETS / TRANSMISSION LINE LOADING MARGIN / VOLTAGE SECURITY ASSESSMENT

KOMSON DAROJ : LOSS ALLOCATION AND CONGESTION MANAGEMENT IN BILATERAL MARKETS. THESIS ADVISOR : ASSOCIATE PROFESSOR BUNDHIT EUA-ARPORN, Ph. D., 175 pp.

Many electric supply industries around the world are on the pressure of changing from vertically integrated to more competitive markets, of which some of them have already been operating under competitive environment for a number periods of time. Among those electricity markets, various trading arrangements have been examined and improved for several years.

In this dissertation, the concept of managing bilateral transactions under feasible and infeasible modes is studied. According to this management some transmission-related services, i.e. transmission loss and congestion cost allocation methodology are proposed based on contributory degree of each transaction. In addition, a methodology to evaluate transmission loading margin is proposed. This margin has a close relationship with voltage instability phenomenon and can be used for transmission planning and on-line voltage security assessment purposes. A slack-bus independent loss allocation method, based on a marginal loss concept of a specified source and sink under bilateral transaction, has also been proposed. However, a key contribution of this dissertation is on congestion management methodology under a bilateral market. The proposed method can be classified into two procedures, i.e. congestion relief and congestion cost allocation procedures. For a congestion relief procedure, it employs an objective function of minimizing congestion relief cost. For the congestion cost allocation methodology, the product of contracted power from each transaction and its Power Transfer Distribution Factor (PTDF) of the congested line is proposed as an index to allocate the congestion cost.

Department. Electrical Engineering...... Student's signature. Komson

Field of study. Electrical Engineering... Advisor's signature. B. Eua-arporn

Academic year. 2006......................

ACKNOWLEDGEMENTS

The author wishes to give a special thanks to my advisor, Associate Professor Dr. Bundhit Eua-arporn, for his valuable guidance, suggestions, and sacrifice to fulfil this dissertation and work throughout the study of this program.

The author also thanks to chairman and examination committee, for their fruitful suggestions and useful recommendations.

Thanks are also expressed to all of my friends for their constant encouragement and helps during the study.

Finally, the author expresses his deepest appreciation to his beloved family for their inspirations, understandings, and endless supports.

สถาบันวิทยบริการ
จุฬาลงกรณ์มหาวิทยาลัย

Table of Contents

List of Tables

TABLE **PAGE**

List of Figures

FIGURE **PAGE**

Nomenclatures

ACPTDF	Power Transfer Distribution Factor formulated by an AC method
AGC	Automatic Generation Control
ATC	Available Transfer Capability
AVR	Automatic Voltage Regulator
BM	Balancing Mechanism
CM	Congestion Management
CPF	Continuation Power Flow
DCPTDF	Power Transfer Distribution Factor formulated by a DC method
DisCos	Distribution Companies
DTS	Dispatcher Training simulator
ED	Economic Dispatch
EGAT	the Electricity Generating Authority of Thailand
EMS	Energy Management System
ESB	Enhanced Single Buyer
ESI	Electric Supply Industry
GenCos	Generation Companies
GridCo	Transmission Company
HFB	Hopfield Bifurcation
HVDC	High Voltage Direct Current
IPPs	Independent Power Producers
ITL	Incremental Transmission Loss
LFC	Load Frequency Control
LLI	Line Loading Index
LLM	Line Loading Margin
LRIC	Long Run Incremental Cost
LRMC	Long Run Marginal Cost
LSI	Line Severity Index
MCP	Marginal Clearing Price
MCQ	Marginal Clearing Quantity
MEA	the Metropolitan Electricity Authority
NERC	the North Electricity Reliability Council

สถาบันวิทยบริการ
จุฬาลงกรณ์มหาวิทยาลัย

NESA	the New Electricity Supply Arrangement
NETA	the New Electricity Trading Arrangement
OLTC	On Load Tap Changer
OPF	Optimal Power Flow
PEA	the Provincial Electricity Authority
PTDF	Power Transfer Distribution Factor
PX	Power Exchange
REDCo	Regulated as Electricity Delivery Company
SCADA	Supervisory and Data Acquisition
SCED	Security Constrained Economic Dispatch
SCOPF	Security Constrained Optimal Power Flow
SCs	Scheduling Coordinators
SET	Stock Exchange of Thailand
SIB	Singularity Induced Bifurcation
SNB	Saddle Node Bifurcation
SO	System Operator
SPPs	Small Power Producers
SRIC	Short Run Incremental Cost
SRMC	Short Run Marginal Cost
SSS	Steady State Stability
SupplyCo	Supply Company
TFS	Transaction Feasibility Study
TLR	Transmission Loading Relief
TOA	Transmission Open Access
TOs	Transmission Owners

CHAPTER 1

INTRODUCTION

1.1 Power System Operation in Vertically Integrated System

A power system generally comprises generation, transmission, distribution systems and demand. Electric energy is transferred from generation to load through transmission and distribution systems. In a vertically integrated system, generation and transmission systems may be bundled together and owned by a single utility, thus monopoly by its nature. Expansion of generation and transmission facilities are periodically planned, constructed to maintain system reliability. The concept of reliability is normally divided into two aspects, i.e. adequacy and security. Adequacy is defined as the ability of the system to supply the aggregate electric power and energy requirements of consumers at all times. Security is the ability of the system to withstand sudden disturbances. As results of good planning, resources and capacity reserve are sufficient for real time operation.

Traditional power system operation relies on the concept of control areas, i.e. single or multiple, under the supervision and control of System Operator (SO). In general, the SO operates the system according to defined rules, codes, or standards which every control area have to act accordingly. The codes and standards provide guidance to power system operation, which can be generally characterized into three operating states, i.e. normal, emergency, and restorative states. Most operating conditions occurred in normal states, which can be defined as the system ability to response the simultaneous minute to minute change of demand. In practice, a power system may be considered as transiting from one to other normal states, which can be defined as a quasi steady state condition. Balancing between generation and demand is analyzed under the topic of Load Frequency Control (LFC) which is normally performed automatically using Automatic Generation Control (AGC) [1], [2].

Apart from the generation/demand balancing, the control signal which is sent to adjust the generation is generally satisfied the objective of minimum operational cost while reliability of the system is still maintained. Operation under this normal state does not concern only maintaining system frequency. Sufficient operating reserve needs to be provided, normally based on N-1 criterion, throughout the system in case of contingency.

Meanwhile normal operation is continuing, real-time status and condition of the system are monitored and assessed. The closed to real-time information is required by SO for decision making to perform preventive measures to maintain the system within a normal state at all times. Accordingly, some credible contingencies e.g. generation/demand and transmission line outages can be analyzed in advance to find a proper corrective action that can restore the system controllability. The state transition diagram of a power system as mentioned above is described in details as shown in Figure1.1 [3]. To achieve in those desired functions, the SO requires some effective tools to handle dynamic behavior, and large and complexity of the system. The tools e.g. state estimator, unit commitment, economic dispatch or optimal power flow, dynamic security assessment, and etc., are normally used by most utilities through the traditional EMS/SCADA [4]-[6]. To provide more details, the basic and generally used functions of EMS/SCADA are presented in the next section.

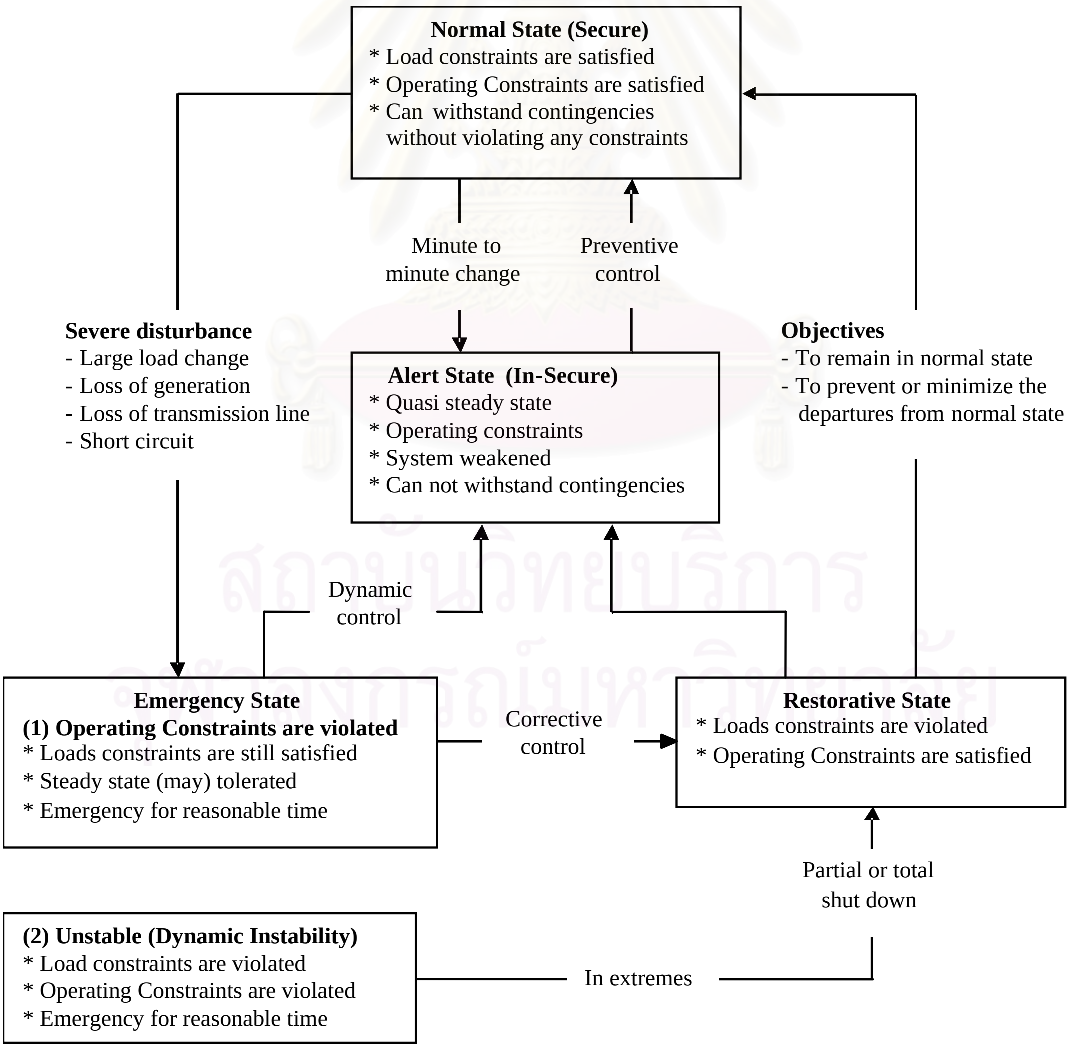

Figure 1.1 State transition diagram of power system in operation and control [3]

1.1.1 Energy Management System (EMS/SCADA)

EMS/SCADA [6], which is later called EMS, is a client/server computer system composed of EMS and SCADA software together with telecommunication and metering equipments. EMS is application software installed in main server computers at utility control centers used for multi-objective purposes in on-line and/or off-line modes. For off-line study, one can use various functions for power system planning. Another application in this mode is to get system operators to be familiar with their system by assuming abnormal condition via a man-machine interactive server called Dispatcher Training Simulator (DTS). The role of EMS in ensuring reliability and economic operation of a power system is significant both in the past and under competitive environment especially after 2003 blackouts in North America and Europe [7]. It has been recognized that many problems which lead to system disintegration could have been prevented or alleviated if more robust and accurate EMS applications are in services [8], [9]. In general, EMS functions are composed of three modules, i.e. network application, generation application, and dispatcher training simulator modules. Typical functions normally used by various utilities are listed below [10].

- Network Model Builder
- Power Flow Calculations
- Economic Dispatch /Optimal Power Flow
- State Estimator
- Contingency Analysis
- Voltage Reactive Power Control
- Automatic Generation Control
- Generation Planning
- Hydro-thermal Optimal Scheduling
- Unit Commitment
- Load Forecast
- Voltage Stability
- Transient Stability Control

Some of the EMS functions, which are the background concerned in this dissertation, are clarified as below.

Economic Dispatch (ED) and Optimal Power Flow (OPF) [2] are optimizing tools for power system operation and planning. Economic dispatch can be stated as the problem of how to schedule generating units to minimize the operational costs in real time. Optimal Power Flow is an extensive tool of economic dispatch due to its several objective functions and the capability to handle various constraints. Before the deregulation has become highly recognized, development of the OPF falls into two aspects [11]. Firstly, we need to incorporate practical constraints e.g. environmental constraints, stability constraints etc., into an OPF problem. Secondly, there are needs to search for a new optimization method to efficiently solve the OPF problem. Several techniques e.g. Newton, quadratic programming, PQ decomposition, and linear programming methods are generally employed. In addition, for security purposes, Security Constrained Economic Dispatch (SCED) or Security Constrained Optimal Power Flow (SCOPF) method which takes into account severe contingency outages [2], [11] can be used as an extension to traditional ED or OPF. The credible contingencies can be obtained from a contingency analysis module. However, some new concerns on OPF arise in competitive markets where the price of power is determined by competitive mechanism.

Security assessment is a term used to describe the process for ensuring all system parameters being in a normal state, i.e. voltages within specified limits, no power lines overloaded etc. [12]. In general, a power system may face a contingency, which may lead to an alert state. In such case, it means that the system is operating in a normal state but insecure due to violation of some operating constraints. To prevent from operating in an alert state, the system requires preventive strategies. For some severe contingencies, power system may turn from normal to an emergency state. In this case, the system needs rapid corrective actions in order to restore the system to a restorative state, then an alert state, and finally a normal operating state. If the corrective actions fail, the system will face the risk of partial load curtailment or total load shedding in the extreme. To help operators take action in time, on-line dynamic security assessment program will be executed and security level of power system needs to be identified when a contingency occurs [13]. The frequency of running the security analysis program depends on operating sophistication of the system. In post-contingencies, the program will give some useful suggestion to the operator or automatically take corrective action itself e.g. providing additional reactive power, rescheduling generation or shedding load to restore the system [14].

In order to reduce the risk of corrective action failure, some OPF programs take those severe contingency cases into account as constraints as recently proposed for Spanish electricity market [15]. The voltage or transient instability may be the results obtained from post-contingency evaluation thereby they can be included as constraints in OPF [16] - [18]. In a large power system, it is impossible to assess all contingencies on-line. Thus, contingency analysis method is needed to select only some severe cases to reduce computation time [2]. Consequently, contingency ranking according to their severities is conducted. Only selective severe cases are included in preventive strategies to enhance security of power system.

Voltage control is one of the main functions most utilities interested in nowadays [19]. Voltage control can be implemented in three hierarchical. Primary voltage control is the traditional strategies by utilizing On Load Tap Changer (OLTC), capacitor banks and Automatic Voltage Regulator (AVR) which is embedded as a part of an excitation system [3], [20], [21]. Secondary voltage control can be done through regulating voltage magnitude of specified load buses [22], [23]. Tertiary voltage control is the method scheduling reactive power resources owing to defined objective [24] e.g. minimize transmission power loss and maximize distance to voltage instability condition.

1.2 Deregulation in Electric Supply Industry [25], [26]

The fundamental goal of restructuring is to replace the regulated, vertically integrated, centrally controlled system with the one primarily based on market mechanism. The motivation is to lower prices and provide customer with satisfied choice. A key objective of the deregulation in electric supply industry is the separation of transmission system from generation and distribution systems and opens to access by all entities. The essence of restructuring is the encouraging of competition among generation, whereas transmission and distribution are generally considered as natural monopolies which should be regulated.

1.2.1 Hierarchical Level of Deregulation

There are various models of restructuring. In wholesale Electricity markets, several generation entities compete to sell their energy. Competition may be introduced into retail sales to provide customers choices among different retail companies and retailers can compete for market share by offering competitive prices and new services. In general, electricity supply structures can be categorized in four basic models as described below.

1.2.1.1 Monopoly

In this model, power system operation is a full integration within a single service area. The control and management of generation, transmission and distribution is bundled to be one utility. Independent Power Producers (IPPs) and Small Power Producers (SPPs) are allowed under utility regulations. There is no competition taking place in any levels. Demand side has no choice to make a contract with satisfied generation.

1.2.1.2 Single Buyer Model

A single power purchasing and selling agency is the only authorized agent to selling electric energy to wholesalers and large customers directly. Competition encourages in generation side including IPPs and SPPs, thereby provides choices for the buyer.

1.2.1.3 Wholesale Competition Model

In this model, the transmission is open to access. Generation can sell electric energy directly to wholesalers and large customers. Thus, distribution companies are allowed to buy power from generation then distribute later to their customers in retail markets. However, customers still have no choice to directly contact with other generations or distribution companies.

1.2.1.4 Retail Competition Model

This model is a fully transmission open to be accessed by any entities. Generations, distribution companies and customers are free to make multilateral transaction with other entities. Hence, this is the closest to fully competitive model.

1.2.2 Entities under Restructured Systems

Under deregulated structure, the system can be segregated into various segments which can be presented with different roles and responsibilities, which can be described below.

- Generation Companies (GenCos) are the power plant owners. In most competitive markets, GenCos are allowed to compete.
- IPP is an entity who plays an important role in electric supply industry. In liberalized markets e.g. Thailand, IPPs have no incentive to compete with others kind of generations according to their long term take-or-pay power purchasing agreement.
- Distribution Companies (DisCos) and Retailers are entities who play an important role in a distribution system. DisCos are normally restricted to maintain distribution network reliability. In contrast, retailers are separated from DisCos and have to provide electric energy sales to end customers.
- Transmission Owners (TOs) are entities who are established in liberalized markets to provide transmission access and services in a non-discriminatory manner. This to ensure that transmission entities are separated from generation and have no incentive in financial benefits.
- System Operator (SO) should be a supreme entity to manage all trading without financial interest. In some utilities, this entity is also a transmission ownership. The role and responsibilities of SO regarding maintaining reliability and security of the system can be varied widely according to various reasons, which can be additionally described in section 1.2.3.
- Power Exchange (PX) is an entity who matches between demand and supply using bid and offer accumulated from both sides in pool-based markets. The typical objective of matching is to maximize social welfare. The time horizon of matching is normally perform in day-ahead, hour-ahead and real-time markets.
- Scheduling Coordinators (SCs) is an entity that aggregate participants in trading using different protocol from PX and SO. The SCs may or may not be integrated as a part of operation according to the markets rule.

1.2.3 Roles and Responsibilities of System Operator

In general, role and responsibilities of the SO in all electricity industry structure is to maintain system reliability especially in a real time control mode. These responsibilities do not change whether electricity industry is deregulated or not. However, some activities under the responsibility of SO concerning operation and planning in a competitive environment are changed considerably due to the separation into various entities.

The fundamental functions that SO in a new era must be performed in operation-planning stage are listed below.

- Coordinate among participants in the market
- Prepare for power system scheduling
- Perform power system dispatch
- Determine and broadcast available transfer capability (ATC)
- Calculate and charge all participants for transmission-related services

Due to the presence of power pool and bilateral contracts may exist in the same market, the SO also has responsibility to coordinate of trading among them. Accordingly, some administration functions listed below must be performed by the SO.

- Run a power pool where participants can bid to buy and sell energy by accumulating bid and offer from them
- Develop a preferred schedule for the pool
- Manage bilateral and multi lateral transactions
- Manage and coordinate submissions from SCs

To achieve in real time balancing mechanism, SO must perform ancillary services provision function as listed below.

- Own and provide some keys ancillary services for satisfactory of grid operation
- Purchase ancillary services from markets participants
- Provide ancillary services to transmission users
- Plan and commission own ancillary services

In this dissertation, the concepts of managing bilateral and multi lateral transactions can be separated into two modes, i.e. feasible and infeasible transactions, defined in Chapter 4. According to this management some transmission-related services, i.e. transmission loss and congestion cost allocation methodology are proposed based on each transaction contribution, which will be additionally described in Chapters 4 and 6 respectively. Regarding ancillary services procurement, some services e.g. reactive power and active power from non-committed units, are also highlighted. The benefits of using these ancillary services in congestion management are analyzed in Chapter 6. However, reactive power has influence on voltage security. Therefore, the transmission loading margin is also proposed in this dissertation in Chapter 5. In Chapter 7, two situation, i.e. co-existence of bilateral and pool trading in the same market and the presence of multiple congested lines are described and tested with a 28-bus of Thailand region 3 system.

As transmission adequacy is also a key in deregulation issues, transmission facilities must be provided by SO to participants. These must be performed since planning through real time operating stage.

The SO has three objectives, i.e. security maintenance, service quality assurance and promotion of economic efficiency and equity. To achieve these objectives, the SO may be authorized to set the rules for transactions between generation and demand, scheduling and dispatch of generators, loads and network services, and energy markets. Generally, the SO is set up according to the market structure, which can be classified into MicroSO, MinSO and MaxSO as described below [26], [27].

A. MicroSO

The MicroSO is an observer of ensuring reliability and security of system operation without involving in markets coordination and scheduling. It is separated from real time control activities. However, it can observe system to ensure adequacy of reserves and others pertinent ancillary services. In addition, it can coordinate measures to manage the congestion. Thus, market intervention is allowed only in case preferred schedules are infeasible. Function performed accordingly is at a minimum responsibility required by all types of the SO. Responsibility of the MicroSO among other entities can be shown in Figure 1.2 [26].

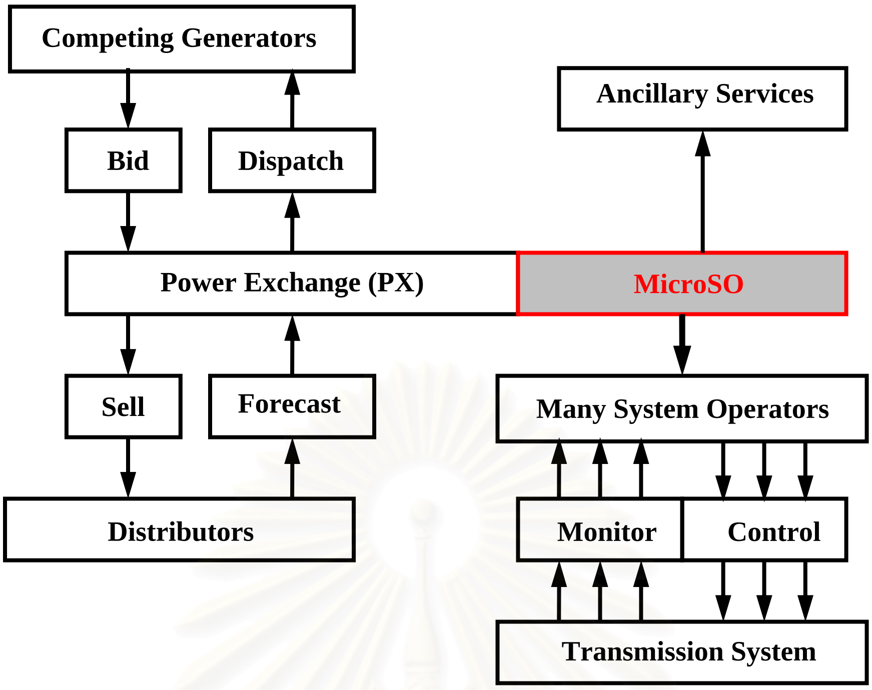

Figure 1.2 MicroSO responsibilities

B. MinSO

This type of SO is defined for the case where the SO is separated from the PX like MicroSO. Consequently, it is restricted to perform functions that maintain system security. Thereby, it is fully responsible for real time system control. In other word, its scientific merit is based on coordinated multilateral trades under bilateral markets [28]. Responsibility of the MinSO among other entities can be shown in Fig 1.3.

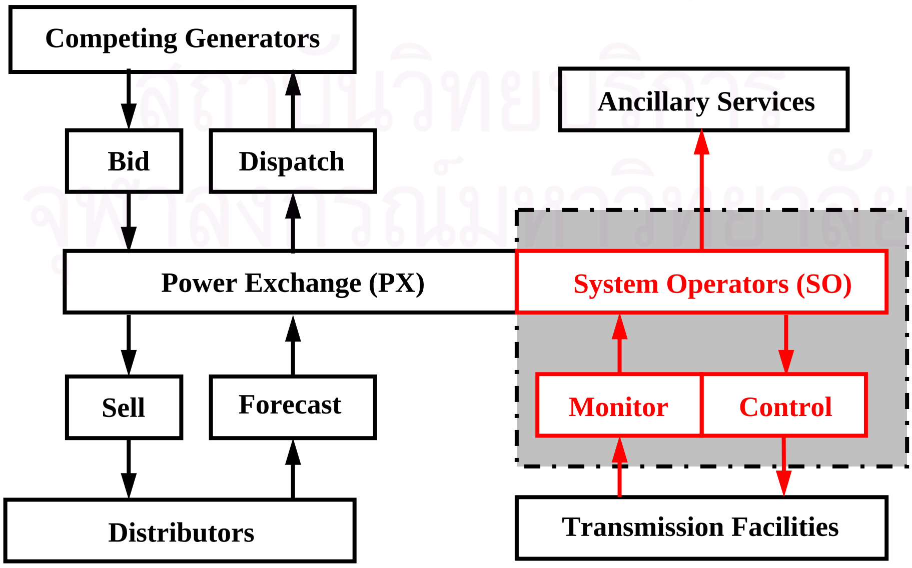

Figure 1.3 MinSO responsibilities

C. MaxSO

This type of SO has full responsibilities to the market by performing functions of MinSO and PX. Thus MaxSO requires and accumulates data, i.e. bids and offers from all participants, and forecasted load to perform the unit commitment and dispatch owing to maximizes social welfare. It also has responsibility to manage the congestion and calculate settlement charges. This type of the SO is proposed based on UK-Poolco before it is substituted by The New Electricity Trading Arrangement (NETA). Responsibility of the MaxSO among other entities can be shown in Figure 1.4.

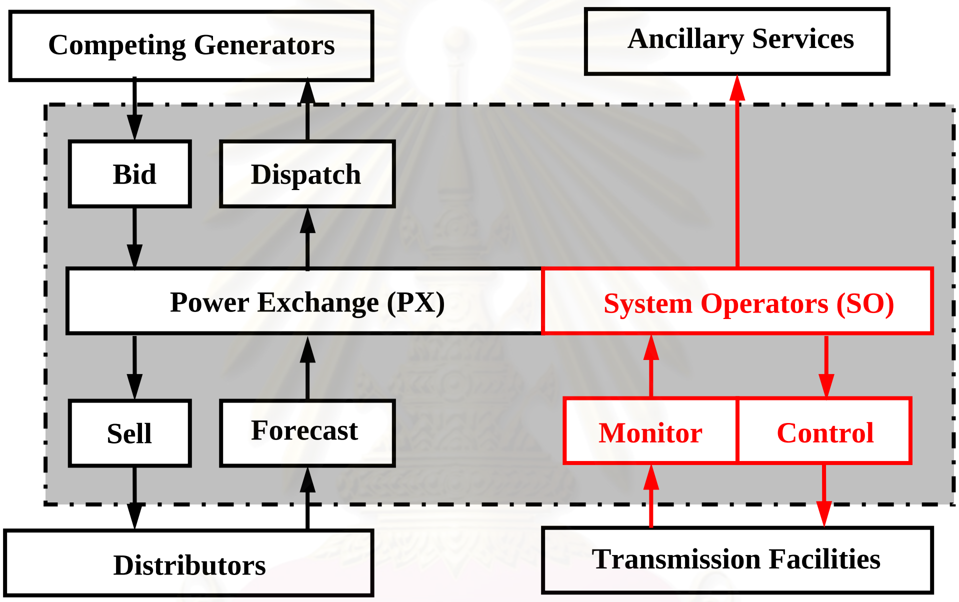

Figure 1.4 MaxSO responsibilities

1.2.4 Trading Arrangements Model

Normally, trading in a restructured system can be arranged into three models, i.e. power pool, pool and bilateral contracts, and multilateral trade models as described hereafter.

A. Power Pool

A Power pool is generally defined as a centralized electric market where proposed bids and offers from demands and generations are cleared under management of PX. Clearing mechanism is performed in a non-discriminatory manner based on a specified method, which in general to maximize social welfare. In this approach, the winners in bidding mechanism are paid and bought according to the system Marginal Clearing Price

(MCP) with their associated Marginal Clearing Quantity (MCQ). Bidding process is performed in forward markets, day-ahead and hour-ahead, and real-time balancing market. Trading arrangement in some country e.g. Chile, Argentina and East Australia fall into this category. The basic structure of trading in a power pool is shown in Figure 1.5.

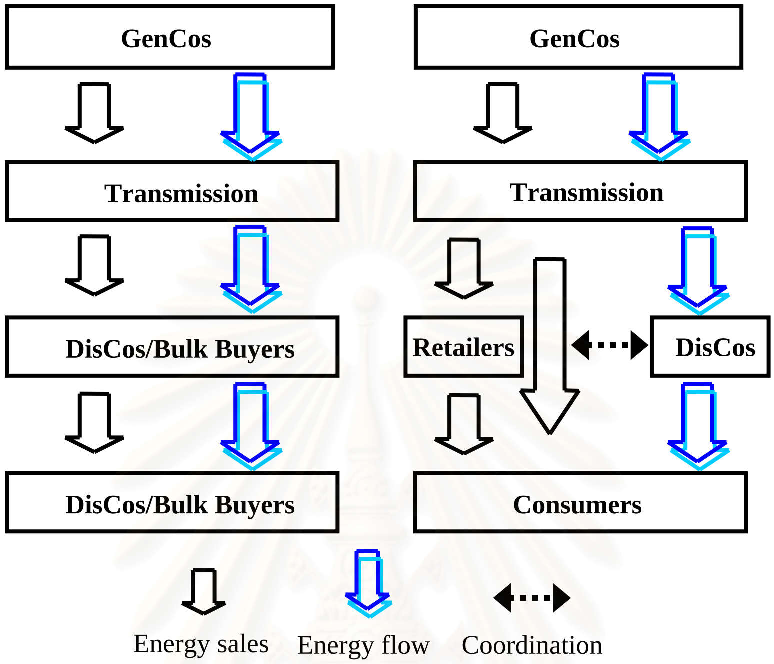

Figure 1.5 Trading in a power pool

B. Pool and Bilateral Trades

This structure is practical and used widely in most markets e.g. PJM, Spain, Nordpool etc., due to the presence of pool and bilateral/multilateral transaction in the model, which is separated into a market and a security sectors. The pool market is taken care by the PX whereas the bilateral contracts established by the SCs. Apart of those functions that performed by SO, the SO also holds a superior position over the PX and SCs to maintain system security. Market participants have flexibility to acquire their energy by bidding into the pool or make a bilateral contract with each other. The basic structure of trading with pool and bilateral contracts is shown in Figure 1.6.

C. Multilateral Trades

In practice, bilateral/multilateral transactions coexist with a power pool. In extremis, pool and PX disappear, the SO in this case is the MinSO thus the trade is allowed without intervention as long as transaction is feasible. However, trading in a power pool is needed for balancing between generations and demand in real-time. This model is shown in Figure 1.7.

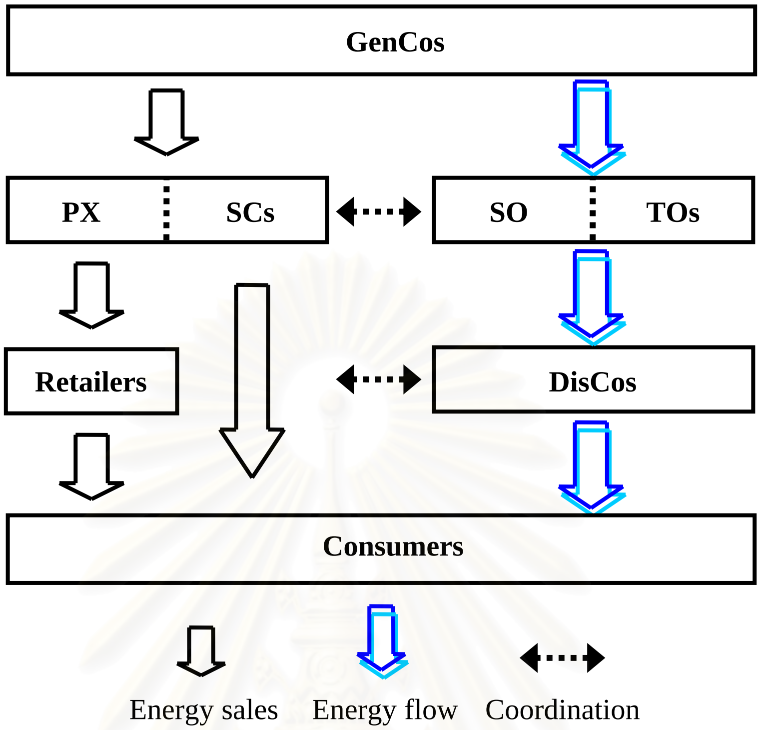

Figure 1.6 Trading with pool and bilateral contracts

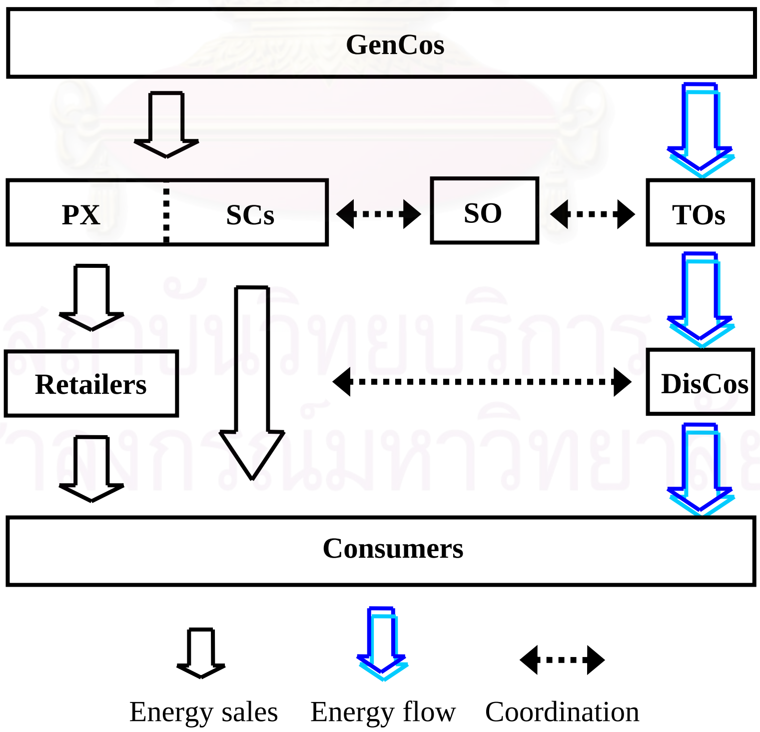

Figure 1.7 Structure with bilateral/multilateral trades only

1.2.5 Ancillary Services

Ancillary services are defined as all those necessary activities that SO acquires from provision entities to maintaining reliable operation and ensuring the required degree of quality and security. Activities defined under the preview of ancillary services are shown in Table 1.1[29].

Table 1.1 Ancillary services and their definitions

Service	Description	Time Scale
System control	The control-area operator functions that schedule generation and transactions before the fact and that control some generation in real-time to maintain generation/load balance, with a focus on reliability, not commercial, activities, including generation/load balance, transmission security, and emergency preparedness	Seconds to hours
Reactive supply and voltage control from generation	The injection or absorption of reactive power from generators to maintain transmission-system voltages within required ranges	Seconds
Regulation	The use of generation equipped with governors and automatic generation control to maintain minute-to-minute generation/load balance within the control area to meet the North America Electricity Reliability Council (NERC) control performance standards	~1 minute
Operating Reserve (**S**pinning)	The provision of generating capacity (usually with governors and automatic-generation control) that is synchronized to the grid and is unloaded that can respond immediately to correct for generation/load imbalances caused by generation and transmission outages and that is fully available within 10 minutes	Seconds to <10 minutes
Operating reserve (**S**upplemental)	The provision of generating capacity and curtailable load used to correct for generation/load imbalances caused by generation and transmission outages and that is fully available within 10 minutes	<10 minutes
	(Unlike spinning reserve, supplemental reserve is not required to begin responding immediately.)	
Energy imbalance	The use of generation to correct for hourly mismatches between actual and scheduled transactions between suppliers and their customers	Hourly
Load following	The use of generation to meet the hour-to-hour and daily variations in system load	Hours
Backup supply	Generating capacity that can be made fully available within one hour; used to back up operating reserves and for commercial purposes	30 to 60 minutes
Real-power-loss replacement	The use of generation to compensate for the transmission-system losses from generators to loads	Hourly
Dynamic scheduling	Real-time metering, telemetering, and computer software and hardware to electronically transfer some or all of a generator's output or a customer's load from one control area to another	Seconds
System-black-start capability	The ability of a generating unit to go from a shutdown condition to an operating condition without assistance from the electrical grid and to then energize the grid to help other units start after a blackout occurs	When outages occur
Network-stability services	Maintenance and use of special equipment (e.g. power-system stabilizers and dynamic-braking resistors) to maintain a secure transmission system	Cycles

1.3 Electric Supply Industry Restructuring Experience

Toward a road of electric supply industry restructuring, power pool is the first electricity market established and operated successfully until it is questioned due to some criticisms. Lesson learned from a power pool crisis results in delaying some electric supply industries for restructuring and promoting new trading arrangements. This section provides root-cause of a power pool crisis and the establishment of New Electricity Trading Arrangements (NETA), which is background and directly related to the core of this dissertation.

1.3.1 Power Pool Crisis

Power pool is a market with centralized mechanism for dispatching generation in advanced to meet forecast demand through forward markets both in day-ahead and hour-ahead markets. The operational price is based on a marginal pricing basis with all committed generators/loads are paid the same price. Although a power pool is successful for arranging the trades in a number of ways, over the years of operation it also attracted many criticisms.

In [30], energy prices of 14 electricity markets are investigated and recorded. Over many years of investigation, the energy prices can be classified into three types, i.e. stable, one bad period or season, and chaotic markets. Stable markets, e.g. England & Wales, Spain, and Scandinavia, have consistent seasonal price patterns and low levels of volatility in power price. Price excursions can be related to load, which in turn usually reflects extreme weather events. Consumers in such a market could reasonable face the power market through demand side management. There is little backlash against deregulation in stable markets. One bad period markets as exemplified by California, Alberta and New Zealand, generally have the characteristics of stable markets except for a period of high price. Alberta and California had extended periods of high price (more than 2.5 times overall average price) due to various reasons, which will be mentioned later. In these markets there has been a backlash against deregulation. A similar period in New Zealand could be attributed to a rare weather event, and the backlash is not severe. Australian power markets have erratic price patterns and very high volatility that is not related to load or weather; the markets show high variation from year to year and season to season.

For power pool customers who encountered with price volatility, some questions are raised concerning the traditional trading arrangements and need for the revision due to unreasonable electricity price especially in a spot market. Some inappropriate points that need for revision and always argued by various customers can be listed below [31]-[33].

- The offer prices submitted by generators into the auction are not reflective of their operational costs and hence pool prices had not tracked downwards with reductions in generating costs. We may say that, pool facilitated the exercise of market power at the expense of customers by enabling all generators to receive a uniform price. However, in various circumstances the market being dominated by a small number of generators, which contributed to the marginal clearing price. This is open an opportunity for generation to play a game of bidding.
- According to clearing mechanism, the customers don't know their energy price however they must expense on the basis of marginal clearing price, which inhibited supply side price pressure.
- Demand inelasticity in power pool has limitation on customer's involvement and protect them from the price spike.
- The complexity and opacity of the pool price setting process and the lack of competition in price setting inhibited the development of derivatives markets and reduced liquidity in the contracts markets. This resulted in high margins on the financial contracts struck between generators and customers, thereby further raising prices to customers above those that would have prevailed with more competitive arrangements.
- The power pool governance arrangements are inflexible and precluded change or delayed reform.

According to a normal market rules designed for power pool, some crisis of trading electricity arises in California Electricity Markets. During May 2000 - 2001, California was confronted with an unprecedented electricity crisis that threatened to undermine the reliability of its electricity system, weaken its economy, and impact energy markets throughout the western part of the United States. Although, the crisis is initiated from a complex mixture of root causes however some causes mentioned here can be described below [34]-[35].

- Lack of sufficient generating capacity in California and throughout the U.S. western region.
- Inadequate transmission infrastructure.
- Inadequate demand responsiveness or lack of demand elasticity.
- Lack of forward contracting.
- Forward scheduling that resulted in the huge reliance on the spot market.

Lacking of generation and transmission infrastructure together with demand inelasticity and lack of forward contracts have influence from markets rule, which cannot send an economic signal to a new investment and cause gaming. These anomalies encouraged several long term solutions for the California electric markets to perform efficiently and competitively. The new design to overcome above problem results in real implementation as below.

- State regulation needs to adapt to markets and focus on ensuring that load is covered with fixed-price contracts rather than after-the-fact prudence reviews of contracts. Sufficient long-term contracts must be in place for a majority of the load to hedge against spot market price volatility.
- There must be significant investments in new generation resources, and fast-track permitting must continue to expedite development of new supply in California to bring supply in line with demand. The generation fuel resource mix should also be diversified so that electricity customers are not overly susceptible to the price volatility of natural gas.
- Transmission constraints must be removed so that generation can be efficiently moved to where it is needed.
- End-use customers must be allowed to see reasonable price increases so that they can make informed efficient decisions about their energy use. Tools that would enable customers more control over their energy use would include the use of real-time meters and innovative pricing options.

With the California crisis, electricity markets around the world questioned themselves to verify their market rules and reform the existing markets with the new paradigm [31], [32], [36]-[41]. Some countries in Latin America e.g. Chile, Argentina, Peru, Bolivia, Colombia, Brazil, Venezuela, Mexico, and Ecuador are on the progress for second-stage reforms [39]. The Californian crisis motivated a healthy preoccupation about the correct design of the regulatory framework in Spain about the situation and the mechanisms to guarantee generation supply [40]. Additionally, lessons learned from electricity crisis contributed to the progress of electricity restructuring in developing countries including Thailand [41], which is presented in section 1.3.3.

In summary, problems found in California's electricity crisis delayed the process of restructuring of vertically integrated system in several countries. Moreover, electricity markets worldwide reform their market rules or trading arrangements, which will be presented in the next section.

1.3.2 The New Electricity Trading Arrangements (NETA) [31]

The New Electricity Trading Arrangements (NETA), implemented in England and Wales in March 2001 is an arrangement where the physical trading of electricity through a power pool is kept to a minimum, to overcome price spike of the previous UK-Poolco model. It should be noted that, some parts of framework of trading in bilateral/multilateral transactions in this dissertation is based on NETA. Overview of the markets under NETA can be shown in Figure 1.8.

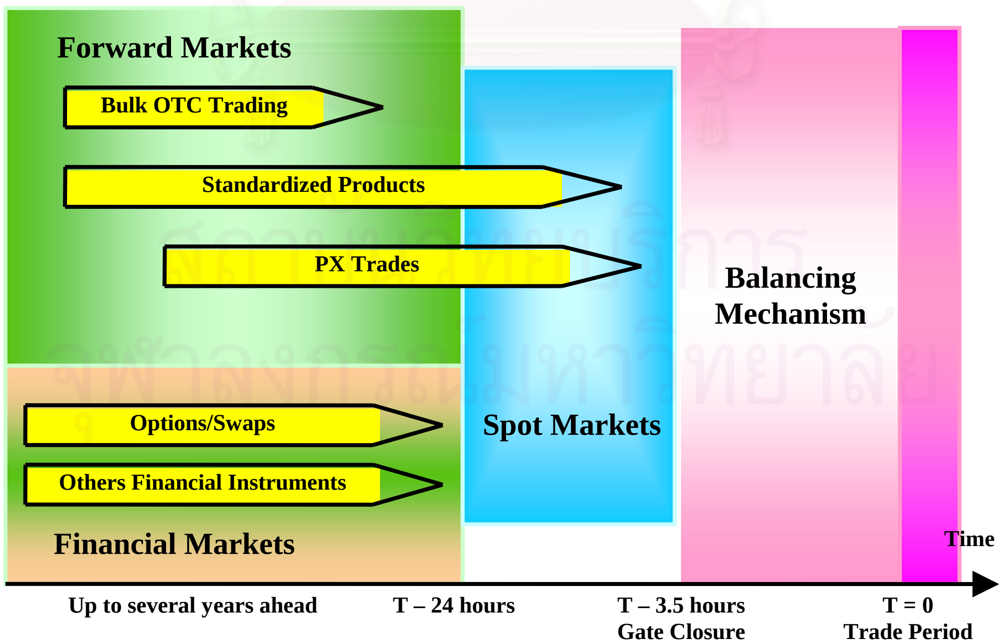

Figure 1.8 Overview of markets under NETA

The vast majority of trading is based on bilateral contracts. In response to the needs of market participants, a number of different trading options have emerged, including:

- forward and futures markets including on-line services, which allow contracts for electricity to be struck up to several years ahead,
- short term power exchanges, where participants have the opportunity to fine tune their contract positions in a simple and accessible way,

The bilateral/multilateral trading is operated without intervention by the regulator and market participants have complete freedom to organize their trading activities before the time of gate closure which during the first year of NETA is set at 3.5 hours and reduced to one hour on July 2, 2002. According to the trades, market participants have to notify their contracted volumes correspond to their intended profile of demand for that period and location of generation and demand contracted to the SO. Thereafter, the SO has control of the system by adopting the Balancing Mechanism (BM) to ensure that generation and demand are matched with the quality and security level of the system is maintained. The BM is a voluntary ancillary services market, which is used by the SO to procure frequency response, reactive power and reserve and even to resolve transmission constraints. As a result, NETA is designed to encompass the need for the following aspects:

- a two-sided market, with demand fully incorporated,
- (contractually) firm bids and offers, to enable costs and risks to be reduced and shared efficiently,
- bilateral contracting rather than a centralized market as the heart of the arrangements, to put greater competitive pressure on generators and encourage innovation and customer responsiveness in suppliers,
- flexible governance arrangements to ensure that the arrangements could respond in a timely fashion to changing market requirements,
- centralized real time balancing and settlement arrangements, to allow the system to be balanced and to target appropriately those balancing costs.

During the first year of market operation under NETA, it found that NETA has fared in terms of three main performance measures, i.e. the liquidity and transparency of the wholesale markets, developments in wholesale and retail prices, and balancing performance. Besides NETA, bilateral transactions in others markets of various countries are increased continuously over times as shown in Table 1.2 [42].

Table 1.2 Percentage of energy trade under bilateral contracts of various markets

Market	Country	Bilateral	Liquidity
NETA	UK**	97-98%	2-3%
Powernext	France**	98%	2%
EXAA	Australia**	98%	2%
ERCOT	Texas**	95-98%	2-5%
EEX	Germany**	91%	9%
APX	Netherlands**	89%	11%
Nord-Pool	Norway-Sweden-Finland-Denmark**	71-72% 50%	28-29% 50%
NYISO	New York**		
PJM	Pensylvania-New Jersy-Maryland*	64%	36%
IPEX	Italy***	68%	32%
NZEM	Newzeland*	20-30%	70-80%
OMEL	Spain**	15%	85%

Average liquidity of 2001; ** Average liquidity of 2003; *** Average liquidity of April 2004; **

1.3.3 Deregulation of Electric Supply Industry (ESI) in Thailand [41]

According to the Government's policy, restructuring of the ESI of Thailand has begun since 1990. The reasons for restructuring are aimed to improve efficiency, lower electricity price, and to cope with financial debts. The proposal of deregulation can be divided into three stages as described below.

The first recommended structure of Thai ESI, a power-pool based model, started in March of 2000, and was expected to be implemented with a full competition by the year 2003. According to the proposed model [43], generation companies, PowerGens, and IPPs have to bid the electric energy price and its quantity to a power pool. Additionally, the model allows PowerGens/IPPs for trading outside the pool through bilateral contracts. The distribution companies, DisCo, and supply company, SupplyCo, are regulated as electricity delivery company, REDCo, have responsible to provide the electricity to all consumers. The retail company, RetailCos, is allowed to compete in providing the electricity to non-captive consumers through the transmission company, GridCo, and DisCo. Characteristic of the proposed power pool model can be described in Figure 1.9.

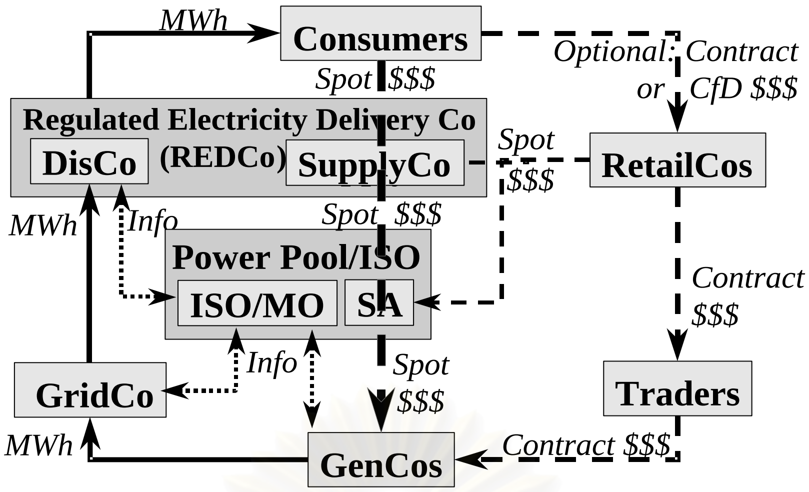

Figure 1.9 The proposed power pool model of Thailand ESI

According to some weak points in a power pool model e.g. may result in highly volatile pool price, in associated with California's crisis. The second stage of the power pool model is revised under the name "the New Electricity Supply Arrangement (NESA)", which is a bilateral based market. Under NESA, most of transactions are bilateral contracts with a system balancing mechanism. In the year 2004, the Electricity Generating Authority of Thailand (EGAT), owned and operated 56.52% of power generation and transmission systems in Thailand, is expected to unbundle into GridCo and three generation companies. The NESA encourages PowerGens and independent power producers to compete in selling electricity to retailers and large consumers through bilateral contracts. The regulated GridCo owns and operates the high voltage transmission system under the instruction of the SO. In distribution systems, the Metropolitan Electricity Authority (MEA) in Bangkok and vicinity and Provincial Electricity Authority (PEA) in the rest of Thailand will be transformed into the regulated electricity delivery companies, REDCos. Each REDCo, combining the distribution and supply companies, DisCo and SupplyCo respectively, deliver and sell electricity to consumers. DisCo owns and operates the low voltage distribution system whereas SupplyCo sells the electricity to captive consumers. In addition, commercial retail companies, RetailCos, compete in selling electricity to non-captive consumers. The imbalances between contractual and physical electricity consumption in real time are handled by a balancing mechanism in balancing market (BM). This model is based on the NETA of England and Wales. Structure of Thai ESI under NESA is shown in Figure 1.10.

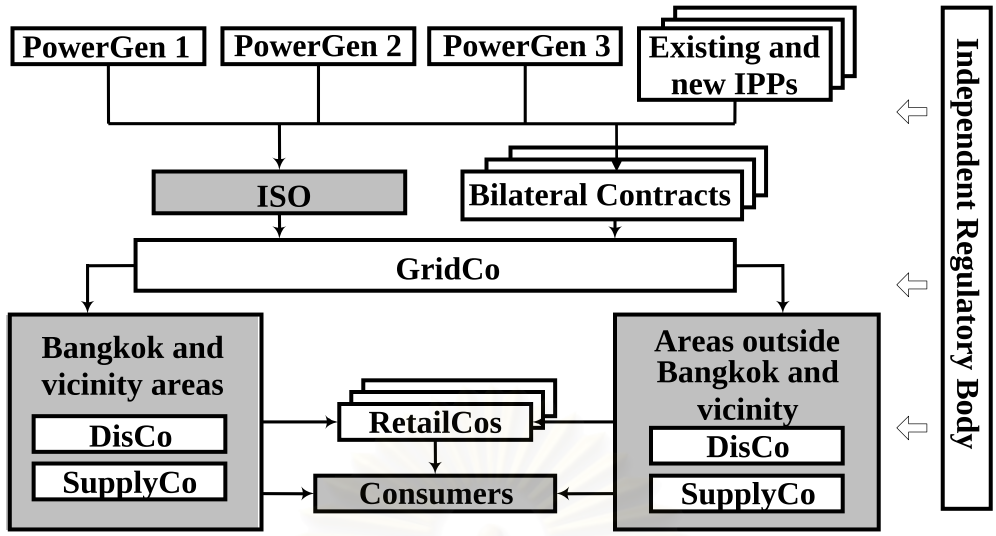

Figure 1.10 The proposed NESA for ESI of Thailand

On September 2003, the Cabinet withdrew its resolution of NESA. Subsequently, on December 2003, the Cabinet approved the new ESI structure, called the Enhanced Single Buyer (ESB) model, proposed by the Ministry of Energy. This is the third stage of ESI reform in Thailand. The ESB Model still maintains the Electricity Generating Authority of Thailand (EGAT) as the only power buyer authorized to sell power to the Metropolitan Electricity Authority (MEA) and the Provincial Electricity Authority (PEA). Some EGAT regulatory work will be transferred to a newly-established Regulatory Body that will oversee the power industry. This new body will determine e.g. power tariffs, bidding process for new power plants, fuel types, and power plant locations. Then EGAT will become another power producer who can participate in the bidding for new power plants that will sell power to the grid in the same manner as other private power producers. The Regulatory Body's Board of Commissioners will be under the supervision of the Ministry of Energy; this Board will comprise 7 members, from both public and private sectors, who have expertise in the energy, economic, finance, and legal fields.

Regarding the privatization of the state enterprises in Thai power sector, EGAT plan to transform into a limited liability company and listed on the Stock Exchange of Thailand (SET). Thus, EGAT needs to separate its accounting in generation and transmission Business in order to become fully transparent and to promote maximum efficiency. For MEA and PEA, they will remain in the distribution and retail business. MEA and PEA accounting are also need to be separated into the distribution and retail business by the same reasons. MEA and PEA plan to be listed on the SET by the end of 2004.

Finally, the Supreme Administrative Court judged that the process of transforming of EGAT into a corporation is illegal after spent about four months in seeking truth. The court rules that the two royal decrees, one served as EGAT Plc's charter and the other ordered the dissolution of the status of EGAT, that supported the process are revoked and all the past preparations for privatization are nullified. As a result of this verdict, EGAT will remain a state enterprise and all the plans for its stock market listing will be cancelled.

However, it is widely accepted that the deregulation for more competition in Thailand is avoided. A bilateral-based market model is one of the future ESI models which is of interest in this dissertation. The foreseen problem e.g. transmission congestion, security operation, which can occur in the existing ESI structure, will be investigated. Solutions will be analyzed and consequently leads to proposed management schemes.

1.4 Dissertation Overview

This dissertation deals with the framework of congestion management problem in bilateral markets. Although, most electricity market transaction can be performed both in a power pool and bilateral contracts. However, some electricity markets e.g. NETA, Powernext, EXAA, and ERCOT, are dominated by bilateral/multilateral contracts. In such markets, trading in a power pool is limited in a spot market through balancing mechanism especially in case of no congestion. This situation is recognized as trading in a normal situation; all preferred transactions are feasible. For this condition, this dissertation proposes loss allocation method, which is one of the debated issues under the context of Transmission Open Access (TOA). In case of congestion, transaction revision is needed. In our framework, we formulate this as an optimization problem of minimizing the congestion relief cost, which can be described in Chapter 6. As a result, those revised transactions may not specify for their source and sink. Hence, loss allocation in case of congestion is out of the scope of this dissertation. Trading in bilateral markets with some loss allocation methods and various objective functions of congestion relief procedures are conducted through a simple 3-bus system in Chapter 3. However, others loss allocation and the proposed methods are also mentioned in Chapter 4. In case of congestion, this dissertation considers procuring of some ancillary services, i.e. reactive power of capacitor banks, emergency start units and interruptible load in a spot market via bidding mechanism to relief the overloaded line. In addition, cost is allocated fairly to the participants who contributed to this line. To verify congestion condition, transmission line thermal model is represented in MVA thereby necessity of reactive power flowing and re-scheduling is also emphasized on. As a result, the voltage stability and security margin is considered and included as a main part of this work. In summary, the proposed framework can be classified into four main parts, i.e. loss allocation, congestion relief, congestion cost allocation, and voltage security assessment, which can be described below.

1) Loss allocation method

   The proposed loss allocation method is based on a slack bus independent concept of a specified source and sink. In practice, only the real power is contracted, whereas the contribution of the reactive power is neglected. However, the significance of reactive flow will be described in other topics concerning the voltage security margin of a transmission line, which will be presented in Chapter 4.

2) Voltage security assessment

   The proposed voltage security assessment method is formulated on the P-Q plane of a particular line, which is easy to visualize and can be used as a candidate method for on-line monitoring purpose. In addition, the proposed method can be adapted to verify transmission system inadequacy, which can be used for transmission planning purposes. This proposed method will be presented in Chapter 5.

3) Congestion relief procedure

   The congestion relief is another key process in this dissertation. Both real and reactive flows are taken into account using MVA thermal limit model associated with the objective function of minimizing congestion. Procuring some ancillary services, i.e. reactive power of capacitor banks, emergency-start units, and interruptible load takes place in a spot market via bidding mechanism to relief the congestion. This procedure will be presented in Chapter 6.

4) Congestion cost allocation

   The congestion cost allocation employed in this dissertation is based on the product of contracted power from each transaction and its Power Transfer Distribution

Factor (PTDF) of the congested line. The PTDF can be formulated either on AC and DC power flow. The error between these two approaches is then compared. In addition, the congestion cost allocation methodology between bilateral and pool markets and the presence of multiple congested lines is also proposed. Overall details can be found in Chapter 6, which has been applied to a 28-bus of Thailand region 3 system in Chapter 7. Details arrangement in the dissertation can be summarized below.

In Chapter 2, influences of transmission system under the context of TOA, i.e. transmission pricing and loss allocation, and transmission operating limit are overviewed.

In Chapter 3, transaction framework of trading in bilateral markets with their associated terms is firstly defined. Then analysis is conducted through a simple 3-bus system.

In Chapter 4, the methodology of allocating transmission loss for bilateral contracts is proposed based on an incremental slack bus independent concept.

In Chapter 5, the method for voltage security margin assessment is proposed.

In Chapter 6, the framework of congestion management in bilateral markets with reactive power consideration is proposed and tested with a 6-bus system.

In Chapter 7, two situation, i.e. co-existence of bilateral and pool trading in the same markets and the presence of multiple congested lines are analyzed and tested with a 28-bus of Thailand region 3 system.

In Chapter 8, conclusion and contributions of the dissertation together with future works are presented.

Flowchart of the overall framework can be shown in Figure 1.11.

สถาบันวิทยบริการ
จุฬาลงกรณ์มหาวิทยาลัย

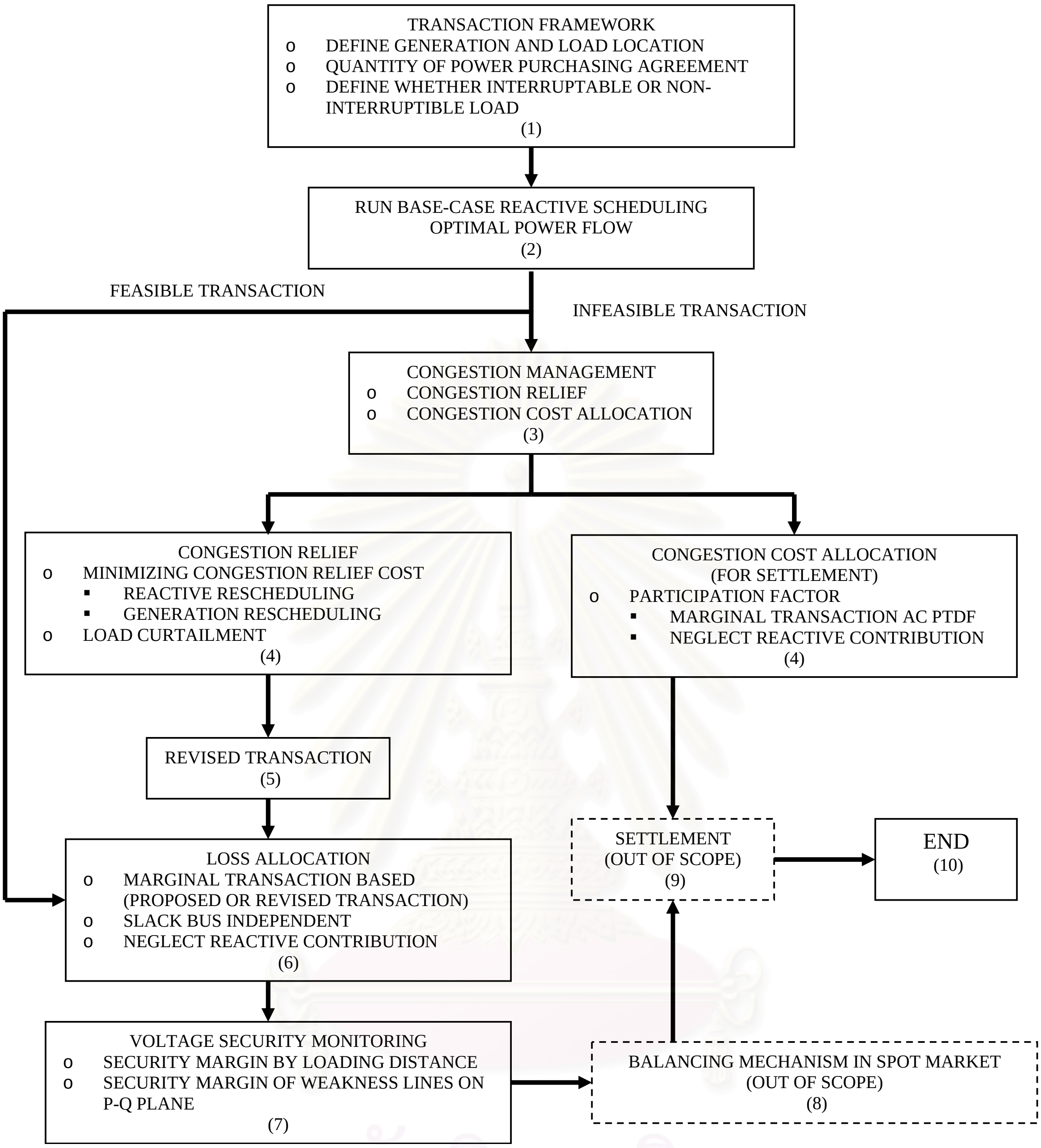

Figure 1.11 Flowchart of the overall framework

The overall framework of this dissertation starts from the SO acquires required information of transaction, i.e. amount of contracted power and locations of source and sink from all participants. Then, the SO performs the Transactions Feasibility Study (TFS) using power flow or OPF tools. In case of no congestion, the preferred transaction is feasible; the SO has to evaluate the loss caused by a particular transaction according to the preferred transaction. In the presence of congestion, the preferred transaction is infeasible and the SO has to use other means e.g. real and reactive power re-scheduling and load curtailment to relief the congestion. These means are ancillary services, which can be procured in a spot market via bidding mechanism. Then the additional cost, which is the congestion relief cost, must be allocated among participants according to their transmission usage. Meanwhile, voltage security assessment program is performed to monitor and maintain system security within a specified value. The security margin is defined as a loading margin on the transmission line P-Q plane. It should be noted that even though the actual response of generation always differs from the schedule due to various reasons e.g. uncertainty of forecasted load and outages, the proposed scenario as mentioned above should be adopted in advance. In a real time normal state, SO must perform the balancing mechanism by acquiring ancillary services in a spot market to balance the system. Then, the settlement will be done after the transaction in a spot market has been finished. However, both the balancing mechanism and settlement is not considered in this dissertation.

1.5 Objectives and Scope of Works

The objectives of this dissertation can be described as follows:

- to propose loss allocation method for feasible transactions under bilateral market, which is based on a slack bus independent concept of a specified source and sink,
- to propose voltage security assessment method,
- to propose congestion relief procedure for a bilateral market, and
- to propose congestion cost allocation method for transactions under bilateral market,

The scope of the works can be summarized as follows:

- impact of the reactive power to transmission loss is neglected,
- balancing mechanism is neglected,
- transmission usage based for allocating the congestion cost is adopted, and
- an actual EGAT system will be used for the test of the proposed methods.

1.6 Conclusion

Background of the dissertation is presented in this chapter. Operation in the vertically integrated market structure using basic EMS functions is briefly described in section 1.1. In section 1.2, some key issues under power system restructuring e.g. level of deregulation, entities of the market, trading arrangement models, role and responsibility of the SO in a competitive environments and definitions of ancillary services, are presented. Experience of ESI restructuring of various markets including ESI of Thailand is analyzed in section 1.3. In section 1.4, overall framework of this dissertation has been presented.

สถาบันวิทยบริการ
จุฬาลงกรณ์มหาวิทยาลัย

CHAPTER 2

INFLUENCES OF TRANSMISSION SYSTEM

2.1 Transmission Loss

Transmission loss occurred in real time operation is a trivial issue in a vertically integrated system due to non-intervention of the third party. For a restructured system, the transmission loss has to be fairly allocated or charged among participants. The loss allocation is recognized as one of the transmission services. In spot pricing of electricity, [44] - [47], the nodal price which aggregates these concerned components, e.g. real and reactive power injected at each node, will be described in section 2.1.1 and its application is presented in section 2.1.2. Operating limits of a transmission line is reviewed in section 2.2 and the transmission cost allocation will be presented in section 2.3.

2.1.1 Components of a Nodal Price [47]

Consider a system of *n* bus, let $P=\left(p_1,p_2,...,p_n\right)$ and $Q=\left(q_1,q_2,...,q_n\right)$, where *P* and *Q* represent real and reactive power demands of *bus-k*, respectively. State variables in power system operation i.e., voltage magnitude and its angle, are defined as $X=\left(x_1,x_2,...,x_n\right)$. In a general Optimal Power Flow (OPF) problem, it can be formulated as

$$Min \qquad f\left(X,P,Q\right) \tag{2.1}$$

$$s.t. \qquad G\left(X,P,Q\right)=0 \tag{2.2}$$

$$H\left(X,P,Q\right)\le 0 \tag{2.3}$$

where

$f\left(X,P,Q\right)$ is a short-term fuel cost,

$G\left(X,P,Q\right)$ is a power flow equation, and

$H\left(X,P,Q\right)$ is an inequality constraints represent limits of all variables.

From the above equations, a Lagrangian function can be formulated as

$$L\left(X,\lambda,\rho,P,Q\right)=f\left(X,P,Q\right)+\lambda G\left(X,P,Q\right)+\rho H\left(X,P,Q\right) \tag{2.4}$$

where $\lambda = \left(\lambda_1, \lambda_2, ..., \lambda_{n1}\right)$ and $\rho = \left(\rho_1, \rho_2, ..., \rho_{n2}\right)$ are the Lagrangian multipliers associated with (2.2) and (2.3) respectively. In practice, only the real power is considered for the optimal solution of (2.4), which can be presented as a nodal price of *bus-k* as shown in (2.5).

$$\begin{aligned} \pi_{p,k} &= \frac{\partial L\left(X, \lambda, \rho, P, Q\right)}{\partial p_k} \\ &= \frac{\partial f}{\partial p_k} + \lambda \frac{\partial G}{\partial p_k} + \rho \frac{\partial H}{\partial p_k} \end{aligned} \tag{2.5}$$

where $\pi_{p,k}$ of (2.5) is a nodal price corresponding to the real power injected at *bus-k*, which can be decomposed into three terms. The first term represents an incremental fuel cost. The second term is an incremental transmission loss whereas the final term is zero if the system inequality constraints are not violated. If some inequality constraints, e.g. transmission line flow, bus voltage, etc., are violated, this component will be activated at the involved buses. However, for actual implementation in markets the components in (2.5) can be modified following the market rule to satisfy all participants. For example, the second and the third terms of a nodal price defined in (2.5) depend on choices of the slack bus. However, in an actual system there is no physical existent of the slack bus. Therefore, if a slack bus is assigned the inequity merchandising surplus between generation and demand causes unfair charges to all participants. Thus, modification is needed for an actual implementation, which will be discussed in Chapters 4 and 6.

2.1.2 Implementation of Spot Pricing Theory [45], [46]

For actual implementation of a spot pricing of electricity in a power pool, a fuel cost based is replaced with a price based mechanism that resulting in a uniform price, which is a social welfare price obtained from a bidding process. For an objective of social welfare maximization, the Marginal Clearing Price (MCP) and Marginal Clearing Quantity (MCQ) can be obtained from an intersection point between demand bid and generation offer as shown in Fig. 2.1.

The MCP obtained from a bidding process substitute the first term of (2.5), which is an energy price of buy/sell in a market. In addition, it represents the cost of transmission loss services that all participants must be incurred as reflected in the second term of (2.5).

Nevertheless, this formula should not be directly implemented in this way, since the slack bus is arbitrarily selected in practice, resulting in slack bus dependent price. Accordingly, other methods used for charging or allocating the transmission loss are needed, which will be briefly discussed in section 2.1.3. The loss allocation method for transaction under bilateral markets, which is independent from a choice of a pre-selected slack bus, will be proposed in Chapter 4.

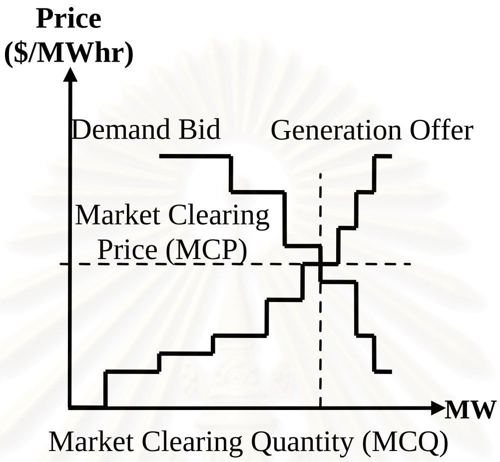

Figure 2.1 MCP and MCQ of a bidding process

2.1.3 Transmission Loss Management

Loss management in an electricity market is a methodology to allocate or charge all participants for their contribution to transmission loss. There are distinctions between the procedures of allocating and charging for transmission loss. Loss allocation method can be defined as a process of dividing total transmission loss to fractions and then distributed to all participants according to their degree of contribution for dispatching or procuring additional power to compensate their own loss. Hence, this scheme must be performed in advanced [48]-[50]. In contrast, charging for transmission loss can be defined as a process of reimbursing cost of transmission loss according to the degree of contribution [51]-[59]. Accordingly, it must be performed in a settlement process after the real time dispatch. The common procedure of both methods either allocating or charging the power loss is to find the degree of participation. The procedure is a complex issue since loss is basically a nonlinear function of all participants and there is no physically meaningful measurement scheme to determine the loss caused by each particular participant. This challenge opens the opportunity to propose any sensible loss allocation schemes. The following principles form the basis for evaluating potential models [60].

- Loss management should be accurate and reflect the cause of its cost

This principle is a key consideration by which most aspects of loss calculation requires a good understanding of all variable impacts to the quantity of loss and an effective incorporation of those variables into the model. Accordingly, amount of generation/load and network topology should be taken into account to send appropriate price signals to reinforce efficient grid use decisions on both short term scheduling and long term generation planning basis.

- Loss management should be straightforward, easy to understand, simple to administer and reasonably predictable

Since accuracy of the loss allocation is important to facilitate a fair competition, any participants should be able to determine the losses attributable to their usage with minimal effort and prior to the usage. The SO should be able to manage loss without undertaking complex ongoing calculations and in a way that can be reasonably replicated.

- Loss management should be consistent for all system users

Since, loss is a physical attribute of the transmission system it should be allocated consistently to all participants in a non-discriminatory manner. There is only one loss allocation methods implemented in a system.

- Loss management should not be gamed

In developing a loss allocation model, opportunities or incentives for participants to artificially shift or avoid appropriate loss responsibility should not be allowed.

- Loss management must be consistent with market design

This means that all participants should be able to provide losses or purchase them as services from the provision entity. In addition, it should be easily accounted for in the congestion management process and appropriate into the settlement process.

In general technical literatures, the proposed loss allocation procedures fall into one of the four categories as described below.

a) Pro-rata method [61]

A Pro-rata method [61] is proposed to allocate transmission loss based on the amount of active power injected/withdrawal at that bus. To clarify, consider the system composed of N_G generation buses and N_L load buses. Assume that transmission losses, denoted by *TTL*, are shared equally among generation and demand sides. Accordingly, loss of the generation and demand sides can be allocated as shown in (2.6) and (2.7) respectively.

$$PL_{Gm} = 0.5TTL.\frac{P_{Gm}}{\sum_{i=1}^{N_G} P_{Gi}} \tag{2.6}$$

$$PL_{Lk} = 0.5TTL.\frac{P_{Lk}}{\sum_{i=1}^{N_L} P_{Li}} \tag{2.7}$$

where

PL_{Gm} is the amount of loss shared to generation at *bus-m*, and

PL_{Lk} is the amount of loss shared to load at *bus-k*, and

P_{Gm} is the amount of power generated from generation at *bus-m*, and

P_{Lk} is the amount of power withdrawal by load at *bus-k*, and

This method is convenient to be implemented due to topology and operating status of the network are neglected. As a result, remote generators/demands are subsidized by the expense of all others. Thus, unfair charge is occurred. However, some electricity markets e.g. Spain and England and Wales, use the Pro-rata scheme for the transmission loss charging.

b) Incremental loss method [49], [50], [59]

In this method, loss is assigned to generators/demands based on the so-called Incremental Transmission Loss (ITL) coefficients. Normalization is performed after the assignment since this allocation procedure typically results in over-recovery. This scheme takes network topology and operating status into account. However, the ITL coefficients obtained from any buses depend on choice of a slack bus, thus it is a discriminatory method and must be agreed by pool agents beforehand on the selection of the slack bus.

c) Proportional sharing method [51]-[56]

This method required for a power flow pattern in association with a linear proportional sharing principle. This principle states that *"the power flow reaching a bus from any power line splits among the lines evacuating power from the bus proportionally* *to their corresponding power flows,”* which is neither provable nor disprovable. Sometimes this method is called Power Flow Tracing.

d) Other methods [57]

Besides the methods mentioned above, Z-bus loss allocation based on electric theorem can be implemented.

2.2 Transmission Operating Limits

Congestion condition on a transmission system is occurred if a transmission line has reached its operating limits. Generally, for steady state operation, there are three types of line limits i.e. thermal, steady state stability (SSS) and voltage stability limits [62]. Details of each limit are described below.

2.2.1 Transmission Line Thermal Limit

Thermal limit is the most common constraint that limits the power transfer capability through a transmission line. Operating beyond the thermal limit can lead to unacceptable sag between the two supporting towers. The sag depends mainly on conductor’s temperature and tension. The conductor temperature relies on two modes of heat transfer, i.e. heat absorption and dissipation. The heat absorption is the heat transfer mode that can increase the conductor temperature i.e., transmission real power loss (I^2R) and solar energy, while the mode of heat dissipation i.e., convection and radiation, would be reduced the conductor temperature. In addition, these environmental parameters in association with conductor tension, stressed during construction, cannot be controlled, whereas only the apparent power flow is a controllable variable depending on the operating condition which is easy to monitor [63]-[65].

- MVA thermal limit model

In general calculation, the amount of current, real power, or apparent power flowing through line rather than conductor temperature is used for thermal limit consideration. However, the MVA flow will be used in this paper since the MVA thermal constraint on π model of transmission line as shown in Fig. 2.2 can be expressed in (2.8) and (2.9).

$$P_{ij}^2 + Q_{ij}^2 \leq S_{ij}^2 \tag{2.8}$$

$$P_{ji}^2 + Q_{ji}^2 \le S_{ij}^2 \tag{2.9}$$

where P_{ij}, Q_{ij} and P_{ji}, Q_{ji} are the real and reactive power flowing from *bus-i* $\rightarrow$ *j* and *bus-j* $\rightarrow$ *i* respectively. S_{ij} is the apparent power flow, which is represented as thermal limit of this line in MVA. The terms P_{ij}, P_{ji}, Q_{ij} and Q_{ji} can be written as (2.10)-(2.13).

$$P_{ij} = V_i V_j Y_{ij} \cos\left(\theta_{ij} - \delta_i + \delta_j\right) - V_i^2 Y_{ij} \cos\theta_{ij} \tag{2.10}$$

$$P_{ji} = V_i V_j Y_{ij} \cos\left(\theta_{ij} + \delta_i - \delta_j\right) - V_j^2 Y_{ij} \cos\theta_{ij} \tag{2.11}$$

$$Q_{ij} = V_i^2 Y_{ij} \sin\theta_{ij} - V_i^2 Y_c - V_i V_j Y_{ij} \sin\left(\theta_{ij} - \delta_i + \delta_j\right) \tag{2.12}$$

$$Q_{ji} = V_j^2 Y_{ij} \sin\theta_{ij} - V_j^2 Y_c - V_i V_j Y_{ij} \sin\left(\theta_{ij} + \delta_i - \delta_j\right) \tag{2.13}$$

where V_i, δ_i and V_j, δ_j are the voltage magnitude and angle at *bus-i* and *bus-j* respectively. Y_{ij} and θ_{ij} are the magnitude and angle of elements of bus-admittance matrix at row-*i* and column-*j*, and Y_c is a half of line charging admittance of the line connected between *bus-i* and *bus-j* .

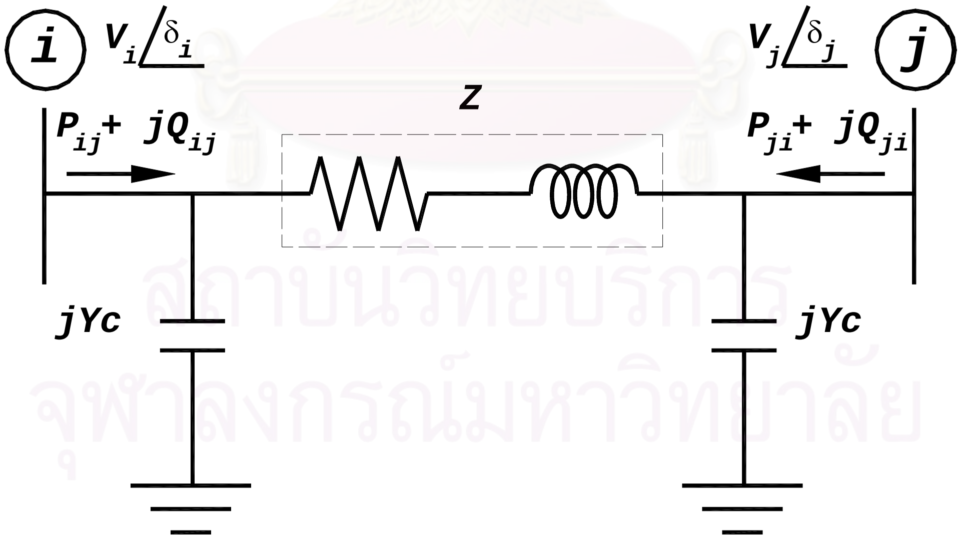

Figure 2.2 The π model transmission line connected between *bus-i* and *bus-j*

For simplicity, only the sending end apparent power is considered due to the reason that in case of congestion the sending end always hits the limit before the receiving end which will be described in the following section.

2.2.2 Steady State Stability Limit

Steady state stability (SSS) limit is the limit of a line according to the maximum power transfer theorem. Operating beyond this limit is impossible. SSS limit depends on voltage magnitude at both end and line parameters i.e. resistance, susceptance and especially reactance of the line. Practically, the SSS limit may be presented using an interconnected transmission line, which transfers a certain amount of power between utilities. In [66], the relationship of active and reactive powers flowing from a sending end bus as shown in Fig. 2.1can be expressed in (2.14) and (2.15).

$$P_{ij} - V_i^2 G = -V_i V_j Y_{ij} \cos(\theta + \delta_i - \delta_j) \tag{2.14}$$

$$Q_{ij} - V_i^2 (B - B_c) = -V_i V_j Y_{ij} \sin(\theta + \delta_i - \delta_j) \tag{2.15}$$

where

V_i is the voltage magnitude at *bus-i*,

δ_i is the angle of V_i,

Bc is the half of line charging susceptance,

Y_{ij} is the magnitude of line admittance between *bus-i* and *bus-j*, where $\vec{Y}_{ij} = G - jB$,

θ is the angle of Y_{ij}^*, $\theta = \tan^{-1}(B/G)$

Taking the square of both sides of (2.14) and (2.15) and then adds together resulting in (2.16).

$$\left[P_{ij} - V_i^2 G\right]^2 + \left[Q_{ij} - V_i^2 \left(B - B_c\right)\right]^2 = \left(V_i V_j Y_{ij}\right)^2 \tag{2.16}$$

Analogously, the active and reactive power flow from receiving end viewpoint can be expressed as (2.17) and (2.18), resulting in (2.19) as shown below.

$$P_{ji} + V_j^2 G = V_i V_j Y_{ij} \cos(\theta - \delta_i + \delta_j) \tag{2.17}$$

$$Q_{ji} + V_j^2 (B - B_c) = V_i V_j Y_{ij} \sin(\theta - \delta_i + \delta_j) \tag{2.18}$$

$$\left[P_{ji} + V_j^2 G\right]^2 + \left[Q_{ji} + V_j^2 \left(B - B_c\right)\right]^2 = \left(V_i V_j Y_{ij}\right)^2 \tag{2.19}$$

The sending and receiving end operating circle associated with the thermal limit circle can be shown as in Fig. 2.3.

Equations (2.16) and (2.19) represent circle diagrams on a P-Q plane with radius of $V_iV_jY_{ij}$ and centers at the coordinate $\left(V_i^2G, V_i^2B - V_i^2B_c\right)$ and $\left(V_j^{\,2}G, V_j^{\,2}B - V_j^{\,2}B_c\right)$ respectively. This means that, the feasible operating points on the sending and receiving end bus must lie on the operating circles which are state in (2.14) and (2.17) respectively. In another word, the operating circles are the power locus diagrams for a constant bus voltage magnitude. In addition, from (2.14) and (2.17), the maximum power transfer at both sides occurs at different point. According to (2.14), the maximum power transfer from the sending end to the receiving end is $V_i^2G + V_iV_jY_{ij}$ when $\delta_i - \delta_j = 180^o - \theta$. On the other hand, the maximum power at a receiving end bus can be determined from (2.17) as $V_iV_jY_{ij} - V_i^2G$ when $\delta_i - \delta_j = \theta$. The angle θ is generally slightly less than 90^o, thereby the maximum power transfer is generally limited by the power at the receiving end bus [62].

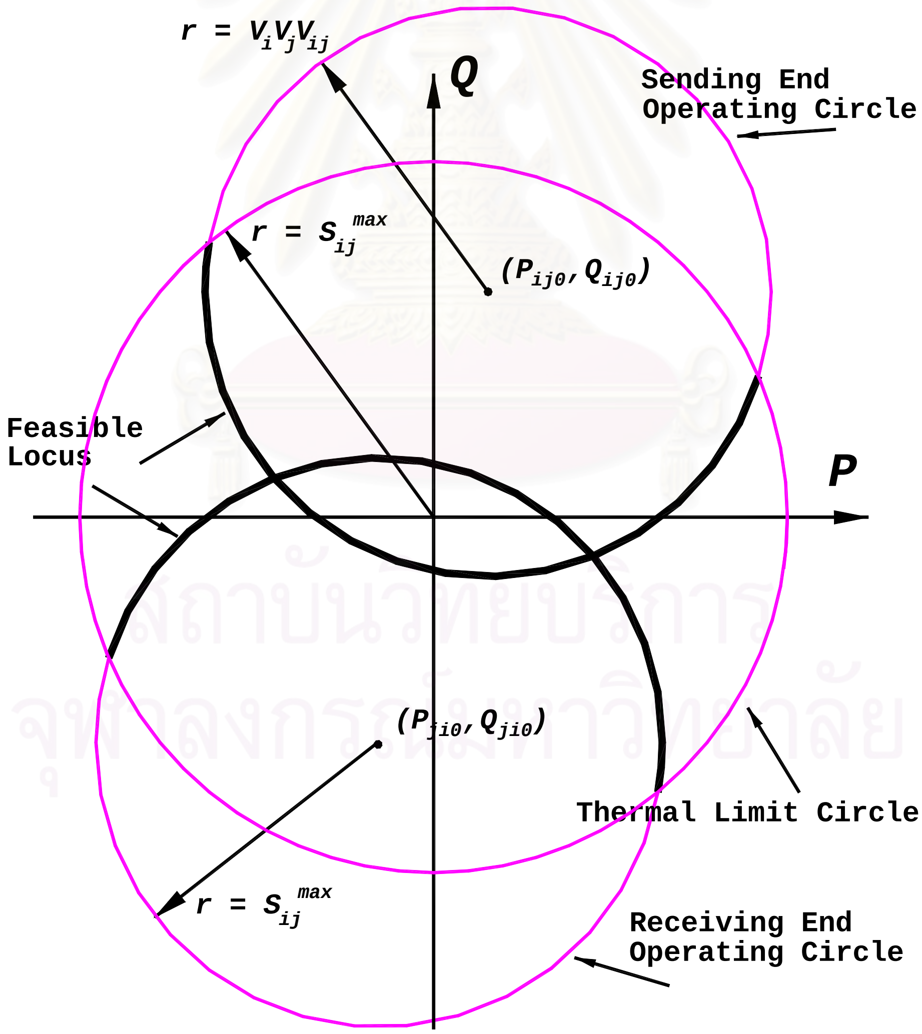

Figure 2.3 The sending and receiving ends operating circles and the thermal limit circle

สถาบันวิทยบริการ
จุฬาลงกรณ์มหาวิทยาลัย

2.2.3 Voltage Stability Limit

This kind of limit is formulated on the assumption that the remote bus cannot maintain its voltage magnitude [67]-[71]. The static voltage stability limit on a transmission line can be developed based on the equivalent model of a transmission line connected between *bus-i* and *bus-j* as shown in Fig. 2.4.

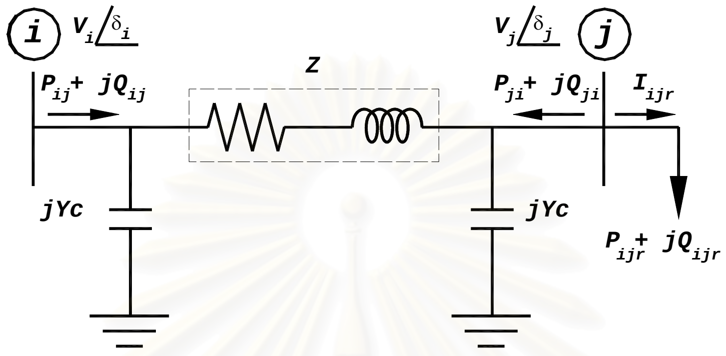

Figure 2.4 The π model transmission line for voltage stability limit

For a considered line, we assume that real power flows from *bus-i* to *bus-j*, and fictitious load current and apparent power at a current operating point of the receiving end are I_{ijr} and $P_{ijr} + jQ_{ijr}$ respectively.

We can formulate relationship based on generalized ABCD parameters [71] as follows:

$$V_i\angle\delta_i = AV_j\angle\delta_j + BI_{ijr} \tag{2.20}$$

where *A=1+ZYc* and *B=Z*. The complex form of *A* and *B* can be expressed as shown in (2.21).

$$A = a_1 + ja_2 \ and \ B = b_1 + jb_2 \tag{2.21}$$

The receiving end current, I_{ijr}, can be expressed as in (2.22).

$$I_{ijr} = \left(P_{ijr} - jQ_{ijr}\right)/V_j\angle-\delta_j \tag{2.22}$$

Substitute A and B from (2.21) and I_{ijr} from (2.22) into (2.20) resulting in (2.23).

$$V_i\angle\delta_i = \left(a_1 + ja_2\right)V_j\angle\delta_j + \frac{\left(b_1 + jb_2\right)\left(P_{ijr} - jQ_{ijr}\right)}{V_j\angle-\delta_j} \tag{2.23}$$

Rearrange (2.23) resulting in (2.24).

$$V_i V_j = \left(a_1 V_j^{\,2} + b_1 P_{ijr} + b_2 Q_{ijr}\right) + j\left(a_2 V_j^{\,2} + b_2 P_{ijr} - b_1 Q_{ijr}\right) \tag{2.24}$$

Equation (2.24) can be rewritten as shown in (2.25).

$$c_1 V_j^{\,4} + \left(c_2 P_{ijr} + c_3 Q_{ijr} - V_i^2\right) V_j^{\,2} + c_4\left(P_{ijr}^{\;2} + Q_{ijr}^{\;2}\right) = 0 \tag{2.25}$$

where $c_1 = a_1^{\,2} + a_2^{\,2}$, $c_2 = 2\left(a_1 b_1 + a_2 b_2\right)$, $c_3 = 2\left(a_1 b_2 - a_2 b_1\right)$ and $c_4 = b_1^{\,2} + b_2^{\,2}$.

Equation (2.25) can be expressed in a quadratic form as (2.26).

$$a\left(V_j^{\,2}\right)^2 + b\left(V_j^{\,2}\right) + c = 0 \tag{2.26}$$

where $a = c_1$, $b = c_2 P_{ijr} + c_3 Q_{ijr} - V_i^2$ and $c = c_4\left(P_{ijr}^{\;2} + Q_{ijr}^{\;2}\right)$.

The solution of (2.25) is the square of the receiving end voltage, which can be calculated from (2.27).

$$V_j = \sqrt{\frac{-b \pm \sqrt{b^2 - 4ac}}{2a}} \tag{2.27}$$

It is obvious that (2.27) has two solutions. A solution lies on the lower part of the P-V curve and is unstable, whereas the other solution on the upper half is a stable one, which can be expressed by (2.28).

$$V_j = \sqrt{\frac{-b - \sqrt{b^2 - 4ac}}{2a}} \tag{2.28}$$

The point where the two trajectories, i.e. stable and unstable, are joined is the nose or bifurcation point. In addition, it is the point where the maximum power can be transferred, which is the condition stated in (2.29).

$$b^2 - 4ac = 0 \tag{2.29}$$

Substitute the coefficients of the quadratic equation from (2.26) into (2.29) and rearrange, we obtain (2.30).

$$\left(c_2^{\,2} - 4c_1 c_4\right) P_{ijr}^{\;2} + \left(c_3^{\,2} - 4c_1 c_4\right) Q_{ijr}^{\;2} - 2c_2 V_i^2 P_{ijr} - 2c_3 V_i^2 Q_{ijr} + 2c_2 c_3 P_{ijr} Q_{ijr} + V_i^4 = 0 \tag{2.30}$$

The relationship between P_{ijr} and Q_{ijr} of (2.30) is a locus of the collapsing point on the P-Q plane which separates the operating points into feasible and infeasible regions as shown in Fig. 2.5.

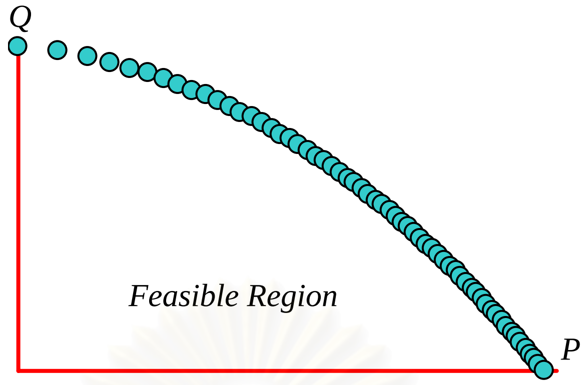

Figure 2.5 Voltage stability boundaries of (2.30)

To clarify, we rewrite (2.30) as shown in (2.31).

$$E_1\left(P_{ijr}^c\right)^2+E_2\left(Q_{ijr}^c\right)^2+E_3P_{ijr}^c+E_4Q_{ijr}^c+E_5P_{ijr}^cQ_{ijr}^c+E_6=0 \tag{2.31}$$

where the superscript c is denoted for the collapsing point and $E_1=\left(c_2^{\,2}-4c_1c_4\right)$, $E_2=\left(c_3^{\,2}-4c_1c_4\right)$, $E_3=-2c_2V_i^2$, $E_4=-2c_3V_i^2$, $E_5=2c_2c_3$, $E_6=V_i^4$. For a given P_{ijr}^c we can calculate Q_{ijr}^c, or vice versa using (2.32) and (2.33) respectively.

$$c_5\left(Q_{ijr}^c\right)^2+c_6Q_{ijr}^c+c_7=0 \tag{2.32}$$

$$c_8\left(P_{ijr}^c\right)^2+c_9P_{ijr}^c+c_{10}=0 \tag{2.33}$$

where

$c_5=\left(c_3^{\,2}-4c_1c_4\right)$, $c_6=2c_3\left(c_2P_{ijr}^c-V_i^2\right)$, $c_7=\left(c_2^{\,2}-4c_1c_4\right)\left(P_{ijr}^c\right)^2-2c_2V_i^2P_{ijr}^c+V_i^4$,
$c_8=\left(c_2^{\,2}-4c_1c_4\right)$, $c_9=2c_2\left(c_3Q_{ijr}^c-V_i^2\right)$, $c_{10}=\left(c_3^{\,2}-4c_1c_4\right)\left(Q_{ijr}^c\right)^2-2c_3V_i^2Q_{ijr}^c+V_i^4$.

Occasionally, the term c_5 or c_8 in (2.32) and (2.33) is zero. In such case, the above equations are reduced to linear form. Then $Q_{ijr}^c=-c_7/c_6$ and $P_{ijr}^c=-c_{10}/c_9$.

2.3 Congestion Cost Allocation [46] - [47]

The basic principle for transmission congestion charging in a power pool is based on spot pricing theory; embed in a nodal price as mentioned in section 2.1.1, where nodal prices can be obtained from dual variables or Lagrangian multipliers, resulting from an

OPF calculation. In this framework, the SO dispatches generation so that the total social welfare is maximized while satisfying the operational and security related constraints. As mentioned earlier, due to a discriminatory concept of a slack bus, this scheme must be performed with agreement of all participants. In practice, to relax the complexity of calculation a zonal pricing may be preferred. Consequently, other schemes [51]-[56] based on generation/load contribution factors to the congested line may be used instead. In contrast, under a bilateral market, source and sink of each bilateral contract is defined explicitly.

2.3.1 Transmission Pricing

A key feature under Transmission Open Access (TOA) is to separate transmission services from generation provision entity. Those services must be charged according to their characteristics and allocated among participants in a non-discriminatory manner. Transmission pricing methodology is a complicated issue under competitive environment. Charging must be performed in a way of providing the correct economic signal reflecting service costs [72] - [79]. In general, pricing methodology of transmission services is promoted to meet the following requirement [72].

- Promote economic efficiency
- Compensate grid companies fairly for providing transmission services
- Allocate reasonable transmission costs among all transmission users
- Maintain reliably of transmission grid
- Ease to implementation.

There are four types of costs associated with transmission services as described below [26].

- *Operating costs* include transmission loss, congestion relief costs and ancillary services provision costs. These operating costs are involved in this dissertation, which will be additionally described in Chapter 6.
- *Recovery of capital costs* of the transmission system investment over their lifetime of the facilities.

สถาบันวิทยบริการ
จุฬาลงกรณ์มหาวิทยาลัย

- *Opportunity costs* are the reliability benefit costs that the grid company incurred as a consequence of maintaining reliability level of services.

- *System expansion costs* include a long-term transmission expansion investment to accommodate with the growth of demand.

There are three main pricing paradigms of transmission usage, i.e. rolled-in, incremental, and composite embedded/incremental paradigms [26]. A brief detail of each can be described below.

A. Rolled-In Transmission Pricing Paradigm

In the Rolled-In pricing paradigm [26], all costs are lumped and allocated to participants according to their usage of transmission services. The existing (embedded) costs need to allocate can be defined as the revenue requirement for all existing facilities plus any new facilities added to the system during life-time contract of the transmission service. The rolled-in pricing paradigm is ease to implement however it is considered to be economically inefficient since it neglects topology of the network. Schematic of the rolled-in transmission pricing paradigm is shown in Fig. 2.6.

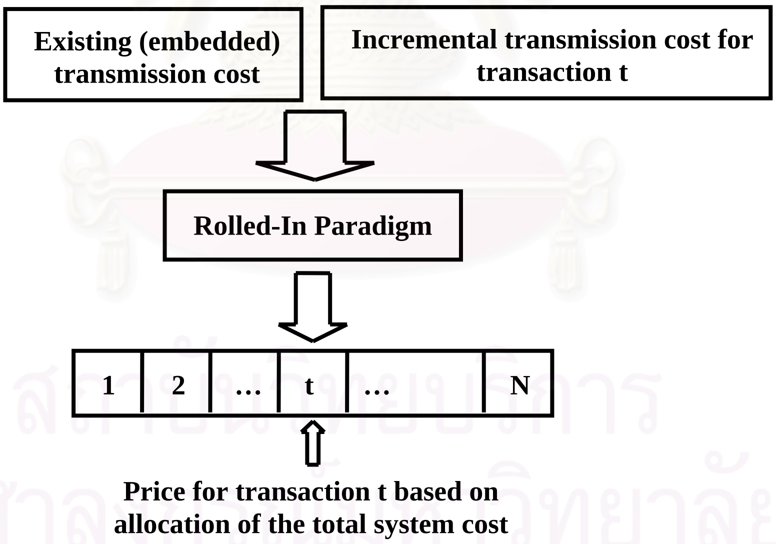

Figure 2.6 Rolled-In pricing paradigm

Several methods under rolled-in paradigm are proposed as below.

- Postage stamp method [77], [78]

A postage stamp rate of transmission service can be calculated simply by allocating the total transmission charges proportionally to the power injected or withdrawal from any buses in the system. In general, this method is considered to be sent incorrect economic signal by neglecting network topology and operating status.

- Contract path method [74]

Under a contract path method, transmission service providers and customers agree on a fictitious flow path between a specified source and sink. The charge is occurred from this fictitious path, which is virtually found without power flow study. Compared with the postage stamp method, the contract path takes the distance between source and sink into account.

- Distance based MW-Mile method [76]

This method is modified from the contract path method in such a way that takes into account the amount of power between source and sink. However, the concept of a fictitious flow path is replaced with an airline distance, without considering the network topology and conditions. Thus, a wrong economic signal is still existed in this method.

- Power flow based MW-Mile method

This method is recommended since it takes into account the real network conditions and amount of the contracted power. Moreover, it uses power flow results to obtain a correct signal before allocating the cost to all participants. There are several concepts proposed under this method e.g. MW-mile, modulus, and zero-counter flow methods. A more detail of each method can be found in [78].

B. Incremental Transmission Pricing Paradigm

Incremental transmission pricing paradigm is referred to revenue requirements paid for any new facilities that are specifically attributed to the transmission service customer. In contrast to rolled-in pricing paradigm, this scheme is considered to promote economic efficiency due to both network topology and operating condition are taken into account however it is complex to implement. Schematic of the incremental transmission pricing paradigm is shown in Fig. 2.7.

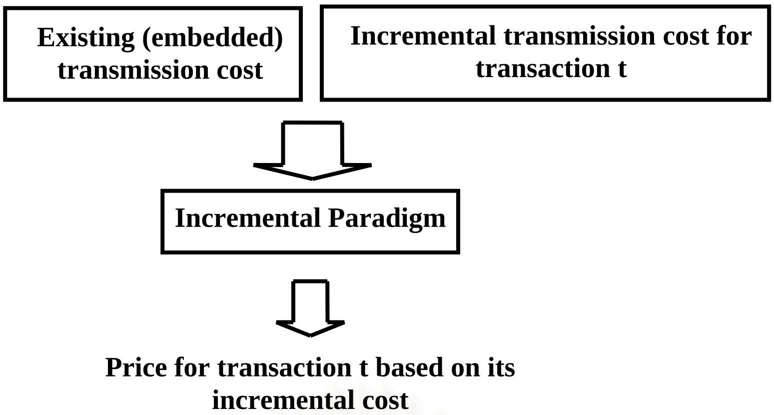

Figure 2.7 Incremental pricing paradigm

Several methods under incremental transmission pricing paradigm are proposed as below [75], [79].

- Short-run incremental cost (SRIC) pricing
- Long-run incremental cost (LRIC) pricing
- Short-run marginal cost (SRMC) pricing
- Long-run marginal cost (LRMC) pricing
- Composite Embedded/Incremental Transmission Pricing Paradigm

This paradigm includes the existing system costs and the incremental costs of transaction. Charging is based on two components of the methods described in A and B as shown in Fig. 2.8.

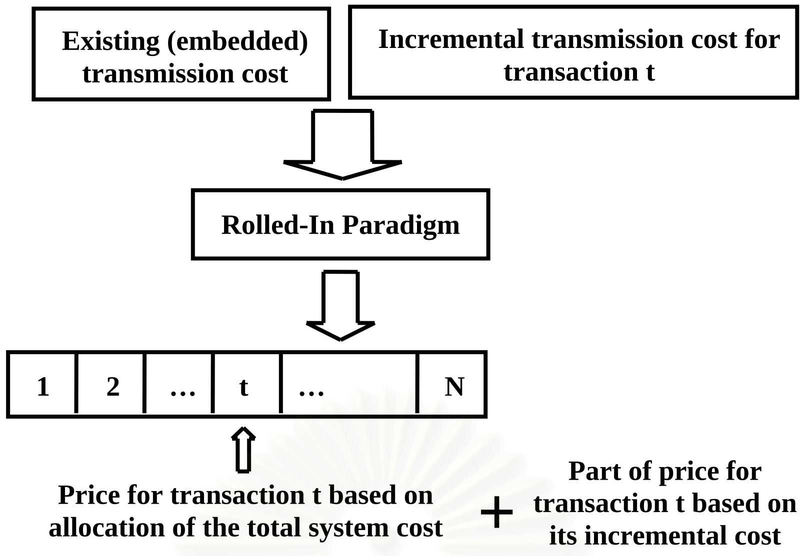

Figure 2.8 Composite embedded/incremental transmission pricing paradigm

2.4 Conclusions

In this chapter, three components of a nodal price formulated based on a spot pricing theory and a real implementation under a pool-based market is presented. Besides, topics under Transmission Open Access (TOA) regarding transmission services charge i.e. transmission loss and transmission pricing, which is studied parallel to a spot pricing theory, are described. In addition, transmission operating constraints, i.e. thermal, steady state stability and voltage stability limits, related to operating parameters e.g. real and reactive power flow through line and voltage magnitudes of the both ends are presented.

CHAPTER 3

TRADING IN BILATERAL MARKETS

3.1 Transaction Framework in Bilateral Markets [80], [81]

3.1.1 Definition of Transaction

Under a bilateral market, buyers and sellers can deal directly. The energy price depends on negotiation and the third party may not be allowed to know. However some information, i.e. locations of source and sink, together with contracted volume must be submitted to the SO, who will accumulate all received contracts to coordinate the trade and then broadcasts to all participants. Accordingly, it is important to clarify the meaning of the word transaction as a bilateral exchange of power between buying and selling entities. A transaction contract can be made both in long-term or short-term basis. Generally, a virtual transaction network can be shown in Fig. 3.1 [80].

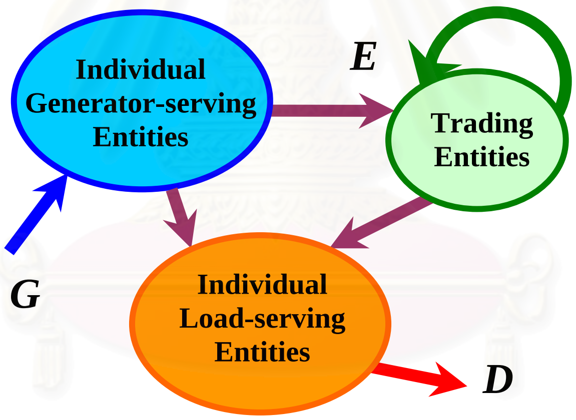

Figure 3.1 Virtual network of transaction among financial entities

The general transaction network shown in Fig. 3.1 consists of three types of financial entities:

(i) the individual generator-serving entities, denoted by *G*, representing the selling interests of individual physical generators

(ii) the individual load-serving entities, denoted by *D*, representing the buying interests of retail loads

(iii) the trading entities, denoted by *E*, which may be of three types: (a) group of generator-serving entities, serving the selling interests of groups of individual generators, (b) group of load-serving entities, serving the buying interests of groups of individual loads, (c) pure trading entities which trade for their own profit with individual or group entities of any kind.

Under these definitions, a utility that owns a number of generators can act as its generator-serving group. An IPP, on the other hand, can act as its own generator-serving entity or independently market its output to a trading entity or to a load-serving entity. Individual loads, can also join to form a group of load-serving entities, or each individual load can find its own suppliers in the market. A power pool is an example of a large load-serving entity that negotiates with all the generator-serving entities.

3.1.2 Transaction Matrix

Once all the virtual flows in a transactions network are determined, they can be systematically represented by a transaction matrix as shown in (3.1).

$$T = \begin{bmatrix} GG & GD & GE \\ DG & DD & DE \\ EG & ED & EE \end{bmatrix} \tag{3.1}$$

Each element of T is a block matrix. The diagonal blocks GG and DD are zero if it is assumed that individual generator-serving entities do not buy from or sell to other individual generator-serving entities or, similarly, that individual load-serving entities do not transact power among each other. In addition, the diagonal terms of EE are zero reflecting the fact that a trading entity does not trade with itself. The remaining terms of T are defined as follow;

- GD_{ik} is scheduled power from generator at *bus-i* to serve load at *bus-k*
- DG_{ki} is power received by load at *bus-k* from generator at *bus-i*
- GE_{ik} is scheduled power from generator at *bus-i* to serve entity at *bus-k*
- EG_{ki} is power received by entity at *bus-k* from generator at *bus-i*
- ED_{ik} is scheduled power from entity at *bus-i* to serve load at *bus-k*
- DE_{ki} is power received by load at *bus-k* from entity at *bus-i*
- EE_{ik} is scheduled power from entity at *bus-i* to entity at *bus-k*

- EE_{ki} is power received by entity at *bus-k* from entity at *bus-i*

The above definition of the elements in transaction matrix *T* excludes transmission loss. Thus the matrix *T* can be called "lossless transaction matrix". The contribution of transmission loss assigning to each transaction methodology is proposed in Chapter 4. It should be noted that elements of *DG, EG,* and *DE* are the power received, while the remaining "sending" transactions are *GD, GE,* and *ED*. In addition, some transactions among trading entities must also be positive, e.g. transaction between a group generation entity and a group load entity. In the wholesale model, there are many groups of load-serving entities, which increase the dimensions of the corresponding matrices. Finally, in the retail model, generation and load allow making a contract directly; thereby elements in *GD* and *DG* may not be zero. The virtual transaction matrix of Fig. 3.1 composes of all possible trades that can be occurred under a bilateral contract market. However, in this dissertation we neglect the trading entity, *E*. Thus, a bilateral contract is a simple contract between generation and demand.

3.2 Trading with Feasible Transactions

Under bilateral markets, the SO requires transacted information, i.e. contracted volume in MW, and locations of source and sink, from all participants. Then, the SO performs feasibility studies based on the preferred transaction using power flow or optimal power flow tools. At this stage, it is required to verify existence of congestion conditions. In case of no congestion, the preferred transaction is feasible, the SO is just responsible to match between demand and supply in real time using balancing mechanism. Regarding transmission loss, the SO has several ways to allocate the loss, which will be examined later. In the presence of congestion, however, the preferred transaction is infeasible and the SO has to find other means, e.g. generation rescheduling to relieve the congestion. After actual transactions, settlement will then be performed. However, both balancing mechanism and settlement is out of scope of this dissertation. The flowchart of trading under bilateral markets regardless of congestion can be shown in Fig. 3.2.

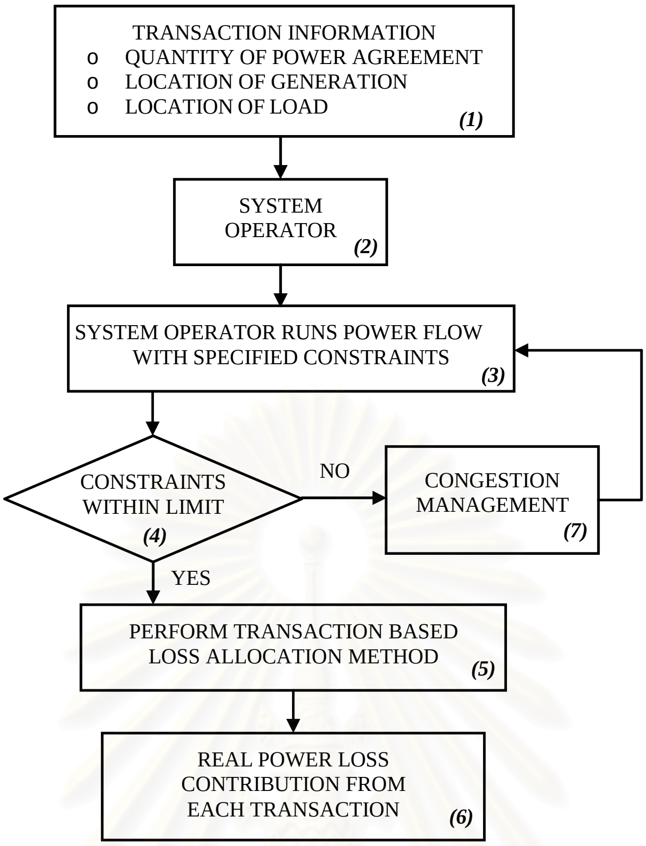

Figure 3.2 Trading under feasible transaction of bilateral markets

To clarify the concept of trading with feasible transaction, we adopt a 3-bus system shown in Fig. 3.3 as an example. In this system, all buses compose of generation and demand. Generation may be selected to commit or de-commit for a specified period depends on market mechanism. The preferred transactions are accumulated by the SO and can be shown in Table 3.1. Transmission line parameters can be found in Table 3.2.

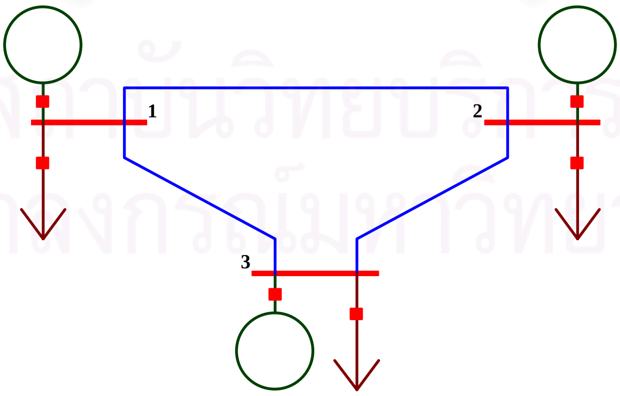

Figure 3.3 Network topology of a 3-bus system

For simplicity, the MW model is used as line thermal limit. According to the framework purposed in Fig. 3.2, the concept of loss management will be firstly clarified.

We assume that, for a preferred transaction in Table 3.2, the real-time demand at every bus in of the forecasted value and there is no contingency, and congestion. The SO responsibility is only to perform balancing mechanism by procuring loss services.

Table 3.1 Transaction information

Transaction No.	Quantity (MW)	Source Bus No.	Sink Bus No.
1	100	1	1
2	40	1	2
3	60	1	3
4	100	2	2
5	40	3	2
6	60	3	3

Table 3.2 Transmission line data

Bus		R	X	Thermal
From	To	(p.u.)	(p.u.)	Limit (MW)
1	2	0.05	0.25	80
1	3	0.04	0.2	60
2	3	0.04	0.2	60

From Table3.1, transactions No. 1, 4 and 6 have no contribution to the flow in the transmission system flow and thereby are neglected from this analysis. Thus only transactions No. 2, 3 and 5 are considered in the calculation.

In the simulation, all bus voltage magnitudes are regulated at 1 p.u. and loss service serving unit is a generation located at bus No. 1. As a consequence, we found that the transmission loss is 2.76 MW. The power flow solutions can be shown in Fig. 3.4.

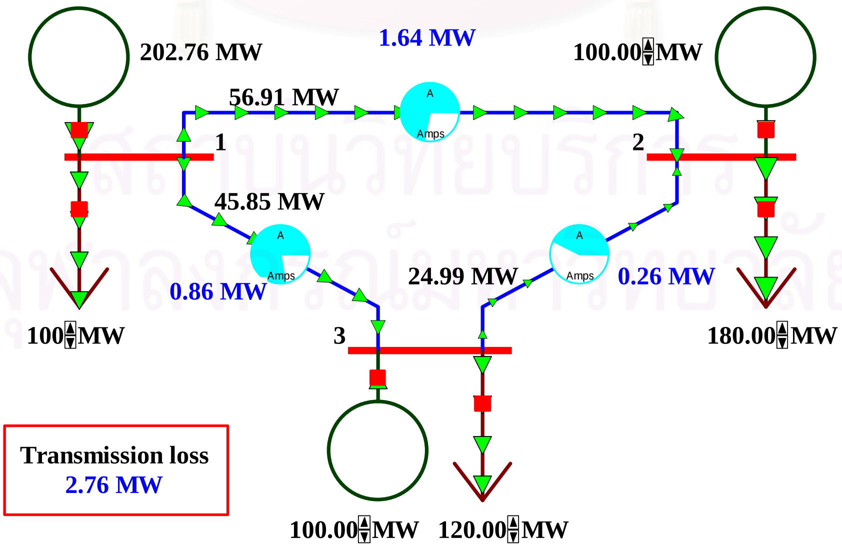

Figure 3.4 Power flow result of preferred transactions

From an example, net generation injected into bus No. 1 is 102.76 MW, including loss of 2.76 MW, whereas net loads taken from the system at buses No. 2 and 3 are 80 and 20 MW respectively. Results from the two loss allocation methods, i.e. pro-rata and power flow tracing methods are presented below.

Under the pro-rata method described in section 2.2, net generation and load equally share for the loss. Thus, 1.38 MW of loss is shared to generation No.1. Likewise, 1.38 MW of loss is shared among loads, which means that 1.104 and 0.276 MW of loss are shared to load at bus No. 2 and 3 respectively.

For power flow tracing [60], generation from bus No. 1 supplies the load at bus No. 2 through a parallel path flow i.e., line connected between buses No. 1 and 2 amount 56.91 MW, and indirect path from line connected between buses No.1 to 3 and 3 to 2. According to a pro-rata method [61], transmission loss is allocated according to (2.6) and (2.7). Thus, loss of the line connected between buses No. 1 and 2 of 1.64 MW is shared equally, 0.82 MW, to generation at bus No. 1 and load at bus No. 2. For line connected between bus No.1 and 3, loss 0.86 MW is shared equally to generation No.1, 0.43 MW, and among loads at buses No. 2 and 3. From proportional sharing assumption, load at bus No. 2 contributes to loss of 0.191 MW, 20/(20+24.99) of 0.43 MW. Likewise, load at bus No. 3 contributes to loss of 0.239 MW, 24.99/(20+24.99) of 0.43 MW. For loss of 0.26 MW occurs at line connected between bus No. 3 and 2, generation at bus No. 1 and load at bus No.2 are shared equally of 0.13 MW. Comparison of loss allocation between pro-rata and power flow tracing methods is shown in Table. 3.3.

Table 3.3 Pro-rata and power flow tracing loss allocation methods

Bus	Amount of allocated loss (MW)	
No.	Pro-rata	Power flow tracing
1	1.38	0.82+0.43+0.13=1.38
2	1.104	0.82+0.191+0.13=1.141
3	0.276	0.239

Advantage of loss allocation under this approach can be listed as below.

- It does not require specifying management method advance. Thus it is easy to manage and reduce the SO burden.
- It neglects all uncertainties affected to loss that preferred transaction cannot be dispatched as proposed.

The second approach of manage transmission loss is to allocate it in advance. The loss is under responsible of all participants. After all participants know their loss contribution, they can compensate it by acquiring for loss services from loss serving entities. The former approach is suitable for implementation in a pool-based market, which exposes a uniform marginal clearing price (MCP). In contrast, the second approach is appropriate for transaction under bilateral markets for a fair competition in the sense that energy price depends on negotiation between the two entities. In this dissertation, the proposed loss allocation method relying on the latter concept will be presented in more detail in Chapter 4.

3.3 Congestion Management in Bilateral Markets

For an example in section 3.2 if the line connected between buses No. 1 and 3 is tripped, the congestion will occur on line connected between buses No. 2 and 3 due to a power flow of 105.78 MW, as shown in Fig. 3.5.

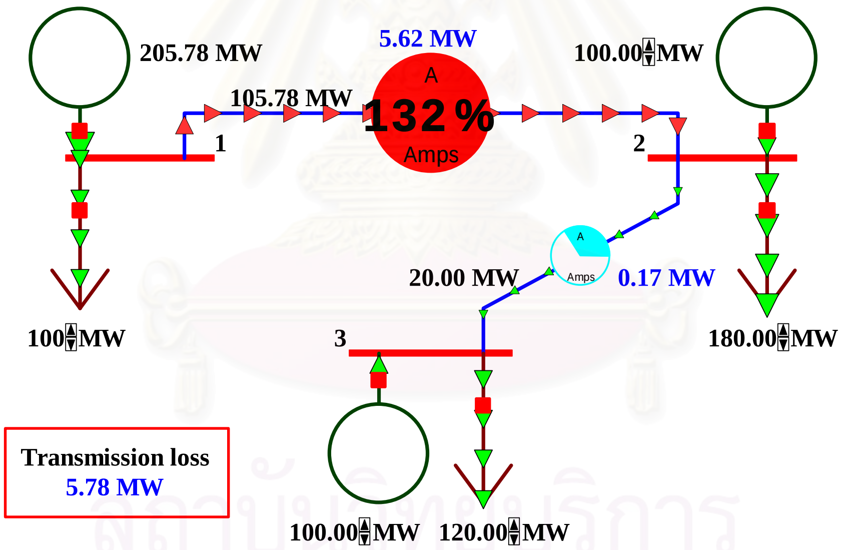

Figure 3.5 Power flow result after line connected between bus No. 1 and 3 is tripped

Due to the presence of congestion, the SO must perform a congestion management program to alleviate the overloaded line. There are several objective functions proposed in literatures to manage the congestion [26]. Some of these objective functions will be discussed in the next section. With any means of congestion management, it may result in the additional cost. For a zero sum congestion management method, as a result, this cost must be allocated among participants. This procedure will be discussed and analyzed in section 3.3.2. It should be noted that if generation re-dispatch cannot alleviate the

สถาบันวิทยบริการ
จุฬาลงกรณ์มหาวิทยาลัย

congestion, a load curtailment program is needed.

3.3.1 Objective Functions of Congestion Management

In case of congestion, the preferred transaction cannot be dispatched. Thus, it needs generation re-scheduling or load curtailment methods to alleviate the congestion, which will result in operating the market deviated from the preferred transaction. In general, there are three main types of objective function for generation re-scheduling and curtailment methods, which can be stated below.

A. Minimize congestion relief cost

In this scheme, all available means, e.g. generation re-dispatching and load curtailment, have to submit a "willingness to accept price" to the SO in case they are requested to relief the congestion. For means that are acquired for congestion management they will receive reimbursement as they bid. In an example, we assume the submitted bids price as shown in Table 3.4.

Table 3.4 Bid price for congestion management

Bus No.	Bid Price ($/kWh)	
	Generation Re-scheduling	Load Curtailment
1	10	15
2	15	20
3	20	25

Solution of the congestion management with minimizing congestion cost is shown in Fig. 3.6.

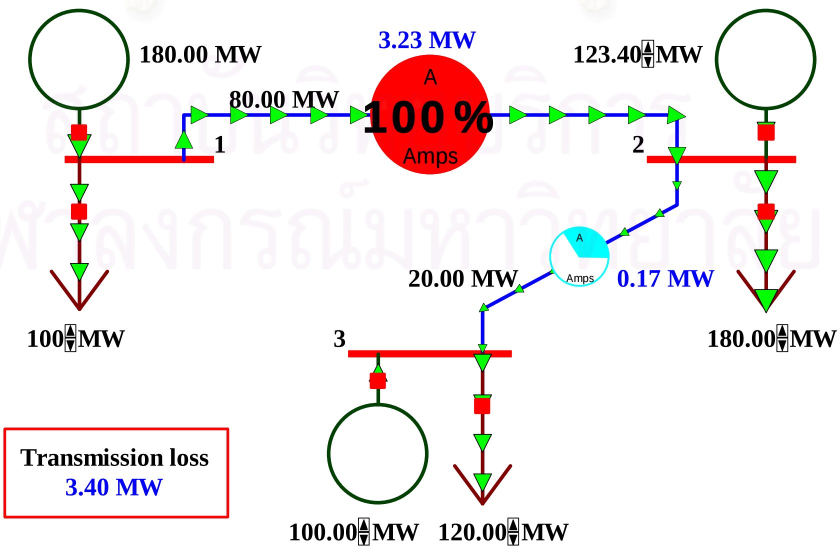

Figure 3.6 Minimizing the congestion cost power flow

If the generation at bus No. 2 has reached a maximum limit at 120 MW, it cannot dispatch as in the case of Fig. 3.6. The curtailed load of 3.4 MW at bus No. 2 is selected additionally to satisfy the objective function. Hence, the new solution can be shown as Fig. 3.7.

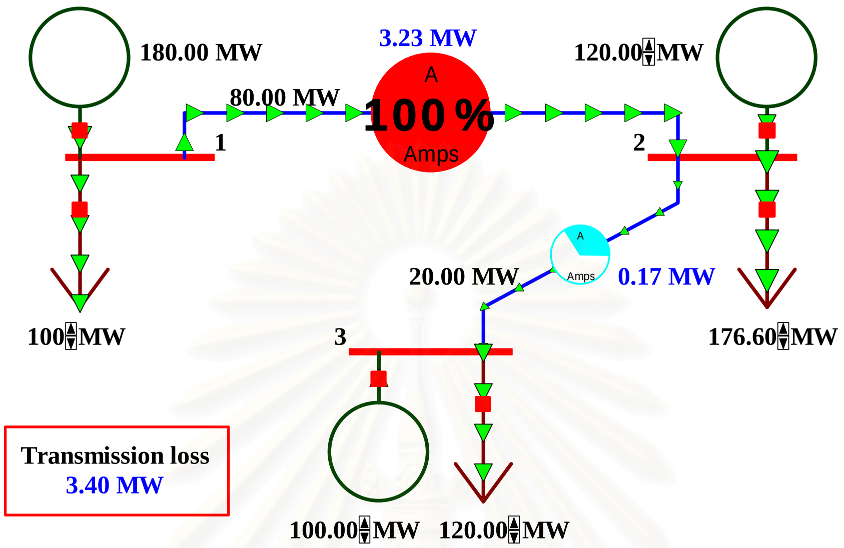

Figure 3.7 Power flow with curtail load at bus No. 2

This objective function is adopted in this dissertation in associated with congestion cost allocation method based on transmission usage index called the Power Transfer Distribution Factor (PTDF). The PTDF is an index revealing participation of each transaction of a specified source and sink to real power flow of a specified line [82]-[86]. It is first formulated using a DC power flow. Detail of PTDF formulation can be found in Appendix B. Details of the proposed congestion management method will be described detail later in Chapter 6.

B. Minimize the deviation from preferred transaction [26]

The objective function of generation re-scheduling in this scheme is to minimize the amount of power deviated from preferred generation dispatch. Deviation is normally defined as the sum of square of amount power differs from the preferred transaction. A quadratic programming is normally used to solve the problem. The disadvantage of this scheme is that it neglects the congestion relief cost and may result in an unnecessary curtailment. Thus, it cannot reflect a correct market signal.

For this objective function, power flow solution is shown in Fig. 3.8.

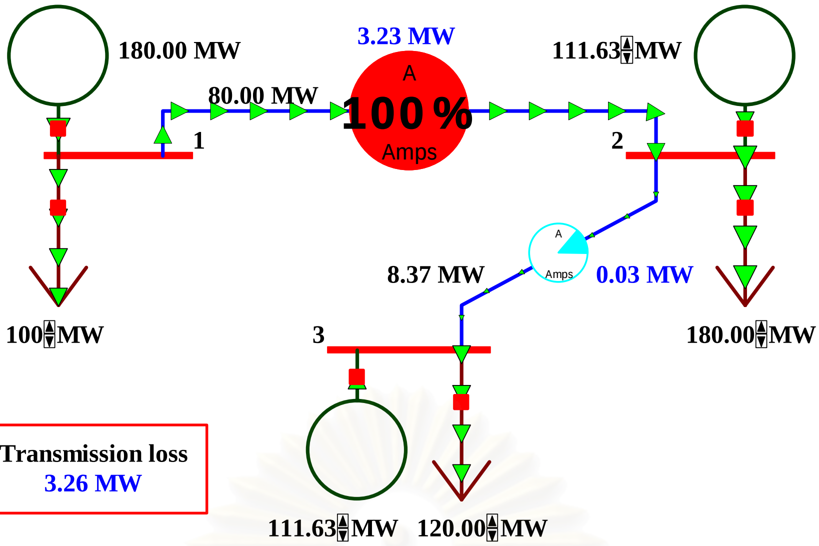

Figure 3.8 Minimizing sum square of deviations power flow

C. Non-firm Transaction curtailment following TLR procedure [87], [88]

This scheme is firstly proposed by the NERC known as a transmission loading relief (TLR) procedure and quite differs from the first two objectives. Using this scheme the SO has to curtail the same amount of power both in generation and load of a transaction based on its PTDF of the congested line times this contracted quantity. The curtailed transaction will not receive reimbursement due to the fact that all transactions involved in the congested line are curtailed in a fair sense. Accordingly, there are several transactions involved in the process and led to an unnecessary curtailment [89], [90].

Power flow solution adopted this objective function is shown in Fig. 3.9.

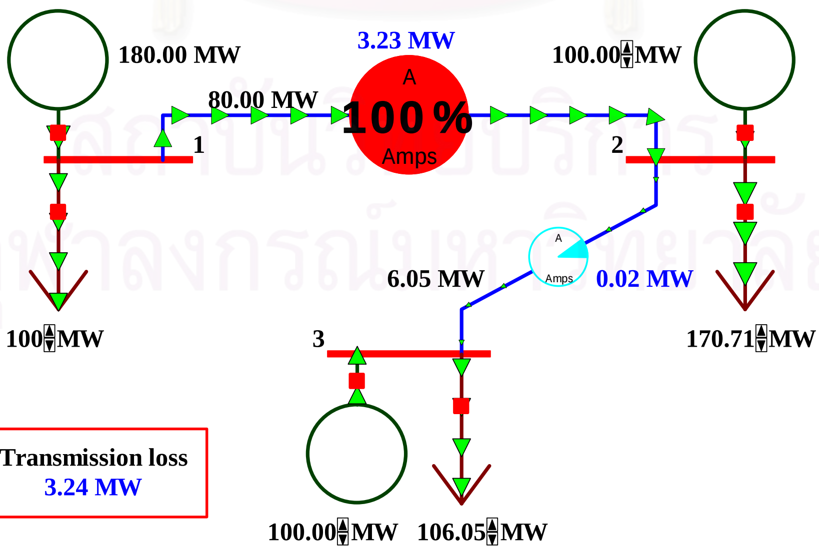

Figure 3.9 Transaction curtailment based on PTDF

Transactions No. 2 and 3 have the same PTDF due to the absence of parallel path flow, power flow radically from bus No. 1 to 3. However, their contribution to line flow is different owing to their contracts have difference quantity. It should be noted that, transaction No. 5 does not contribute to the congested line, Thus it does not involve in the curtailment. In general, the obtained solution is not a complete congestion management scheme since it leaves burden to the SO to re-coordinate the curtailed transactions.

3.3.2 Congestion Cost Allocation

There are two main approaches generally adopted to allocate congestion cost i.e., game theory [91]-[93] and transmission usage index [83]-[86]. The PTDF is a marginal method reveals participation of line flow of a specified line from a specified source and sink. Congestion cost of various objective functions from section 3.3.1 with PTDF based cost allocation can be shown in Table 3.5.

Table 3.5 Summary of congestion cost and congestion cost allocation

Objective	Congestion Cost (1000 $)	Congestion Cost Allocation for Transaction No. (1000 $)		
		2	3	5
A	23.78x0.2x10+23.4x15 = 398.56	159.42	239.14	0
A with G2 reaches limit	23.78x0.2x10+20x15+3.4x20 = 415.56	166.22	249.34	0
B	23.78x0.2x10+11.63x15+11.63x20 = 454.61	181.80	272.71	0
C	Non (According to the TLR procedure)	-	-	-

3.4 Conclusion

This chapter provides a background of trading in a bilateral market. First, definition of a transaction with key information that participants must submit to the SO is presented. For a feasible transaction, a loss allocation method is briefly described. In contrast, a congestion management, which can be divided into congestion relief and congestion loss allocation procedures, is performed if the preferred transaction is infeasible. Several congestion management approaches are presented using a 3-bus system.

CHAPTER 4

LOSS ALLOCATION IN BILATERAL MARKETS

4.1 Introduction

Transmission loss allocation is one of the debating issues in deregulation of electric supply industry. It is a procedure to allocate or charge all participants for system real power loss. Although it is widely accepted that loss is a nonlinear function of all participants and there is still no any physical measurement scheme for determining the real power loss caused by each participant. However, the loss allocation method is a challenge issue and still widely opened for debating. The method should be based on a reasonable assumption, fair for all participants, cannot be gamed, and consistent with market design [60]. Schweppe et al. included the term of incremental cost of loss due to generation and load into a spot price of electric energy [46], which has been later aggregated into a nodal price of a pool-based market [47]. Nevertheless, there are two main weak points found in an actual implementation, which causes unfair charges to participants. Firstly, the non-existent of a slack bus in a real system and secondly, the inequity merchandising surplus between generation and demand occurred in [45], [47]. Accordingly, electricity tracing based method in association with a proportional sharing assumption is proposed to overcome the inconsistency of the incremental transmission loss [51]-[56]. In addition to the tracing based method, other reasonable methods for allocating loss were proposed in [57] and [58]. The main distinctions between incremental-based method presented for a pool market and the methods proposed in [51]-[58] are the presence of the slack bus concept and the way of managing loss. For the incremental loss concept, it can be obtained from either two different power flow calculation or sensitivity analysis. On the other hand, methods in [51]-[58] can directly calculate the contribution of each participant to the loss from each power flow pattern. Though the incremental loss is inconsistent according to the selected slack bus, however, this impact can be diminished for a specified source and sink under a bilateral contract. In [48], a fictitious flow path between a contracted source and sink based on equivalent incremental power exchange between generators and loads is defined to formulate a unique incremental loss allocation for a pool dispatch. In [59], transmission loss resulting from bilateral transactions is allocated at each simultaneous time step by adjusting loss serving generating units. It should be noted that in [48] and [59] the choice of a slack bus still has slightly influence to the uniqueness of the solution. Comparison among various loss allocation methods is conducted in [61]

As a result, a methodology for allocating transmission loss in bilateral markets is proposed in this dissertation. The loss contributed by each transaction is a key value that the system operator (SO) should know for fair settlement in an ex-post time. To facilitate a slack bus independent concept, transmission loss contributed from each feasible transaction is calculated and then allocated to each transaction for separately dispatching in the real-time.

4.2 Framework for Bilateral Transaction

The definition and framework for bilateral/multilateral contracts have already been defined in [58], [80], [81]. However, some terms should be preliminary clarified as described below.

4.2.1 Definition of a Transaction

Transaction can be defined as a bilateral selling/buying contract of electrical energy between a generation and a demand entity.

4.2.2 Transaction Matrix

The transactions defined above can be represented by a transaction matrix with dimension of *n x n*, where *n* is a number of buses in the system. We can categorize the transaction matrix into three types as described below.

4.2.2.1 Preferred Transaction Matrix

The preferred transaction matrix is defined as a matrix whose elements are the quantity of the contracted power made between a pair of generation and load without considering loss. The row and column of each element represents the location or bus of generation and load of each transaction. A typical format of the matrix is shown by (4.1).

$$T^P = \begin{bmatrix} t_{1,1} & \cdots & t_{1,n} \\ \vdots & t_{i,j} & \vdots \\ t_{n,1} & \cdots & t_{n,n} \end{bmatrix} \tag{4.1}$$

where

$t_{i,j}$ is the amount of power from *bus-i* generator contracted to serve the *bus-j* load, and n is the number of buses in the system.

The summation of all elements in the i^{th} row of the matrix represents generation from *bus-i* for various loads in the j^{th} column. The sum of all elements in the j^{th} column of this matrix represents the contracts of load at *bus-j* made with generation at any *bus-i*.

The SO can develop the preferred transaction matrix from the transaction contract submitted from all participants. Then, the SO will develop a loss allocation matrix to share the real power loss from each transaction.

4.2.2.2 Loss Allocation Matrix

We can define the loss allocation matrix as (4.2).

$$L = \begin{bmatrix} 0 & L_{1,2} & \cdots & L_{1,n} \\ L_{2,1} & 0 & \cdots & L_{2,n} \\ \vdots & \vdots & \ddots & \vdots \\ L_{n,1} & L_{n,2} & \cdots & 0 \end{bmatrix} \tag{4.2}$$

The element $L_{i,j}$ in (2) represents the transmission loss contribution by $t_{i,j}$. It should be noted that the transaction of generation and load at the same bus contribute no power loss in the system. Thus, the diagonal elements of this matrix are zero.

4.2.2.3 Scheduled Transaction Matrix

The scheduled transaction matrix is defined as the summation of the preferred transaction matrix and the loss allocation matrix as shown by (4.3).

$$T^S = \begin{bmatrix} t_{1,1} + L_{1,1} & \cdots & t_{1,n} + L_{1,n} \\ \vdots & t_{i,j} + L_{i,j} & \vdots \\ t_{n,1} + L_{n,1} & \cdots & t_{n,n} + L_{n,n} \end{bmatrix} \tag{4.3}$$

The calculation procedure of the proposed concept can be described hereafter. First, the SO acquires the required information from all participants. Then, the SO performs feasibility studies based on the preferred transaction using power flow or optimal power flow tools. In case of there is no congestion, the preferred transaction is feasible, the SO has to evaluate the loss caused by each particular transaction according to the preferred transaction. In the presence of congestion, however, the preferred transaction is infeasible and the SO has to find other means, e.g. generation rescheduling to relieve the congestion. Since loss management for the congestion case, which may occur just a little period of time compared to overall normal operation period, is not in the scope of this dissertation, only the loss allocation method for the feasible transaction is calculated. The procedures can be illustrated in Fig 4.1.

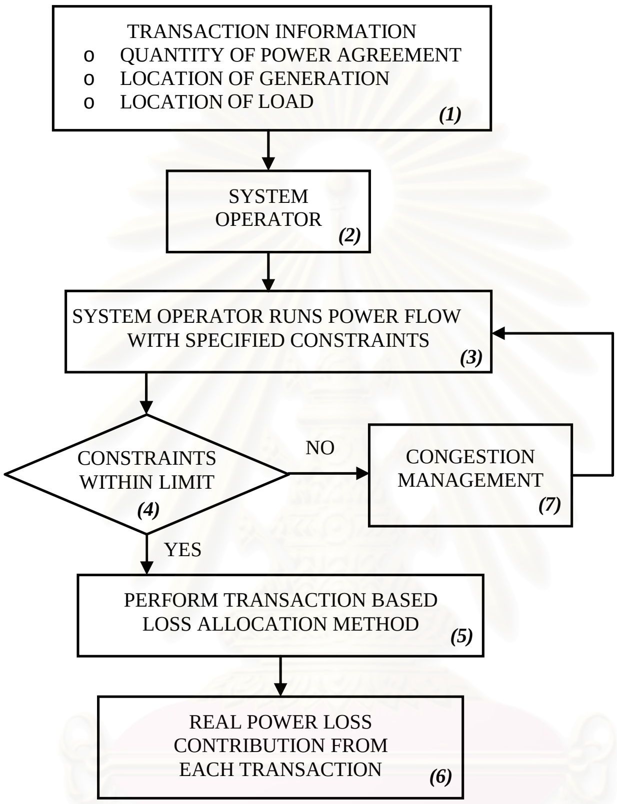

Figure 4.1 Flowchart of the proposed methodology

4.3 Problem Formulation

4.3.1 Incremental Loss Sensitivity Factor

In an AC power flow, real power loss in a transmission system can be expressed by the following equation.

$$P_{loss} = \sum_{a=1}^{n} \sum_{b=1}^{n} |V_a||V_b||Y_{ab}| cos(\theta_{ab} - \delta_a + \delta_b) \tag{4.4}$$

where

$|V_a|$ is the voltage magnitude at *bus-a*,

สถาบันวิทยบริการ
จุฬาลงกรณ์มหาวิทยาลัย

$|V_b|$ is the voltage magnitude at *bus-b*,

$|Y_{ab}|$ is the magnitude of elements of bus-admittance matrix, at *row-a* and *column-b*,

θ_{ab} is the angle of Y_{ab},

δ_a is the angle of V_a, and

δ_b is the angle of V_b.

Contribution of the system loss from the injected power at each bus can be evaluated by calculating $\partial P_{loss} / \partial P_m$ and $\partial P_{loss} / \partial Q_k$. To obtain $\partial P_{loss} / \partial P_m$ and $\partial P_{loss} / \partial Q_k$, the $\partial P_{loss} / \partial \delta_m$ and $\partial P_{loss} / \partial |V_k|$ as defined by (4.5) and (4.6) should be firstly calculated, whereas *m* represents all buses except the slack bus and *k* represents all the load buses.

$$\frac{\partial P_{loss}}{\partial \delta_m} = \sum_{u \in m} \left[\frac{\partial P_{loss}}{\partial P_u} \cdot \frac{\partial P_u}{\partial \delta_m} \right] + \sum_{w \in k} \left[\frac{\partial P_{loss}}{\partial Q_w} \cdot \frac{\partial Q_w}{\partial \delta_m} \right] \tag{4.5}$$

and

$$\frac{\partial P_{loss}}{\partial |V_k|} = \sum_{u \in m} \left[\frac{\partial P_{loss}}{\partial P_u} \cdot \frac{\partial P_u}{\partial |V_k|} \right] + \sum_{w \in k} \left[\frac{\partial P_{loss}}{\partial Q_w} \cdot \frac{\partial Q_w}{\partial |V_k|} \right]. \tag{4.6}$$

These relationships can be presented in a matrix form as (4.7).

$$\begin{bmatrix} \dfrac{\partial P_{loss}}{\partial \delta_m} \\ \dfrac{\partial P_{loss}}{\partial |V_k|} \end{bmatrix} = [J]^T \begin{bmatrix} \dfrac{\partial P_{loss}}{\partial P_m} \\ \dfrac{\partial P_{loss}}{\partial Q_k} \end{bmatrix}. \tag{4.7}$$

where the terms $\partial P_{loss} / \partial \delta_m$ and $\partial P_{loss} / \partial |V_k|$ can be obtained from (4.8) and (4.9) respectively.

$$\frac{\partial P_{loss}}{\partial \delta_m} = \sum_{a=1, \neq m}^{n} |V_m||V_a||Y_{ma}| sin\left(\theta_{ma} - \delta_m + \delta_a\right) \tag{4.8}$$

$$\frac{\partial P_{loss}}{\partial |V_k|} = \sum_{a=1, \neq k}^{n} |V_a||Y_{ka}| sin\left(\theta_{ka} - \delta_k + \delta_a\right) + 2|V_k||Y_{kk}| sin\,\theta_{kk} \tag{4.9}$$

$[J]$ is a Jacobian matrix, which can be divided into J_1, J_2, J_3 and J_4. J_1 is a matrix of *m x m* dimension, of which the diagonal and off-diagonal elements are presented in (4.10) and (4.11) respectively.

$$\frac{\partial P_m}{\partial \delta_m} = \sum_{b=1,\neq m}^{n} |V_m||V_b||Y_{mb}| sin(\theta_{mb} - \delta_m + \delta_b) \tag{4.10}$$

$$\frac{\partial P_m}{\partial \delta_b} = -|V_m||V_b||Y_{mb}| sin(\theta_{mb} - \delta_m + \delta_b), b \neq m , \tag{4.11}$$

J_2 is a matrix of *m x k* dimension, of which the diagonal and off-diagonal elements are shown below.

$$\frac{\partial P_k}{\partial |V_k|} = 2|V_k||Y_{kk}| cos(\theta_{kk}) + \sum_{b=1,\neq k}^{n} |V_b||Y_{kb}| cos(\theta_{kb} - \delta_k + \delta_b) \tag{4.12}$$

$$\frac{\partial P_m}{\partial |V_k|} = |V_m||Y_{mk}| cos(\theta_{mk} - \delta_m + \delta_k), k \neq m , \tag{4.13}$$

J_3 is a matrix of *k x m* dimension, which the diagonal and off-diagonal elements are shown in (4.14) and (4.15).

$$\frac{\partial Q_k}{\partial \delta_k} = \sum_{a=1,\neq k}^{n} |V_k||V_a||Y_{ka}| cos(\theta_{ka} - \delta_k + \delta_a) \tag{4.14}$$

$$\frac{\partial Q_k}{\partial \delta_m} = -|V_k||V_m||Y_{km}| cos(\theta_{km} - \delta_k + \delta_m), m \neq k \tag{4.15}$$

J_4 is a matrix of *k x k* dimension, of which the diagonal and off-diagonal elements are expressed by (4.16) and (4.17).

$$\frac{\partial Q_k}{\partial |V_k|} = -2|V_k||Y_{kk}| sin(\theta_{kk}) - \sum_{b=1,\neq k}^{n} |V_b||Y_{kb}| sin(\theta_{kb} - \delta_k + \delta_b) \tag{4.16}$$

$$\frac{\partial Q_k}{\partial |V_b|} = -|V_k||Y_{kb}| sin(\theta_{kb} - \delta_k + \delta_b), b \neq k \tag{4.17}$$

Using (4.10)–(4.17), (4.7) can be rewritten as shown in (4.18).

$$\begin{bmatrix} \dfrac{\partial P_{loss}}{\partial P_m} \\ \dfrac{\partial P_{loss}}{\partial Q_k} \end{bmatrix} = \begin{bmatrix} J_1 & J_3 \\ J_2 & J_4 \end{bmatrix}^{-1} \begin{bmatrix} \dfrac{\partial P_{loss}}{\partial \delta_m} \\ \dfrac{\partial P_{loss}}{\partial |V_k|} \end{bmatrix} \tag{4.18}$$

The term $\partial P_{loss} / \partial P_m$ represents the loss sensitivity factor, which is defined as an incremental change of real power loss by an incremental change of scheduled power injected into bus, will be used in the next section to formulate the loss contribution index.

The term $\partial P_{loss} / \partial Q_k$ is not used in this dissertation.

4.3.2 Loss Contribution Index

The loss contribution index is defined as an incremental change of loss created by a particular transaction. This term can be obtained by calculating an incremental loss due to the contracted load and generation at *bus-j* and *bus-i* respectively. To obtain this index, the formulation is separated into two cases, according to a location of the generating unit, i.e. at the PV-bus or at the slack bus.

4.3.2.1 Generating Unit Located at a PV-bus

An incremental change of the load at an arbitrary *bus-j*, $-\Delta P_j$, results in changes of system power loss, defined as ΔP_{loss}, of which the relationship can be shown by (4.19).

$$\Delta P_{loss} = -\frac{\partial P_{loss}}{\partial P_j}\Delta P_j \tag{4.19}$$

In a normal power flow calculation, the changes of load and real power loss, which are the consequence of the load change, are compensated by the generation at the slack bus according to the following equation.

$$\Delta P_{slack} = \left(1 - \frac{\partial P_{loss}}{\partial P_j}\right)\Delta P_j \tag{4.20}$$

However, in a bilateral market, this change of demand should be compensated by its generation contracted at *bus-i*, defined as ΔP_i. Similarly, the adjusted generation also influences the change of transmission system loss. To treat the slack bus generation governed from this contract, the net increased generation, expressed on the left hand side of (4.21), must be equal to the sum of the changed demand and loss, expressed on the right hand side of (4.21).

$$\left(1 - \frac{\partial P_{loss}}{\partial P_i}\right)\Delta P_i = \left(1 - \frac{\partial P_{loss}}{\partial P_j}\right)\Delta P_j \tag{4.21}$$

A bilateral transaction contract $T^P_{i,j}$ is defined as the generation at *bus-i* serving load at *bus-j* of $t_{i,j}$ MW. For a fair competition, however, all the committed generators should inject their power equal to the contracted loads, $t_{i,j}$, plus loss, $L_{i,j}$ caused by their transactions. Accordingly, an incremental change of load at *bus-j*, ΔP_j, and generation at *bus-i*, ΔP_i, can be substituted by $t_{i,j}$ and $t_{i,j} + \Delta L_{i,j}$ respectively. From which, (4.21) can be rewritten as (4.22).

$$t_{i,j} + \Delta L_{i,j} = \frac{1 - \dfrac{\partial P_{loss}}{\partial P_j}}{1 - \dfrac{\partial P_{loss}}{\partial P_i}} t_{i,j} \tag{4.22}$$

Consequently, we can rewrite the term $\Delta L_{i,j}$, which is the loss occurred due to this transaction as (4.23).

$$\Delta L_{i,j} = \frac{\dfrac{\partial P_{loss}}{\partial P_i} - \dfrac{\partial P_{loss}}{\partial P_j}}{1 - \dfrac{\partial P_{loss}}{\partial P_i}} t_{i,j} \tag{4.23}$$

4.3.2.2 Generating Unit Located at the Slack Bus

In case of the slack bus generator is contracted with the load of ΔP_j at *bus-j*, the incremental loss due to this transaction can be obtained directly by (4.24).

$$\Delta L_{s,j} = -\frac{\partial P_{loss}}{\partial P_j} t_{s,j} \tag{4.24}$$

where subscript *s* is denoted as the generated power at the slack bus.

The terms $\Delta L_{i,j}$ in (23) and $\Delta L_{s,j}$ in (4.24) are recognized as the loss contribution index of a particular transaction due to the generation at *bus-i* and the slack bus respectively.

4.3.3 Loss-sharing Index

Theoretically, the nature of loss in a system is a nonlinear function of generation and load. Thus, the loss contribution index cannot be applied directly. The actual contribution of loss must be normalized before allocating to particular transactions. Normalization of the loss contribution index is defined as loss-sharing index for each transaction, denotes as $\alpha_{i,j}$, as shown in (4.25).

$$\alpha_{i,j} = \frac{\Delta L_{i,j}}{\sum_{i,j=1}^{n} \Delta L_{i,j}} \tag{4.25}$$

Likewise, loss-sharing index of each PV-bus including the slack bus, denoted as α_i, can also be obtained from (4.26).

$$\alpha_i = \sum_{j=1}^{n} \alpha_{i,j} \tag{4.26}$$

This index in associated with a fine tuned algorithm which will be presented in the next section will be used to obtain the solution, which is independent from different selected slack buses.

4.4 Fine Tuned Algorithm

This section presents a developed fine tuned algorithm to obtain the amount of loss shared by each transaction. The procedure can be described below.

Step 1: Run a power flow program with specified generation. For the first iteration, the specified generation is a case where all PV-bus injected power without compensating for power loss. Thus the slack bus generator is the only one responsible for power loss.

Step 2: Calculate the loss-sharing index for each PV-bus including the slack bus, using (4.25) and (4.26).

Step 3: Calculate the actual loss sharing for each PV-bus as shown by (4.27).

$$L_i = P_i - \sum_{j=1}^{n} t_{i,j} \tag{4.27}$$

For the first iteration, the values of L_i for all the PV-bus are zero since only the slack bus is responsible for the loss.

Step 4: In general, a slight increase of the generation at a PV-bus to share loss from the slack bus results in a small change of loss. Thus, the predicted loss in the system after increasing ΔP_i of each transaction to compensate the loss becomes as (4.28).

$$P_{loss}^{predicted} = P_{loss} + \sum_{i=1}^{N_{PV}} \frac{\partial P_{loss}}{\partial P_i} \Delta P_i \tag{4.28}$$

สถาบันวิทยบริการ
จุฬาลงกรณ์มหาวิทยาลัย

where N_{PV} is a number of PV-buses in a system.

Then the loss shared by generation of all PV-buses based on the loss-sharing index can be expressed by the following equation.

$$\frac{\sum_{i=1}^{N_{PV}} \alpha_i}{\sum_{i=1}^{N_{PV}} \alpha_i + \alpha_s}\left(P_{loss} + \sum_{i=1}^{N_{PV}} \frac{\partial P_{loss}}{\partial P_i} \Delta P_i \right) \tag{4.29}$$

For simplicity, we use β to define the term $\sum_{i=1}^{N_{PV}} \alpha_i /(\sum_{i=1}^{N_{PV}} \alpha_i + \alpha_s)$, which is a contribution ratio of loss for all the PV-bus.

Step 5: The portion of loss defined in (4.29) should be shared by all the generation bus. This relationship can be shown in (4.30).

$$\beta\left(P_{loss} + \sum_{i=1}^{N_{PV}} \frac{\partial P_{loss}}{\partial P_i} \Delta P_i \right) = \sum_{i=1}^{N_{PV}} \left(L_i + \Delta P_i \right) \tag{4.30}$$

The above equation can be rewritten as (4.31).

$$\beta P_{loss} - \sum_{i=1}^{N_{PV}} L_i = \sum_{i=1}^{N_{PV}} \left(1 - \beta \frac{\partial P_{loss}}{\partial P_i} \right) . \Delta P_i \tag{4.31}$$

Step 6: To obtain ΔP_i of each PV-bus while maintaining $\alpha_{i,j}$, the generation at *bus-r* is selected as a reference for loss sharing. The loss sharing index, the actual loss sharing value and the incremental change of generation at this bus are denoted as α_r, L_r and ΔP_r respectively. Then, ΔP_i of each PV-bus can be expressed in term of α_r and ΔP_r as shown in (4.32).

$$\frac{L_i + \Delta P_i}{L_r + \Delta P_r} = \frac{\alpha_i}{\alpha_r} \tag{4.32}$$

Equation (4.32) can be rearranged and rewritten as (4.33).

$$\Delta P_i = \frac{\alpha_i}{\alpha_r}\left(L_r + \Delta P_r \right) - L_i \tag{4.33}$$

For the first iteration, the above equation is reduced to (34).

$$\Delta P_i = \Delta P_r \frac{\alpha_i}{\alpha_r} \tag{4.34}$$

Step 7: Substitute (4.33) to (4.31), then ΔP_r can be obtained from (4.35).

$$\Delta P_r = \frac{\beta P_{loss} - \sum_{i=1}^{N_{PV}} L_i - \sum_{i=1}^{N_{PV}} \left[\left(\frac{\alpha_i}{\alpha_r} L_r - L_i \right) \left(1 - \beta \frac{\partial P_{loss}}{\partial P_i} \right) \right]}{\sum_{i=1}^{N_{PV}} \frac{\alpha_i}{\alpha_r} \left(1 - \beta \frac{\partial P_{loss}}{\partial P_i} \right)} \tag{4.35}$$

Step 8: For ΔP_r from (4.35), ΔP_i can be obtained from (4.33). Then a new value of the specified generation at each bus can be obtained from (4.36).

$$P_i^{new} = P_i^{old} + \Delta P_i \tag{4.36}$$

Repeat steps 1–8 until the specified convergence criteria, i.e. ΔP_i of each PV-bus, is satisfied.

Step 9: After the convergence, the element $L_{i,j}$ of a loss allocation matrix can be obtained from the equation below

$$L_{i,j} = P_{loss} .\alpha_{i,j} \tag{4.37}$$

Finally, the independent slack bus scheduled transaction matrix can be obtained by substituting the value of $L_{i,j}$ in (4.37) to (4.3) to achieve in slack bus independent concept.

4.5 Numerical Example

The proposed method is tested with a modified 6-bus [2] and the IEEE 30-bus system [82]. The comparison of loss allocation between the proposed and a Pro-rata method is also illustrated using the IEEE 30-bus system.

4.5.1 A Modified 6-bus System

For this system, buses *1*, *2* and *3* are generator buses, whereas buses *4*, *5* and *6* are load buses. All the required data are available in Appendix A. The preferred transaction matrix is assumed as below.

$$T^P = \begin{bmatrix} 0 & 0 & 0 & 30 & 30 & 40 \\ 0 & 0 & 0 & 20 & 30 & 30 \\ 0 & 0 & 0 & 30 & 40 & 50 \\ 0 & 0 & 0 & 0 & 0 & 0 \\ 0 & 0 & 0 & 0 & 0 & 0 \\ 0 & 0 & 0 & 0 & 0 & 0 \end{bmatrix}$$

First, we investigate the loss shared by each generator based on various selected slack buses in order to prove that the developed method for loss allocation is independent from slack bus location.

<u>Case 1</u> ***Define bus-1 as slack bus***

The process starts by executing a base-case power flow with generation at *bus-2* and bus-*3* scheduled at 80 and 120 MW respectively. Accordingly, generation at *bus-i* will supply the system loss of 9.2006 MW. Using the algorithm presented in the previous sections, the solution converges within five iterations. The obtained results are shown in Table 4.1.

Table 4.1 System loss shared from generation at each bus of case 1

	Iteration					
	Based case	1	2	3	4	5
G1	9.2006	4.0566	3.8745	3.8679	3.8677	3.8676
G2	0.0000	1.9891	2.0273	2.0282	2.0282	2.0282
G3	0.0000	3.0279	3.1678	3.1734	3.1736	3.1736
Ploss	9.2006	9.0736	9.0696	9.0695	9.0695	9.0695

The loss sharing of each transaction, $\alpha_{i,j}$, can be obtained as below.

$$\alpha = \begin{bmatrix} 0 & 0 & 0 & 0.1095 & 0.1503 & 0.1666 \\ 0 & 0 & 0 & 0.0422 & 0.1031 & 0.0783 \\ 0 & 0 & 0 & 0.0679 & 0.1438 & 0.1383 \\ 0 & 0 & 0 & 0 & 0 & 0 \\ 0 & 0 & 0 & 0 & 0 & 0 \\ 0 & 0 & 0 & 0 & 0 & 0 \end{bmatrix}$$

Finally, the loss allocation matrix can be obtained as below.

$$L = \begin{bmatrix} 0 & 0 & 0 & 0.9931 & 1.3636 & 1.5110 \\ 0 & 0 & 0 & 0.3824 & 0.9353 & 0.7105 \\ 0 & 0 & 0 & 0.6154 & 1.3039 & 1.2543 \\ 0 & 0 & 0 & 0 & 0 & 0 \\ 0 & 0 & 0 & 0 & 0 & 0 \\ 0 & 0 & 0 & 0 & 0 & 0 \end{bmatrix}$$

Case 2 ***Define bus-2 as slack bus***

For this case, the process begins with the generation at *bus-1* and *bus-3* scheduled at 100 and 120 MW respectively. Accordingly, generation at bus-*2* is responsible for the system loss of 8.9804 MW. Using the proposed algorithm, the process converges within five iterations. The obtained results are shown in Table 4.2.

Table 4.2 System loss shared from generation at each bus of case 2

	Iteration					
	Based case	1	2	3	4	5
G1	0.0000	3.7818	3.8654	3.8675	3.8676	3.8676
G2	8.9804	2.1307	2.0296	2.0282	2.0282	2.0282
G3	0.0000	3.1549	3.1744	3.1737	3.1736	3.1736
Ploss	8.9804	9.0674	9.0694	9.0695	9.0695	9.0695

The obtained loss-sharing index and actual loss allocated of each transaction are the same as in case 1.

Case 3 ***Define bus-3 as slack bus***

For this based case, the process starts with the scheduled generation at *bus-1* and *bus-2* of 100 and 80 MW respectively. Accordingly, generation at *bus-2* will take the system loss of 9.005 MW. Using the developed algorithm, the process also converges within five iterations. The obtained results are shown in Table 4.3.

Table 4.3 System loss shared from generation at each bus of case 3

	Iteration					
	Based case	1	2	3	4	5
G1	*0.0000*	*0.0000*	*3.6949*	*3.8609*	*3.8674*	*3.8676*
G2	*8.9804*	*0.0000*	*2.0084*	*2.0283*	*2.0282*	*2.0282*
G3	*0.0000*	*9.0055*	*3.3625*	*3.1801*	*3.1739*	*3.1736*
Ploss	*8.9804*	*9.0055*	*9.0658*	*9.0693*	*9.0694*	*9.0695*

The obtained loss-sharing index and actual loss allocation for each transaction are the same as in cases 1 and 2. It can be seen that, with the proposed method, *G1, G2* and *G3* have to responsible for the loss as 3.8676, 2.0282 and 3.1736 MW respectively, resulting in total system loss of 9.0695 MW. In this case, it means that *G1, G2* and *G3* should be scheduled at 103.8676, 82.0282 and 123.1736 MW respectively.

The above results show that the loss shared from each transaction based on the developed method is consistent and does not depend on the slack bus selection.

4.5.2 The IEEE 30-bus system

For this system, buses *1* and *2* are generation buses, whereas *buses-3, 4, 6-7, 9-10, 12, 14-21, 23-24, 26* and *29-30* are load buses. Generation at *bus-1* has contracts of 243.4 MW for buses 3-8, 12-15 and 18-30, whereas generation at *bus-2* has contracts of 40 MW for buses 2, 10, 16 and 17. The total load of this system is 283.4 MW. Detail of the system is shown in the Appendix A.

We first investigate the results of the loss shared from each generator based on various selected slack buses. The preferred transactions are assumed in Table 4.4.

Table 4.4 The preferred transaction table of IEEE 30-bus system

Transaction No.	Generation Bus	Load Bus	Quantity (MW)
1	2	2	21.7
2	1	3	2.4
3	1	4	7.6
4	1	5	94.2
5	1	7	22.8
6	1	8	30.0
7	2	10	5.8
8	1	12	11.2
9	1	14	6.2
10	1	15	8.2
11	2	16	3.5
12	2	17	9.0
13	1	18	3.2
14	1	19	9.5
15	1	20	2.2
16	1	21	17.5
17	1	23	3.2
18	1	24	8.7
19	1	26	3.5
20	1	29	2.4
21	1	30	10.6

<u>Case 1</u> ***Slack bus as bus-1***

The process starts by executing a base case power flow program with generation at *bus-2* scheduled at 40 MW. Accordingly, generation at *bus-1* will supply the system loss of 17.5985 MW. Using the algorithm presented in section 4, the process converges within three iterations. The obtained results are shown in Table 4.5.

Table 4.5 System loss shared from generation of each bus of, slack bus is *bus-1*

	Iteration			
	Based case	1	2	3
G1	17.5985	17.0235	17.0224	17.0224
G2	0.0000	0.5410	0.5419	0.5419
Ploss	17.5985	17.5644	17.5644	17.5644

Case 2 ***Slack bus as bus-2***

The process starts by executing power flow program with generation at *bus-1* scheduled at 243.4 MW. Accordingly, generation at *bus-2* will supply the system loss of 16.5989 MW. Using the algorithm presented in section 4, the process converges within three iterations. The obtained results are shown in Table 4.6.

Table 4.6 System loss shared from generation of each bus of, slack bus is *bus-2*

	Iteration			
	Based case	1	2	3
G1	0.0000	16.9468	17.0223	17.0224
G2	16.5989	0.6131	0.5421	0.5419
Ploss	16.5989	17.5599	17.5644	17.5644

It can be seen from the results of both cases, Table 4.5 and 4.6, that the system losses from different selected slack buses are equal at loss 17.5644 MW. Contribution of loss from *G1* and *G2* are 17.0224 and 0.5415 MW respectively. The loss-sharing index and the actual loss of each transaction can be obtained and shown in Table 4.7.

Table 4.7 Loss-sharing index and actual loss of each transaction

Transaction No.	Quantity (MW)	$\alpha_{i,j}$	Actual Loss (MW)
1	21.7	0.0000	0.0000
2	2.4	0.0055	0.0968
3	7.6	0.0224	0.3940
4	94.2	0.3995	7.0178
5	22.8	0.0905	1.5894
6	30.0	0.1095	1.9232
7	5.8	0.0096	0.1685
8	11.2	0.0337	0.5927
9	6.2	0.0218	0.3833
10	8.2	0.0302	0.5303
11	3.5	0.0055	0.0974
12	9.0	0.0157	0.2761
13	3.2	0.0129	0.2269
14	9.5	0.0392	0.6888
15	2.2	0.0088	0.1538
16	17.5	0.0662	1.1620
17	3.2	0.0128	0.2240
18	8.7	0.0360	0.6322
19	3.5	0.0158	0.2783
20	2.4	0.0107	0.1882
21	10.6	0.0536	0.9407

4.5.3 Results Comparison

The results from the proposed method are compared with the one obtained from a

Pro-rata method based on the IEEE 30-bus system. In the Pro-rata method, the transaction loss is shared proportionally to its contracted quantity, without considering topological of the network. Detail of a pro-rata method can be found in (2.6) and (2.7) of Chapter 2. For convenience, we compare the results based on the same value of loss, 17.5644 MW as shown in Table 6. We can notice that the transaction No. 1 is neglected since the generation and load are located at the same bus. Thus, total power 261.7 MW of load is considered. Fig. 4.2 illustrates the allocated loss for each transaction between these two methods. The ratio of allocated loss of the proposed method over the Pro-rata method is shown in Fig. 4.3.

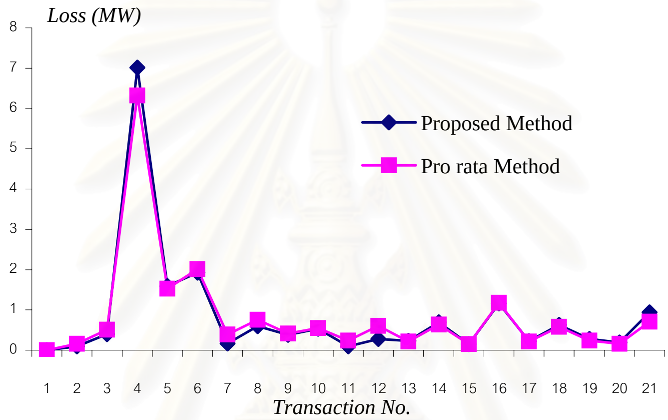

Fig. 4.2 Comparison of actual loss between the Pro-rata and proposed methods

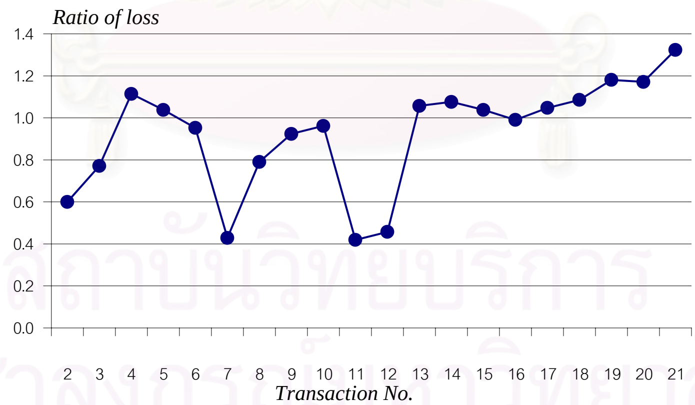

Fig. 4.3 The ratio of loss from the proposed over the Pro-rata methods

From Fig. 4.3, we can notice that transactions No. 7, 11 and 12, contracted by the generation at bus No. 2, have to be responsible for the loss which is less than that of the Pro-rata method. The reason is that the increased generation from bus No. 2 can reduce generation from bus No. 1, which supplies power much higher than bus No. 2. Although transactions No. 3 and 8 are contracted with generation at bus No. 1, they are in the area closed to their generation. Therefore, the loss contribution in this case should be less than those of the Pro-rata. Accordingly, transactions No. 13-21 show that the loss obtained from the proposed method is higher than those of the Pro-rata since all these loads are located far from their generation. The reason is also the same for the case of transaction No. 4.

4.6 Conclusion

In this chapter, we formulate a method of allocating transmission loss for bilateral contracts. The method employs an incremental change of real power to loss based on defined transactions. Thus, network status and topology are taken into account. It can be applied to calculate the loss responsible by any feasible transaction for fair settlement. The effectiveness of the proposed loss management method is that it does not depend on a choice of the slack bus. In addition, the uniqueness of solution can be obtained with the proposed fine tuned algorithm

สถาบันวิทยบริการ
จุฬาลงกรณ์มหาวิทยาลัย

CHAPTER 5

LOADING MARGIN AND TRANSMISSION LINE PERFORMANCE INDICES

5.1 Introduction

Maximum loading capability of a power system is generally limited by steady state and voltage stability limits which practically take place on the transmission system. The interest of evaluating the loading margin of the system according to voltage stability limit is of concerns for decades [83] particularly under competitive environment. Under electric supply industry restructuring, the system may be driven to a heavy loading situation more than in the past, which can cause system blackout in an extremis as recently occurred in a few places worldwide [7], [8]. Since transmission system plays an important role in voltage instability phenomenon and the results obtained from traditional methods, i.e. the system loadability limit and the weakest bus, cannot provide information regarding operating status of a transmission line. Thus, it is necessary to evaluate transmission line loading margin and severity of the transmission system, which can be verified and presented through performance indices. The obtained information can be useful for transmission planning and on-line monitoring purposes.

The loading capability/margin evaluation is traditionally conducted on an entire system. The continuation power flow [84]-[87] is generally employed to calculate such margin. The minimum loading margin for current operating to the closest bifurcation points is calculated and proposed as an index to verify proximity to voltage collapse in [88]-[90]. A method in [91] is proposed to maximize the distance between the current operating to the saddle-node bifurcation points by adjusting the system parameters. In addition, some performance indices obtained from the Jacobian matrix, i.e. the minimum singular value, the minimum eigenvalue, and the determinant of the Jacobian matrix, can be used also as an index to detect proximity to the collapsing point [3]. A comparison of these performance indices is conducted in [92]. Most methods [84]-[91] strictly require wide area system parameters and sufficient mathematical background. In fact, the power system loading capability is normally limited by weak areas. Therefore, only detailed analysis on vulnerable parts is sufficient for decision making. Consequently, the concept of local measurement, i.e. voltage and current at a particular line end, is used in association with appropriate formulation for voltage stability assessment [67]-[70]. The advantage of this approach is to reduce the scale of computation and the complexity of system model. In [71], the P-Q curve corresponds to the static voltage stability relationship for each transmission line is formulated. However, it is derived and tested based on a 2-bus system, thus cannot guarantee to successful implementation in a real system. Transmission line loading margin proposed in this chapter can be calculated independently for each line in association with a given increased line flow direction. The proposed method provides information concerning loading margin of each line, which can be finally used as an index to detect proximity to the collapsing point. In the proposed concept, a P-Q curve is formulated independently for each line at a defined operating point. Then the loading margin corresponding to the specified direction of the increase line flow and the minimum loading margin can be calculated. In addition, two performance indices of a transmission line, i.e. line loading index and line severity index are defined and proposed to use for transmission planning purpose. These indices can be obtained from power system loadability limit calculation with slight modification from a traditional process, i.e. continuation power flow.

In summary, a method for evaluating loading margin and defining the performance indices of each transmission line are proposed in this chapter. The developed methodology can be implemented to assess voltage security margin for an on-line mode. The feasible line flow boundary of each line is firstly formulated on a P-Q plane. Consequently, loading margin in a specified direction of the increased line flow and the minimum loading margin can be calculated. The proposed method can directly evaluate the loading margin on a P/Q mode at an operating point without the need to transform or define loading scenarios. However, any specified loading scenarios are adopted to calculate transmission line performance indices calculation. The indices can be obtained from power system loadability limit, which is generally calculated based on static voltage stability criterion. Information regarding transmission loading margin and their performance indices can then be used for both transmission planning purposes and to detect the proximity to voltage collapse.

5.2 Loadability Limit Calculation by Traditional Methods

In this section, two traditional methods for system loadability limit calculation, i.e.

bifurcation theory and continuation power flow (CPF) are presented. From these methods the point of system voltage collapse can be obtained corresponding to a generation and demand loading scenarios. Consequently, a loading margin can be calculated as a distance from the current operating point to instability boundaries. Detail of both methods can be presented below.

5.2.1 Bifurcation Theory [3], [20], [21], [88]-[91]

Bifurcation theory is a subject used to analyze dynamical mechanism of system instability from the slow change of system parameters. The word bifurcation can be defined as split into two, i.e. stable and unstable regions. Bifurcation analysis requires power system model, which is composed of two types of variables, i.e. *states* and *parameters*. The *states* are variables that varied dynamically during system transients e.g. machine angles, bus voltage magnitudes and angles, and currents in generator windings. *Parameters* are quantities that are regarded as varying slowly to gradually change the system equations e.g. active and reactive power demands at system buses. In a study, the definitions of *states* and *parameters* are an important part of the power system modeling and should be stated explicitly in the study. Generally, there are three types of bifurcation i.e. the saddle node bifurcation (SNB), Hopfield bifurcation (HFB) and singularity induced bifurcation (SIB). Details of the three mode of bifurcation can be described below.

5.2.1.1 Saddle Node Bifurcation

A SNB occurs when the system Jacobian becomes singular in such a way that Jacobian has exactly one zero eigenvalue, and all other eigenvalues have negative real parts. This is the necessary conditions for locating SNB.

In power systems, SNB has a closed relationship with voltage collapse. Accordingly, the system is at its saddle node bifurcation point when it is being stressed to its loadability limit, which can be distinguished from P-V or Q-V curves. The SNB point is also called the point of collapse at which two distinct solutions, i.e. stable and unstable emerge into one solution. There is no solution beyond the SNB point. The system will exhibit voltage collapse immediately after being perturbed beyond the point. The saddle node bifurcation can provide indices to estimate the margin from the current operating point to the bifurcation boundaries. The smallest eigenvalue or critical eigenvalue of the linearized system, or the eigenvector can be used to verify the margin in the parameter space to prevent instability. However, a mapping method is needed transform such margin into a P-Q mode.

5.2.1.2 Hopfield Bifurcation

The HFB corresponds to emergence of a periodic solution from an equilibrium point in a quasi-steady state condition. At a HFB point, the system Jacobian has a pair of imaginary eigenvalues passing the imaginary axis, and no other eigenvalues with non negative real part. These two pure imaginary eigenvalues result in the system's oscillatory modes, depending on the direction of a transversality condition. The system oscillations can exhibit either stable or unstable. The bifurcation is classified to be stable oscillation if it has stable periodic solution due to a stable limit cycle is formed around the unstable equilibrium point. On the other hand, if the periodic solution is unstable occurred where an unstable limit cycle exists around the stable equilibrium point it can be classified as unstable oscillation. Accordingly, it is important in stability analysis to understand the property of limit cycle around the operating point when the system is near a HFB. The studies of HFB are focused on system stability. In practice, system protection can be initiated from a dynamic mechanism, e.g. net damping or frequency dependence of electrical torque and voltage control equipment, and typically triggered by system contingencies. Hence, the system may lose its stability before the point of collapse is reached.

5.2.1.3 Singularity Induced Bifurcation

The singularity-induced bifurcation is a bifurcation in power systems, which can be characterized by the unbound of the system Jacobian eigenvalues at the equilibrium point. A singularity induced bifurcation is the result of singularity of the algebraic part of the linearized power system dynamic algebraic equation model. At this bifurcation point, one of the system state matrix or Jacobian eigenvalues becomes infinity while others remain bounded. The system behavior can not be predicted at the verge to this point due to loss of connectivity between algebraic and differential parts of the system.

5.2.2 Continuation Power Flow (CPF) [3], [20], [21], [84]-[87]

In a real situation, the system will be collapsed at a saddle node bifurcation point, of which the system has no solution beyond this point. In a normal power flow, singularity property of a Jacobian matrix at the verge to collapsing point always annoys the converging even though the system does not reach the limit. To obtain the solution at the collapsing point, a traditional power flow must be modified. The CPF is a power flow version of which the solution can be obtained even the system is operated beyond its loadability limit. The key idea of the CPF is to avoid singularity of the Jacobian matrix by slightly reformulating the power flow equation by applying the locally parameterized continuation technique. Using a CPF, we can trace a P-V or Q-V curve of an interested bus along the system loading trajectory. To trace a complete P-V or Q-V curve, the power flow solution of the modified equation at an interested point can be obtained sequentially until the target point is reached. To enhance calculation speed and accuracy of the solution at the collapsing point, a predictor-corrector scheme is employed. A predictor scheme is adopt generally to find the expected solution in the direction of gradient vector with a specified step length. Then a corrector scheme is used to adjust to the exact point. The key point of adopting a predictor-corrector scheme is an appropriate incremental step, which can be large at the beginning and small or even change a localized parameter at the verge to the collapsing point. However, it should be noted that a CPF require for loading scenarios of generation and demand increasing. Thus, an obtained margin is belonged to a pre-defined scenario.

5.3 Static Voltage Stability Limit on a Transmission Line

The static voltage stability limit on a transmission line can be developed based on the equivalent π model of a transmission line connected between *bus-i* and *bus-j* as shown in Fig. 5.1.

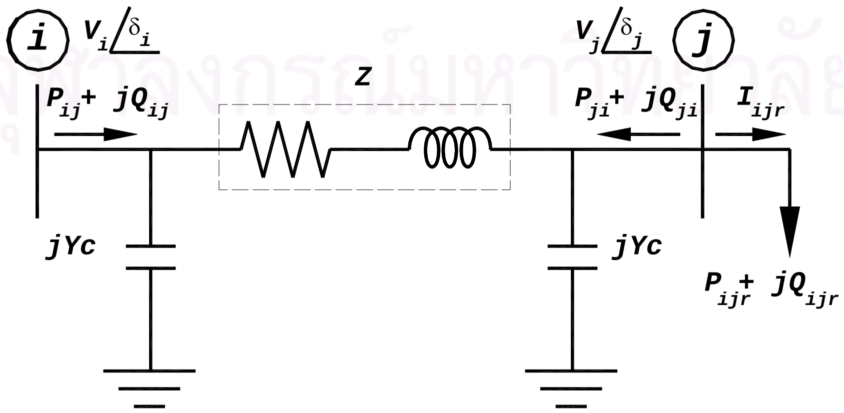

Figure 5.1 The π model transmission line connected between *bus-i* and *bus-j*

We define $V_i\angle\delta_i$ and $V_j\angle\delta_j$ as voltage of *bus-i* and *bus-j* respectively. The series impedance is denoted by *Z*, whereas the half of line charging susceptance is denoted by *Yc*. The apparent power flows from *bus-i* to *bus-j* and vice versa is denoted by $P_{ij} + jQ_{ij}$ and $P_{ji} + jQ_{ji}$ respectively. For a considered line, we assume that real power flows from *bus-i* to *bus-j*, and fictitious load current and apparent power at the current operating point of the receiving end are I_{ijr} and $P_{ijr} + jQ_{ijr}$ respectively.

The relationship based on generalized ABCD parameters can be formulated [71] as follows:

$$V_i\angle\delta_i = AV_j\angle\delta_j + BI_{ijr} \tag{5.1}$$

where *A=1+ZYc* and *B=Z*. The complex form of *A* and *B* can be expressed as shown in (5.2).

$$A = a_1 + ja_2 \text{ and } B = b_1 + jb_2 \tag{5.2}$$

The receiving end current, I_{ijr}, can be expressed as in (5.3).

$$I_{ijr} = \left(P_{ijr} - jQ_{ijr}\right) / V_j\angle -\delta_j \tag{5.3}$$

Substitute A and B from (5.2) and I_{ijr} from (5.3) into (5.1) resulting in (5.4).

$$V_i\angle\delta_i = \left(a_1 + ja_2\right)V_j\angle\delta_j + \frac{\left(b_1 + jb_2\right)\left(P_{ijr} - jQ_{ijr}\right)}{V_j\angle -\delta_j} \tag{5.4}$$

Rearrange (5.4) resulting in (5.5).

$$V_iV_j = \left(a_1V_j^2 + b_1P_{ijr} + b_2Q_{ijr}\right) + j\left(a_2V_j^2 + b_2P_{ijr} - b_1Q_{ijr}\right) \tag{5.5}$$

Equation (5.5) can be rewritten as shown in (5.6).

$$c_1V_j^4 + \left(c_2P_{ijr} + c_3Q_{ijr} - V_i^2\right)V_j^2 + c_4\left(P_{ijr}^{\ 2} + Q_{ijr}^{\ 2}\right) = 0 \tag{5.6}$$

where $c_1 = a_1^2 + a_2^2$, $c_2 = 2\left(a_1b_1 + a_2b_2\right)$, $c_3 = 2\left(a_1b_2 - a_2b_1\right)$ and $c_4 = b_1^2 + b_2^2$.

Equation (5.6) can be expressed in a quadratic form as (5.7).

$$a\left(V_j^2\right)^2 + b\left(V_j^2\right) + c = 0 \tag{5.7}$$

where $a = c_1$, $b = c_2 P_{ijr} + c_3 Q_{ijr} - V_i^2$ and $c = c_4\left(P_{ijr}{}^2 + Q_{ijr}{}^2\right)$.

The solution of (5.6) is the square of the receiving end voltage, which can be calculated from (5.8).

$$V_j = \sqrt{\frac{-b \pm \sqrt{b^2 - 4ac}}{2a}} \tag{5.8}$$

It is obvious that (5.8) has two solutions. A solution lies on the lower part of the P–V curve and is unstable, whereas the other solution on the upper half is a stable one, which can be expressed by (5.9).

$$V_j = \sqrt{\frac{-b - \sqrt{b^2 - 4ac}}{2a}} \tag{5.9}$$

The point where the two trajectories, i.e. stable and unstable, are joined is the nose or the bifurcation point. In addition, it is the point where the maximum power can be transferred, which is the condition stated in (5.10).

$$b^2 - 4ac = 0 \tag{5.10}$$

Substitute the coefficients of the quadratic equation from (5.7) into (5.10) and rearrange, we obtain (5.11).

$$\left(c_2{}^2 - 4c_1c_4\right)P_{ijr}{}^2 + \left(c_3{}^2 - 4c_1c_4\right)Q_{ijr}{}^2 - 2c_2V_i^2P_{ijr} - 2c_3V_i^2Q_{ijr} + 2c_2c_3P_{ijr}Q_{ijr} + V_i^4 = 0 \tag{5.11}$$

To clarify, we rewrite (5.11) as shown in (5.12).

$$E_1\left(P_{ijr}^c\right)^2 + E_2\left(Q_{ijr}^c\right)^2 + E_3P_{ijr}^c + E_4Q_{ijr}^c + E_5P_{ijr}^cQ_{ijr}^c + E_6 = 0 \tag{5.12}$$

where the superscript c is denoted for the collapsing point and $E_1 = \left(c_2{}^2 - 4c_1c_4\right)$ $E_2 = \left(c_3{}^2 - 4c_1c_4\right)$, $E_3 = -2c_2V_i^2$, $E_4 = -2c_3V_i^2$, $E_5 = 2c_2c_3$, $E_6 = V_i^4$.

The relationship between P_{ijr} and Q_{ijr} of (5.12) is a locus of the collapsing point on the P–Q plane which separates the operating points into feasible and infeasible regions. The feasible region is the area in the first and fourth quadrant of the P-Q plane which lies beneath the curve defined by (5.11). The infeasible region is the area besides the feasible region as shown in Fig. 5.2.

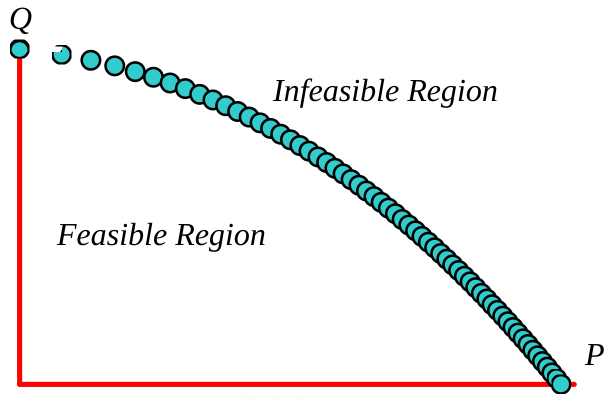

Figure 5.2 Feasible and infeasible region on a P-Q plane

For a given P_{ijr}^{c} we can calculate Q_{ijr}^{c}, or vice versa using (5.13) and (5.14) respectively.

$$c_5\left(Q_{ijr}^{c}\right)^2 + c_6 Q_{ijr}^{c} + c_7 = 0 \tag{5.13}$$

$$c_8\left(P_{ijr}^{c}\right)^2 + c_9 P_{ijr}^{c} + c_{10} = 0 \tag{5.14}$$

where

$c_5 = \left(c_3^{\,2} - 4c_1c_4\right)$, $c_6 = 2c_3\left(c_2P_{ijr}^{c} - V_i^2\right)$, $c_7 = \left(c_2^{\,2} - 4c_1c_4\right)\left(P_{ijr}^{c}\right)^2 - 2c_2V_i^2P_{ijr}^{c} + V_i^4$,
$c_8 = \left(c_2^{\,2} - 4c_1c_4\right)$, $c_9 = 2c_2\left(c_3Q_{ijr}^{c} - V_i^2\right)$, $c_{10} = \left(c_3^{\,2} - 4c_1c_4\right)\left(Q_{ijr}^{c}\right)^2 - 2c_3V_i^2Q_{ijr}^{c} + V_i^4$.

Occasionally, the term c_5 or c_8 in (5.13) and (5.14) is zero. In such case, the above equations are reduced to linear form. Then $Q_{ijr}^{c} = -c_7 / c_6$ and $P_{ijr}^{c} = -c_{10} / c_9$. We defined the distance between the current operating point and the point on a P-Q curve as a loading margin, which will be presented in the next section.

5.4 Loading Margin Calculation

In this section, the loading margin for a specified direction and the minimum loading margin for each line are formulated. Details of each calculation can be presented below.

5.4.1 Loading Margin for a Specified Direction

The predicted collapsing point is the intersection between the voltage stability curve, defined in (5.12), and the line passing through the current operating point in the direction of a specified gradient vector, $\Delta P_{ijr} + j\Delta Q_{ijr}$. This vector can be freely specified or used as a predicted gradient vector, computed from a defined loading scenario. Details of the calculation of the predicted gradient vectors of any defined loading scenario are described in Appendix C. The concept to obtain the collapsing point, (P_{ijr}^c, Q_{ijr}^c), is illustrated in Fig. 5.3.

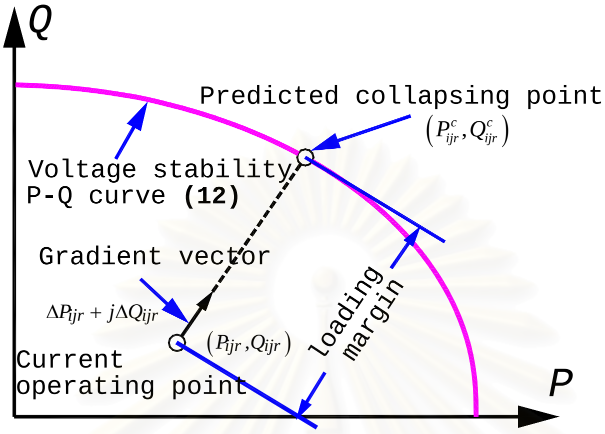

Figure 5.3 The loading margin in a direction of a gradient vector

The predicted collapsing point on the line passing through the current operating point in the direction of a gradient vector can be expressed in (5.15), which is then simplified to (5.16).

$$Q_{ijr}^c = \left(\frac{\Delta Q_{ijr}}{\Delta P_{ijr}}\right) P_{ijr}^c + \left(Q_{ijr} - \frac{\Delta Q_{ijr}}{\Delta P_{ijr}} P_{ijr}\right) \tag{5.15}$$

$$Q_{ijr}^c = MP_{ijr}^c + C \tag{5.16}$$

where $M = \dfrac{\Delta Q_{ijr}}{\Delta P_{ijr}}$ and $C = Q_{ijr} - \dfrac{\Delta Q_{ijr}}{\Delta P_{ijr}} P_{ijr}$.

Substitute (5.16) into (5.12) resulting in (5.17).

$$\left(E_1 + E_2 M^2 + E_5 M\right)\left(P_{ijr}^c\right)^2 + \left(2E_2 MC + E_3 + E_4 M + E_5 C\right) P_{ijr}^c + \left(E_2 C^2 + E_4 C + E_6\right) = 0 \tag{5.17}$$

Substitute the feasible solution of (5.17) into (5.15) to obtain the predicted collapsing point. Then, the line loading margin is defined as the norm of the vector starting from the current operating point to the predicted collapsing point as shown in (5.18).

$$LLM_{ij} = \left\| \left(P_{ijr}^c - P_{ijr}, Q_{ijr}^c - Q_{ijr}\right) \right\| \tag{5.18}$$

5.4.2 The Minimum Loading Margin

A prediction-correction scheme is used to calculate minimum loading margin. The prediction step is used to predict the collapsing point. The correction step is then used to update the predicted solution by neglecting the infeasible portion. The dot product of the two vectors, i.e. the tangent vector and the vector starting from the current operating to the predicted collapsing point is employed to select the feasible portion. The process is continued until these two vectors are perpendicular within a specified tolerance. The concept for minimum loading margin calculation can be illustrated in Fig. 5.4 using nine-step algorithm described below. *Step1* is a pre-process step. Then the prediction is performed by *steps 2* and *3*, whereas the correction is conducted by *steps 4-7*. The process is repeated until satisfying the convergence criteria as defined in *step 8*. Finally, the minimum loading margin is obtained from *step 9*. Detail of each step can be described below.

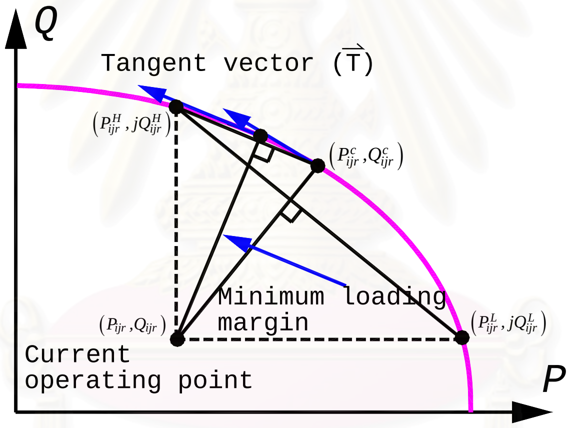

Figure 5.4 The iterative process to obtain the minimum loading margin

<u>*Step 1*</u> Calculate the (P_{ijr}^H, Q_{ijr}^H) and (P_{ijr}^L, Q_{ijr}^L), which are the collapsing points in the direction of the Q and P axis according to (5.12) and (5.13) respectively.

<u>*Step 2*</u> Calculate the slope of the line connecting between (P_{ijr}^H, Q_{ijr}^H) and (P_{ijr}^L, Q_{ijr}^L) as described in (5.19)

$$slope = \frac{\left(Q_{ijr}^H - Q_{ijr}^L\right)}{\left(P_{ijr}^H - P_{ijr}^L\right)} \tag{5.19}$$

<u>*Step 3*</u> Calculate the (P_{ijr}^c, Q_{ijr}^c), which is the predicted collapsing point in the direction of *–1 /slope* using (5.15)-(5.17).

Step 4 Calculate the slope of the P-Q curve at $(P_{ijr}^{c}, Q_{ijr}^{c})$, which can be obtained from (5.20)-(5.21) as follows:

$$F(P,Q) = E_1P^2 + E_2Q^2 + E_3P + E_4Q + E_5PQ + E_6 = 0 \tag{5.20}$$

$$slope = -\frac{\partial F(P,Q)/\partial P}{\partial F(P,Q)/\partial Q} = -\frac{2E_1P_{ijr}^{c} + E_5Q_{ijr}^{c} + E_3}{2E_2Q_{ijr}^{c} + E_5P_{ijr}^{c} + E_4}. \tag{5.21}$$

Step 5 Define the tangent vector according to the slope in (5.21) as stated in (5.22).

$$\vec{T} = -\left(2E_1P_{ijr}^{c} + E_5Q_{ijr}^{c} + E_3\right) + j\left(2E_2Q_{ijr}^{c} + E_5P_{ijr}^{c} + E_4\right) \tag{5.22}$$

Step 6 Calculate the dot product between vector $\vec{T}$ in (5.22) and the vector that starts from the predicted collapsing point and ends at the current operating point.

Step 7 If the dot product in *step 6* is a negative value, replace $(P_{ijr}^{L}, Q_{ijr}^{L})$ by $(P_{ijr}^{c}, Q_{ijr}^{c})$. If the dot product in *step 6* is a positive value, replace $(P_{ijr}^{H}, Q_{ijr}^{H})$ by $(P_{ijr}^{c}, Q_{ijr}^{c})$.

Step 8 Repeat *steps 2* to *7* until the results of the dot product obtained in *step 6* is within a specified tolerance, which implies that the two vectors are perpendicular. This is the condition to guarantee the minimum loading margin.

Step 9 Calculate the minimum loading margin using (5.18).

From the algorithm presented above, the minimum loading margin occurs when $\vec{T}$ perpendicular to the gradient vector defined in (5.23).

$$\vec{G} = \left(P_{ijr}^{c} - P_{ijr}\right) + j\left(Q_{ijr}^{c} - Q_{ijr}\right) \tag{5.23}$$

The minimum loading margin of each line obtained in this section is presented in a unit of MVA, which can be used to verified proximity of the collapsing point.

5.5 Transmission Line Performance Indices

In this section, two performance indices of a transmission line i.e., line loading index and line severity index in association with the calculation methodology are proposed. To calculate these indices, loading scenarios of generation and demand must be defined first. Then, a predicted gradient vector of line flow can be obtained. Accordingly, those indices are finally calculated based on margin in the direction of gradient vector as presented in section 5.3.1. These indices can be calculated in an on-line mode to verify severity of transmission system. Additionally, for off-line study it provides a signal of upgrading or expanding transmission system to enhance the system loadability limit. The calculation process can be presented below.

5.5.1 Scenarios for the Increase of Generation and Demand

We consider firstly a set of buses in the system which is defined as $\mathbb{N} = \{s, G, L\}$, where *s* refers to the slack bus, *G* is a set of generation buses, and *L* is a set of load buses. ΔP_G and ΔQ_G are defined as a set of an incremental change of real and reactive power injected at generation buses, ΔP_L and ΔQ_L are a set of an incremental change of real and reactive power injected to load buses. An incremental change of real and reactive transmission loss is denoted by ΔS_{loss}.

If the load change of $\Delta P_L + j\Delta Q_L$ occurs, all the generation buses must contribute their power for the consequences. This relationship can be expressed in (5.24).

$$\Delta P_G + j\Delta Q_G + \Delta P_L + j\Delta Q_L + \Delta P_s + j\Delta Q_s = \Delta S_{loss} \tag{5.24}$$

We define λ_n as a vector indicating the contribution indices for the increase of generation and demand as described in (5.25).

$$\lambda_n = \left(\lambda_s, \lambda_G, \lambda_L\right) = \left(\lambda_s, \lambda_1, \ldots, \lambda_G, \lambda_{G+1}, \ldots, \lambda_L\right) \tag{5.25}$$

The contribution indices represent the change of generation and demand. If the change in system power loss is neglected for the increase generation and demand, the sum of these indices is zero, and the general relationships can be stated as in (5.26).

$$\left.\begin{array}{l} \sum\limits_{g \in s \cup G} \lambda_g = 1 \\ \sum\limits_{l \in L} \lambda_l = -1 \end{array}\right\} \tag{5.26}$$

Transactions can be defined as a bilateral selling/buying contract of electrical energy between generators and loads.

5.5.2 Gradient Vector and a Predicted Collapsing Point

From a specified loading scenario, we can calculate the gradient vector of each receiving end line flow, denoted by $\Delta P_{ijr} + j\Delta Q_{ijr}$, of which the real and imaginary parts can be expressed in (5.27) and (5.28).

$$\Delta P_{ijr} = \sum_{m \in G \cup L} \left[\frac{\partial P_{ijr}}{\partial P_m} . \Delta P_m \right] + \sum_{k \in L} \left[\frac{\partial P_{ijr}}{\partial Q_k} . \Delta Q_k \right] \tag{5.27}$$

$$\Delta Q_{ijr} = \sum_{m \in G \cup L} \left[\frac{\partial Q_{ijr}}{\partial P_m} . \Delta P_m \right] + \sum_{k \in L} \left[\frac{\partial Q_{ijr}}{\partial Q_k} . \Delta Q_k \right] \tag{5.28}$$

Details of the gradient vector calculation can be found in Appendix C. The terms ΔP_m and ΔQ_k in (5.27) and (5.28) are referred to an incremental change of the real and reactive power at buses *m* and *k* respectively. They can be calculated by (5.29) and (5.30).

$$\Delta P_m = \lambda_m . \Delta P_L, \; m \in G \cup L \tag{5.29}$$

$$\Delta Q_k = \lambda_k . \Delta Q_L, \; k \in L \tag{5.30}$$

Substitute ΔP_m and ΔQ_k from (5.29) and (5.30) into (5.27) and (5.28), then rearrange these equations to result in (5.31) and (5.32).

$$\Delta P_{ijr} = \sum_{m \in G \cup L} \left[\frac{\partial P_{ijr}}{\partial P_m} . \lambda_m \right] . \Delta P_L + \sum_{k \in L} \left[\frac{\partial P_{ijr}}{\partial Q_k} . \lambda_k \right] . \Delta Q_L \tag{5.31}$$

$$\Delta Q_{ijr} = \sum_{m \in G \cup L} \left[\frac{\partial Q_{ijr}}{\partial P_m} . \lambda_m \right] . \Delta P_L + \sum_{k \in L} \left[\frac{\partial Q_{ijr}}{\partial Q_k} . \lambda_k \right] . \Delta Q_L \tag{5.32}$$

The gradient vector, $\Delta P_{ijr} + j\Delta Q_{ijr}$, calculated in this section can be substituted with a specified gradient vector to obtained a predicted collapsing point as described in section 5.3.1.

5.5.3 Transmission Line Performance Indices

The performance indices of transmission line defined in this section can be described below.

5.5.3.1 The Line Loading Index

The line loading index is defined as the ratio of the line loading margin of (5.18) to the apparent power of the predicted collapse point, which can be obtained from (5.33).

$$LLI_{ij} = \frac{\left\| \left(P_{ijr}^{c} - P_{ijr}^{t}, Q_{ijr}^{c} - Q_{ijr}^{t} \right) \right\|}{\left\| \left(P_{ijr}^{c}, Q_{ijr}^{c} \right) \right\|} \tag{5.33}$$

5.5.3.2 The Line Severity Index

The line severity index can be defined as ratio of the norm of the gradient vector to the security margin as shown in (5.34).

$$LSI_{ij} = \frac{\left\| \left(\Delta P_{ijr}^{t}, \Delta Q_{ijr}^{t} \right) \right\|}{\left\| \left(P_{ijr}^{c} - P_{ijr}^{t}, Q_{ijr}^{c} - Q_{ijr}^{t} \right) \right\|} \tag{5.34}$$

Superscript *t* denotes the operating point of the current iteration. It should be noted that the predicted collapsing point employed in both indices, i.e. line loading and line severity indices, obtained from a gradient vector. Simulation results of the proposed method will be presented in the next section.

5.6 Simulation and Results

5.6.1 Loading Margin Evaluation

5.6.1.1 A Two-bus System

The proposed method is firstly illustrated with a 2-bus system, shown in Fig. 5.5.

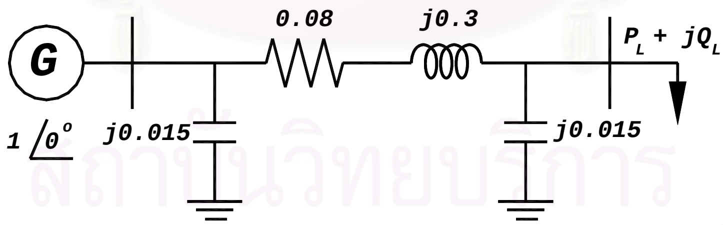

Figure 5.5 A two-bus tested system

The demand is assumed to increase from the current operating to the collapsing point with a constant ratio of reactive to active power equal to 0.5 at 100 MVA base. The demand at the collapsing point, 0.869798 p.u., is obtained from (5.17). Additionally, the margin in the direction of any interested power factor, and the minimum margin can be calculated based on the procedure described in section 5.3. As a result, the margins in the specified direction of various power factors including the minimum margin and its associated power factor are calculated as shown in Table 5.1 and Fig. 5.6 respectively.

Table 5.1 The results of a 2-bus system

Load Level	Demand (p.u.)	Margin in the direction of specified power factors (p.u.)							Minimum margin	
		1	0.9	0.8	0.7	0.6	0.5	0	(p.u.)	P.F
1	0	1.285061	0.978046	0.905438	0.864608	0.839025	0.822853	0.822855	0.808835	0.258950
2	0.20	1.005039	0.753164	0.698775	0.670714	0.655323	0.647869	0.683748	0.646141	0.417571
3	0.40	0.717492	0.528277	0.491165	0.473745	0.465840	0.464026	0.517295	0.463979	0.660927
4	0.60	0.420563	0.303385	0.282651	0.273888	0.270937	0.271805	0.320424	0.270839	0.576563
5	0.70	0.267767	0.190937	0.178067	0.172929	0.171556	0.172692	0.209457	0.171556	0.600076
6	0.75	0.190093	0.134713	0.125694	0.122201	0.121400	0.122408	0.150616	0.121391	0.610445
7	0.80	0.111478	0.078488	0.073270	0.071310	0.070940	0.071647	0.089442	0.070919	0.620032
8	0.85	0.031838	0.022263	0.020793	0.020258	0.020181	0.020414	0.025859	0.020167	0.628923
9	0.869798	0	0	0	0	0	0	0	0	-

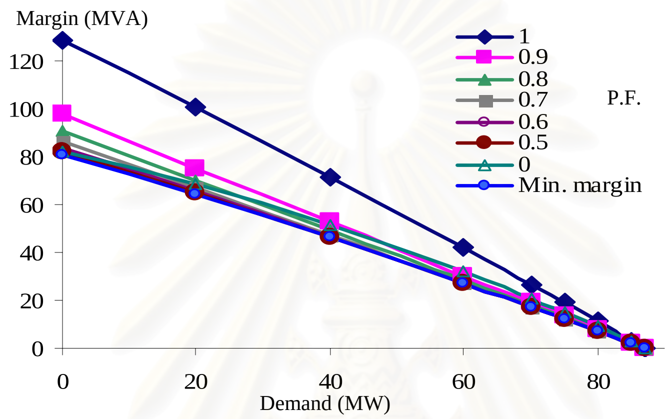

Figure 5.6 The margin in the direction of various P.F. and a minimum margin

5.6.1.2 A Modified 6-bus System

The proposed method is also tested with the same system used in Chapter 4, a modified 6-bus system. However, the initial operating point is different. All the required bus and line data are provided in the Appendix A.

The results of the margins in the direction of gradient vector and the minimum margin as described in section 5.3 are shown in Tables 5.2 and 5.3 respectively.

Table 5.2 The margin in the direction of gradient vector

Line No.	Connecting bus –	bus	Margin (MVA) at Various % of base-case Loading											
			100	110	120	130	140	150	160	170	180	190	200	200.21
1	1	2	221.83	221.55	221.23	220.86	220.43	219.90	219.27	218.46	217.39	215.79	211.64	210.86
2	1	4	68.23	61.29	54.36	47.46	40.57	33.70	26.86	20.04	13.27	6.57	1242.20	0.03
3	1	5	48.35	44.07	39.82	35.59	31.39	27.22	23.09	19.00	14.96	11.03	315.57	219.88
4	2	3	186.95	185.36	183.56	181.50	179.12	176.34	173.03	168.96	163.72	156.23	138.08	134.84
5	2	4	127.40	114.46	101.53	88.62	75.72	62.84	49.99	37.17	24.42	11.81	0.06	0.13
6	2	5	48.14	43.87	39.61	35.36	31.12	26.87	22.62	18.35	14.03	9.62	861.40	476.70
7	2	6	91.75	88.02	84.66	81.80	79.63	78.40	2772.80	1326.90	743.34	452.01	248.66	232.88
8	3	5	57.15	52.11	47.04	41.92	36.76	31.55	26.29	20.96	15.51	9.83	2.39	1.58
9	3	6	227.09	218.61	209.97	201.16	192.14	182.87	173.28	163.33	152.79	141.39	129.73	130.50
10	4	5	54.48	52.35	50.01	47.44	44.60	41.45	37.90	33.84	29.01	22.86	11.60	10.10
11	6	5	60.95	57.48	53.90	50.20	46.34	42.30	38.04	33.48	28.49	22.74	14.02	13.13

Table 5.3 The minimum margin

Line No.	Connecting bus	– bus	Minimum Margin (MVA) at Various % of base-case Loading											
			100	110	120	130	140	150	160	170	180	190	200	200.21
1	1	2	111.11	111.10	111.08	111.06	111.03	110.99	110.93	110.84	111.07	110.42	109.43	109.20
2	1	4	63.43	57.22	50.97	44.69	38.38	32.05	25.69	19.31	12.90	6.48	0.10	0.00
3	1	5	46.08	42.34	38.57	34.76	30.91	27.01	23.05	18.99	14.77	10.22	3.95	3.32
4	2	3	95.91	95.50	94.95	94.23	93.28	92.04	90.38	88.13	85.36	79.96	66.77	64.33
5	2	4	116.82	105.20	93.51	81.76	69.96	58.11	46.24	34.37	22.52	10.79	0.03	0.12
6	2	5	45.23	41.50	37.74	33.94	30.10	26.21	22.26	18.22	14.03	9.54	3.45	2.86
7	2	6	90.72	87.71	84.65	81.53	78.33	75.04	71.60	67.97	64.03	59.35	51.24	50.11
8	3	5	47.79	43.28	38.71	34.09	29.43	24.72	19.98	15.22	10.43	5.62	0.48	0.20
9	3	6	184.83	177.44	169.80	161.88	153.64	145.02	135.91	126.16	115.57	102.80	81.61	78.89
10	4	5	39.87	38.13	36.31	34.39	32.35	30.17	27.79	25.15	22.19	18.24	10.60	9.40
11	6	5	53.36	50.31	47.15	43.86	40.41	36.78	32.92	28.76	24.19	18.78	10.07	9.03

The simulation is performed by increasing generation and demand at various percentage of their base-case until reaching the collapsing point, known from the divergence of power flow solution. Transmission line loss is compensated by slack bus generation. For simplicity, the generation *P* and *Q* limits are neglected. The results show that the demand at the collapsing point is 200.21 % of the base-case.

The results from Tables 5.2 and 5.3 clearly show that bus–*4* is the weakest bus since some lines e.g., lines No. 2 and 5 hit voltage stability limit before the others. In a normal state, the margin in a direction of gradient vector and the minimum loading margin vary accordingly. However, in the heavy load condition, the direction of gradient vectors may not be calculated accurately. Consequently, line loading margin may fluctuate as shown in Table 5.2 and Fig. 5.7. Therefore, the minimum loading margin should be used instead. The margin of the lines connected to bus–*4* in the direction of the gradient vector and the minimum margin are depicted in Fig. 5.7 and 5.8 respectively.

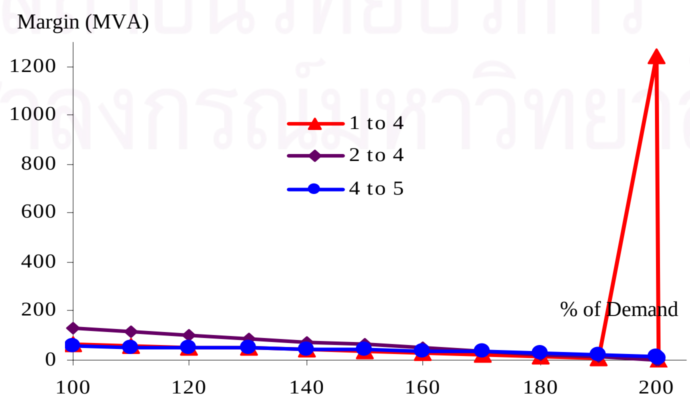

Figure 5.7 The transmission line loading margin in the direction of gradient vector

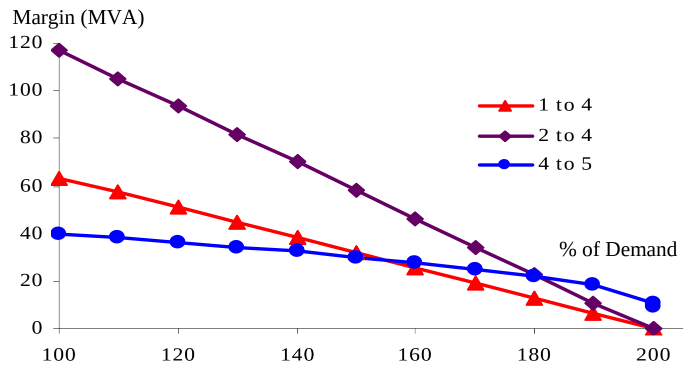

Figure 5.8 The minimum margin of transmission line connected to *bus-4*

5.6.2 Transmission Line Performance Indices Evaluation

The same operating point of section 5.5.1 is used to obtain the transmission line performance indices defined in section 5.4.3. Accordingly, the line loading index and the line severity index defined by (5.33) and (5.34) are shown in Tables 5.4 and 5.5 respectively.

Table 5.4 The line loading index

Line No.	Connecting bus –	bus	Line loading Index at % of base - case Loading											
			100	110	120	130	140	150	160	170	180	190	200	200.21
1	1	2	0.9882	0.9857	0.9829	0.9796	0.9758	0.9712	0.9657	0.9588	0.9496	0.9361	0.9018	0.8956
2	1	4	0.4982	0.4480	0.3978	0.3476	0.2974	0.2474	0.1974	0.1475	0.0978	0.0485	1.0363	0.0002
3	1	5	0.5435	0.4974	0.4513	0.4052	0.3591	0.3129	0.2668	0.2208	0.1750	0.1300	1.0488	1.0123
4	2	3	0.9173	0.9025	0.8859	0.8674	0.8464	0.8224	0.7947	0.7618	0.7211	0.6661	0.5465	0.5269
5	2	4	0.4966	0.4460	0.3956	0.3452	0.2948	0.2446	0.1945	0.1446	0.0949	0.0459	0.0002	0.0005
6	2	5	0.5416	0.4950	0.4483	0.4015	0.3545	0.3072	0.2596	0.2115	0.1625	0.1122	1.0416	1.0456
7	2	6	0.7494	0.7263	0.7051	0.6867	0.6721	0.6628	1.0129	1.0255	1.0412	1.0590	1.0894	1.0948
8	3	5	0.5154	0.4672	0.4191	0.3712	0.3233	0.2755	0.2278	0.1801	0.1320	0.0826	0.0196	0.0129
9	3	6	0.7123	0.6820	0.6512	0.6200	0.5882	0.5556	0.5220	0.4871	0.4500	0.4092	0.3571	0.3549
10	4	5	0.9306	0.9197	0.9070	0.8922	0.8746	0.8533	0.8268	0.7923	0.7440	0.6669	0.4466	0.4044
11	6	5	0.7386	0.7056	0.6706	0.6334	0.5936	0.5505	0.5036	0.4516	0.3924	0.3210	0.2051	0.1927

Table 5.5 The line severity Index

Line No.	Connecting bus –	bus	Line Severity Index at % of base - case Loading											
			100	110	120	130	140	150	160	170	180	190	200	200.21
1	1	2	0.0058	0.0060	0.0064	0.0069	0.0076	0.0086	0.0100	0.0122	0.0160	0.0250	0.2176	6.3104
2	1	4	0.2469	0.2492	0.2569	0.2708	0.2932	0.3281	0.3840	0.4823	0.6828	1.2878	0.0087	10772.7
3	1	5	0.2031	0.2017	0.2040	0.2103	0.2216	0.2397	0.2681	0.3158	0.4035	0.6180	0.1291	5.3836
4	2	3	0.0394	0.0410	0.0433	0.0465	0.0508	0.0568	0.0654	0.0791	0.1032	0.1599	1.4395	42.380
5	2	4	0.2518	0.2547	0.2631	0.2781	0.3020	0.3393	0.3990	0.5046	0.7224	1.3959	186.64	2513.8
6	2	5	0.2073	0.2062	0.2089	0.2158	0.2279	0.2470	0.2771	0.3274	0.4202	0.6477	0.0330	1.6854
7	2	6	0.0817	0.0777	0.0751	0.0737	0.0736	0.0752	0.0022	0.0053	0.0116	0.0287	0.4586	14.387
8	3	5	0.2465	0.2491	0.2569	0.2707	0.2925	0.3261	0.3790	0.4697	0.6475	1.1418	22.061	903.87
9	3	6	0.1102	0.1069	0.1051	0.1050	0.1065	0.1100	0.1162	0.1273	0.1475	0.1945	1.1551	31.222
10	4	5	0.0238	0.0240	0.0247	0.0259	0.0277	0.0303	0.0343	0.0412	0.0542	0.0891	1.3247	45.386
11	6	5	0.0966	0.0960	0.0970	0.0998	0.1048	0.1127	0.1249	0.1451	0.1809	0.2646	1.9784	55.386

As lines No. 2 and 5 hit voltage stability limit before the others. Similar results are also shown in Table 5.4 for line loading index, which are 0.0002 and 0.0005. For more details, line No. 2 is in a more severe condition than line No. 5, seen from severity index of both lines, i.e. 10772.7 and 2513.8 respectively. For the lines connecting between generator buses, i.e. lines No. 1 and 4 are safe from hitting voltage stability limit even in a heavy load condition. However, the security margin of some particular lines may increase rapidly, at proximity to the collapsing point due to direction of the gradient vector cannot be calculated precisely. As discussed earlier in section 5.5.1, the line loading margin in the direction of the gradient vector alone is not suitable to evaluate the capability of line loading. However, this effect has less impact on line loading and line severity indices. As a result, line No.2 and 5 should be considered first to enhance system loadability.

5.7 Application for On-line Monitoring

The voltage security margin assessment has already been included in the present Energy Management System (EMS). The developed methodology can be implemented in an on-line mode. The collapsing surface which presents the relationship among P and Q of the receiving end bus versus various sending end voltage magnitude can be calculated using (5.12) and shown in Fig. 5.9. This surface can be calculated beforehand for each line using its parameters and can be applied for on-line monitoring.

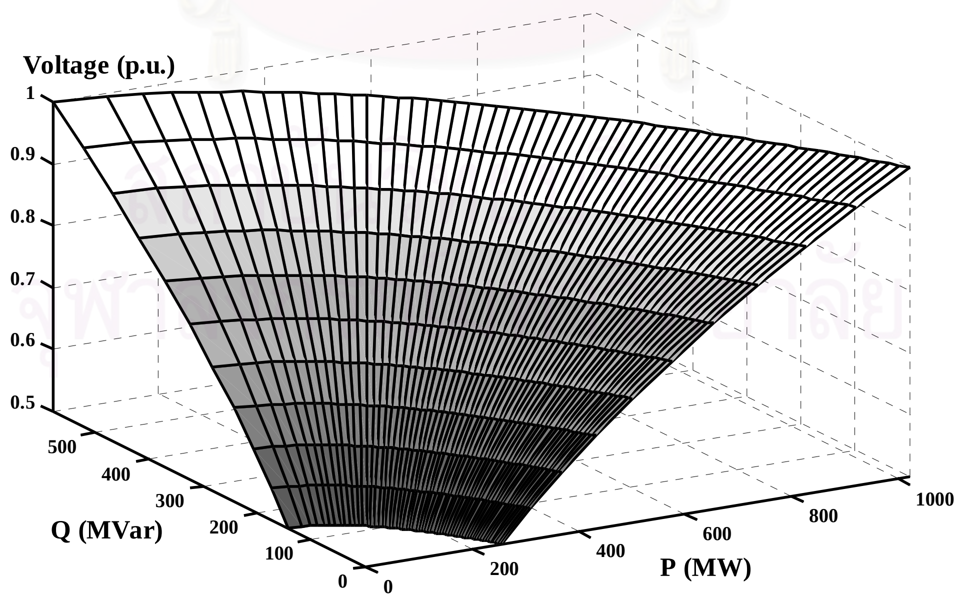

Figure 5.9 Collapsing surface for an interested line

Using the results of the 6-bus system, the minimum margin of all lines as shown in Table 5.3 are illustrated along with their loading trajectory in figures 5.10-5.20. We conduct analysis according to types of bus connected at line ends, i.e. PV to PV, PV to load, and load to load buses. The symbols □ and ○ in the figures represent operating points and their associated collapsing points of the minimum margin respectively.

The results of the line connected between PV to PV buses, i.e. lines No. 1 and 4 are far from voltage collapse as shown in Fig. 5.10 and Fig. 5.11 respectively.

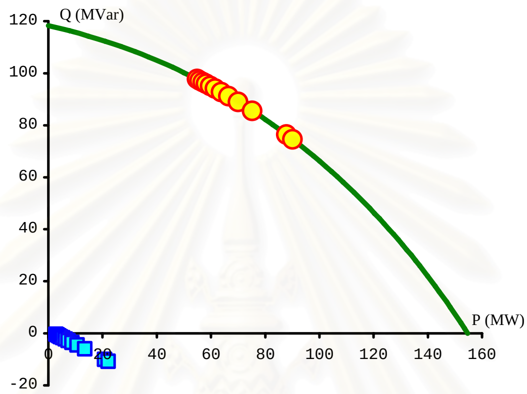

Figure 5.10 Trajectory of operating and collapsing points of line No.1

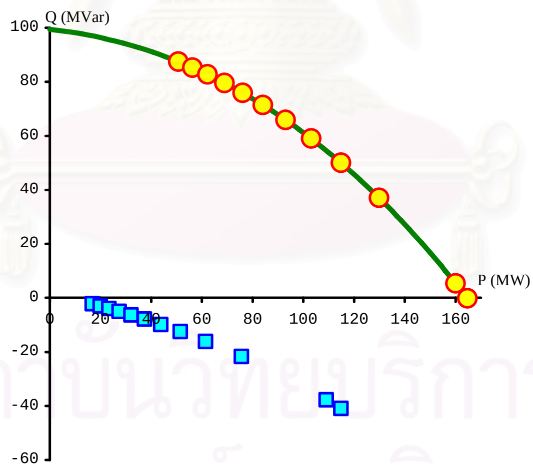

Figure 5.11 Trajectory of operating and collapsing points of line No.4

For the lines connected between PV to load buses, i.e. lines No. 1, 2 and 5-9, we find that lines No. 2 and 5 which are connected to bus-4 are approaching toward voltage stability limit as shown in Fig. 5.12 and 5.14 respectively. Lines connected to bus-5, i.e. lines No. 3, 6 and 8 are also close to the voltage stability limit as shown in Fig. 5.13, 5.15 and 5.17 respectively. In contrast, lines connected to bus-6, i.e. lines No. 7 and 9 still have margin at the collapsing point as shown in Fig. 16 and 18 respectively.

สถาบันวิทยบริการ
จุฬาลงกรณ์มหาวิทยาลัย

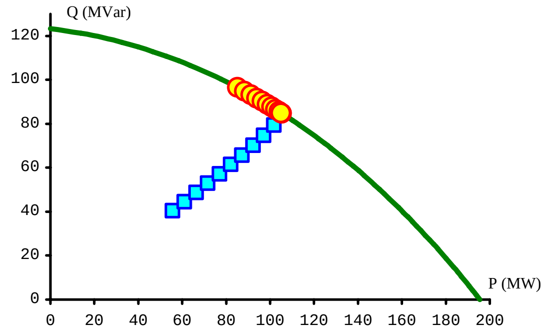

Figure 5.12 Trajectory of operating and collapsing points of line No.2

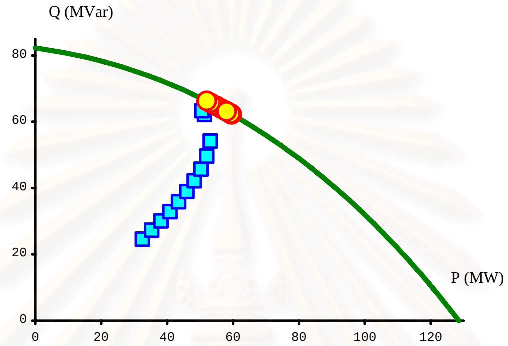

Figure 5.13 Trajectory of operating and collapsing points of line No.3

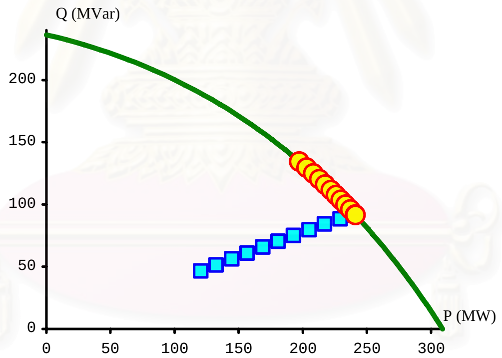

Figure 5.14 Trajectory of operating and collapsing points of line No.5

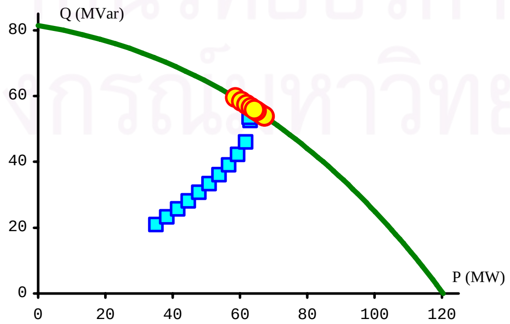

Figure 5.15 Trajectory of operating and collapsing points of line No.6

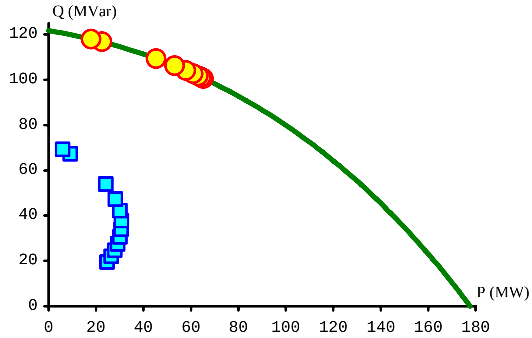

Figure 16 Trajectory of operating and collapsing points of line No.7

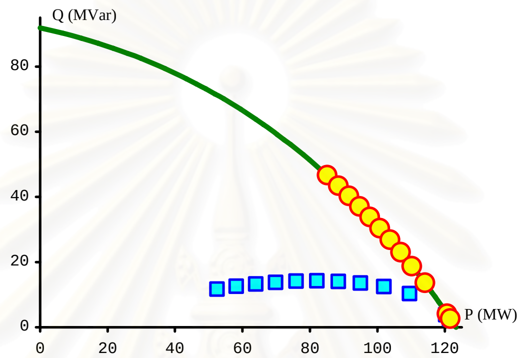

Figure 17 Trajectory of operating and collapsing points of line No.8

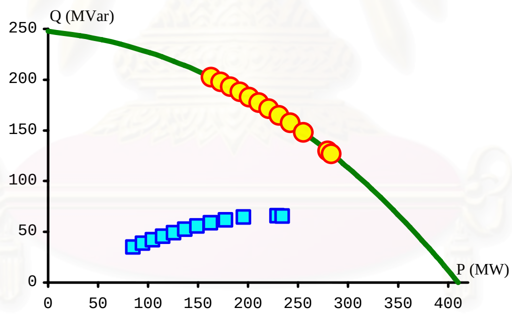

Figure 18 Trajectory of operating and collapsing points of line No.9

For the lines connected between load to load buses, i.e. lines No. 10 and 11, we investigate that it does not hit voltage stability limit. It should be noted that these P-Q curves are not fixed but varied according to the change of its sending end voltage for each loading step as shown for examples in Fig. 5.19 and 5.20 respectively.

It should be noted that, if the sending end bus voltage is not constant, e.g. line No. 10, its P-Q curves can be varied according to the change of sending end voltage magnitude. Consequently, if the sending end voltage magnitude is decreased, the curve in Fig. 5.9 is shrunk along the trajectory. Moreover, this situation can be found in a PV-bus whose voltage magnitude cannot be regulated at a specified value.

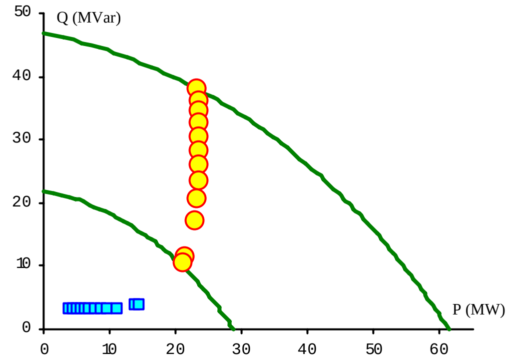

Figure 5.19 Trajectory of operating and collapsing points of line No.10

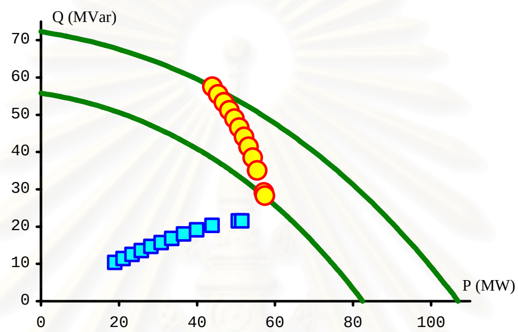

Figure 5.20 Trajectory of operating and collapsing points of line No.11

5.8 Conclusion

In this chapter, the loading margin in a specified direction and the minimum loading margin of each transmission line respected to voltage stability constraints are evaluated first using a static voltage stability criterion. The proposed method provides information concerning loading capability of each line, which can be used as an index to detect voltage collapse phenomenon. In a normal state, the margin in the direction of the gradient vector may be used appropriately due to the system controllability. In a heavy load or emergency situation, one cannot predict the system condition precisely. In such case, the minimum loading margin should be replaced to cope with various uncertainties. The proposed method can be applied for on-line voltage security assessment. In addition, performance indices of a transmission line i.e., line security margin, line loading and line severity indices are defined and can be computed from the calculation process of maximum loading capability of power system with slightly modification from the traditional methods. These indices can be used for transmission planning purposes.

CHAPTER 6

CONGESTION MANAGEMENT IN BILATERAL MARKETS

6.1 Introduction

A bilateral based market is preferable in many countries which are in the privatization or deregulation process, e.g. England & Wales, Vietnam, and Thailand. The New Electricity Trading Arrangements (NETA) proposed for England & Wales has been designed to overcome various problems found in the pool-based markets. In NETA, transaction is dominated by bilateral contracts between generation and demand. Intervention is only allowed to some situations, e.g. emergency and congestion conditions. In other word, the SO in bilateral markets is the MicroSO as described in Chapter 1. Consequently, congestion management methodology in bilateral markets is necessary to manage the amount of power flow especially in case of having high volume of bilateral contracts.

Congestion Management (CM) procedure for bilateral markets proposed in this dissertation is divided into two main parts, i.e. congestion relief and congestion cost allocation. The congestion relief is a procedure of utilizing existing means to alleviate the overloaded line. There are several objective functions adopted for transactions in bilateral markets. The North American Electricity Reliability Council (NERC) proposes a Transmission Loading Relief (TLR) procedure [93], [94] for bilateral transaction curtailment. However, it is argued by [95], [96] that strictly curtailing according to that rule leads to an unnecessary curtailment and cannot provide a correct signal to participants. Other objective functions proposed in [97], [98] is to minimize the least square amount of power deviated from the preferred schedule. In [99], a dispatching methodology based on contingency constrained with a minimum number of adjustments in preferred schedules is proposed. In this dissertation, the objective function of minimizing the congestion re-scheduling cost is used [100], [101]. With this objective, real and reactive power costs in association with MVA transmission line thermal mode are taken into account. Accordingly, it can satisfy all participants with minimum cost incurred. Additionally, the market signal can be sent through contribution of utilizing transmission system in a congestion cost allocation procedure [122]. The congestion cost allocation is defined as a methodology of allocating additional cost from the former procedure to participants in a non-discrimination manner. A transmission usage index called Power Transfer Distribution Factor (PTDF) is adopted in this regard [103]- [107].

Theoretically, constraints limiting transfer capability of a transmission line are conductor thermal, steady state stability, and voltage stability limits [62]. Normally, thermal limit is the most common constraints [100] dominated within zonal network. It is generally controlled through line flows, which can be represented in MW or MVA. The main distinctions between these two models are the complexity/simplicity and correct signals. If one uses the MW model, only real power flow is considered. This may send a wrong signal to the SO in case of heavy reactive power flow since conductor temperature depends on MVA rather than only MW flow [63] – [65]. The MVA based model is an interesting issue to solve congestion problem especially for the system whose reactive resource distributed throughout the network. However, this method should be performed while system security is still maintained.

This chapter emphasizes on congestion management problem in bilateral markets. In addition to real power re-dispatching and interruptible load shedding, this dissertation also takes into account ancillary services, i.e. reactive power and emergency startup units, by treating them as alternative means to relief the congested lines. It is the fact that a bilateral contract is normally made in a long-term basis, whereas the congestion management reflects short-term operation. The entities who offer such means to relief the congestion will receive reimbursement based on their willingness to accept price. The requested real power re-scheduling from committed or non-committed units is paid by its defined price. The price of capacitor utilization and interruptible load is generally offered as a flat rate per MVar and MW respectively. The problem is then solved by a Linear Programming (LP) associated with sensitivity factors. The simulation results are presented in section 6.6.

6.2 Framework for Congestion Management in Bilateral Markets

Transaction under bilateral contracts can be defined as selling/buying of electric energy between each pair of generation and demand for any specified time intervals [80], [81] and can be represented by (6.1).

$$\left[T^m\right]=\left[P^m,G_i^m,L_j^m\right] \tag{6.1}$$

where

$\left[T^m\right]$ is a transaction vector of bilateral contracts defined by vectors *P, G* and *L,*

P^m is a row vector of amount of contracted generation power,

G_i^m is a row vector of generation unit located at *bus-i,* and

L_j^m is a row vector of demand located at bus-j.

Superscript *m* represents the order of a transaction vector. The proposed overall framework and a congestion management methodology can be shown in Fig. 6.1, of which its details will be presented in section 6.5 respectively.

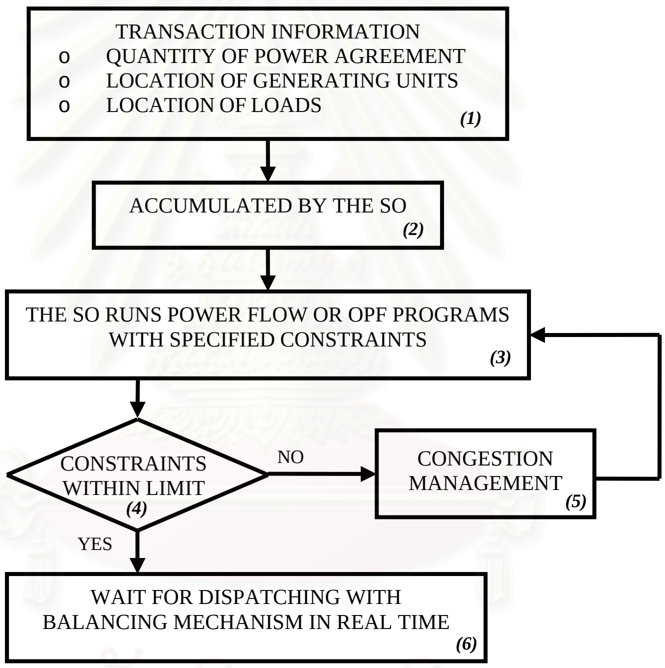

Figure 6.1 Flowchart of the proposed framework

The transaction vector is accumulated by the SO before the gate of each time interval is closed. Then the SO performs transaction feasibility study using power flow or OPF tools. In case of no congestion exists, the preferred transaction is feasible. Accordingly, intervention is not needed, leaving for only dispatching and balancing in real time. In the presence of congestion, however, the preferred transaction is infeasible and the SO has to manage congestion, which consists of two main procedures. Firstly, the SO employs existing means, e.g. generation re-scheduling, load shedding to relief congestion. Secondly, additional cost incurred from the first stage must be allocated in a justified manner to all contributors. Regarding the transmission loss allocation method, it is relaxed in this chapter. The revised transaction cannot specify the source and sink nodes as described in Chapter 4.

6.3 Transmission Line Thermal Limit Model [63] – [65]

6.3.1 Transmission Line Thermal Limit

Thermal limit is the most common constraint that limits the power transfer capability through a transmission line. Operating beyond the thermal limit can lead to unacceptable sag between the two supporting towers. The sag depends mainly on conductor's temperature and tension. The conductor temperature relies on two modes of heat transfer, i.e. heat absorption and dissipation. The heat absorption is the heat transfer mode that can increase the conductor temperature, i.e. transmission real power loss (I^2R) and solar energy, while the mode of heat dissipation, i.e. convection and radiation, would reduce the conductor temperature. In addition, these environmental parameters in association with conductor tension, stressed during construction, cannot be controlled, whereas only the apparent power flow is a controllable variable depending on operating condition which is easy to monitor.

6.3.2 MVA Thermal Limit Model

In general calculation, the amount of current, real power, or apparent power flowing through line rather than conductor temperature is used for thermal limit consideration. However, the MVA flow will be used in this paper since the MVA thermal constraint on π model of transmission line as shown in Fig. 6.2 can be expressed in (6.2) and (6.3).

$$P_{ij}^2 + Q_{ij}^2 \leq S_{ij}^2 \tag{6.2}$$

$$P_{ji}^2 + Q_{ji}^2 \leq S_{ij}^2 \tag{6.3}$$

where P_{ij}, Q_{ij} and P_{ji}, Q_{ji} are the real and reactive power flowing from *bus-i* $\rightarrow j$ and *bus-j* $\rightarrow i$ respectively. S_{ij} is the apparent power flow, which is represented as thermal limit of this line in MVA.

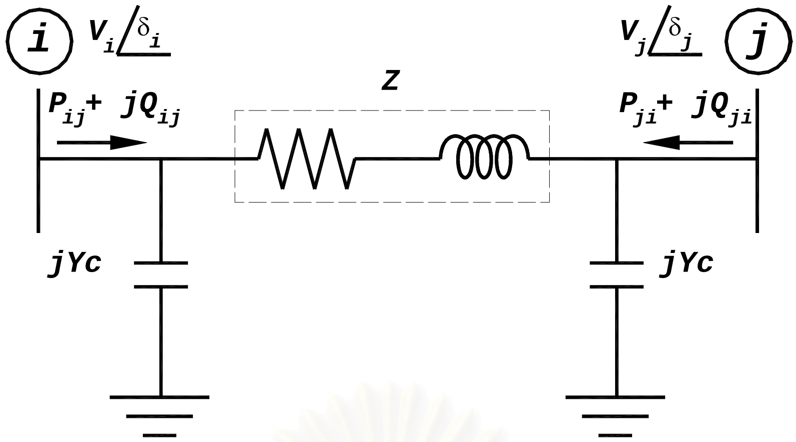

Figure 6.2 The π model transmission line connected between *bus-i* and *bus-j*

The terms P_{ij}, P_{ji}, Q_{ij} and Q_{ji} can be written as (6.4)-(6.7).

$$P_{ij} = V_i V_j Y_{ij} \cos\left(\theta_{ij} - \delta_i + \delta_j\right) - V_i^2 Y_{ij} \cos\theta_{ij} \tag{6.4}$$

$$P_{ji} = V_i V_j Y_{ij} \cos\left(\theta_{ij} + \delta_i - \delta_j\right) - V_j^2 Y_{ij} \cos\theta_{ij} \tag{6.5}$$

$$Q_{ij} = V_i^2 Y_{ij} \sin\theta_{ij} - V_i^2 Y_c - V_i V_j Y_{ij} \sin\left(\theta_{ij} - \delta_i + \delta_j\right) \tag{6.6}$$

$$Q_{ji} = V_j^2 Y_{ij} \sin\theta_{ij} - V_j^2 Y_c - V_i V_j Y_{ij} \sin\left(\theta_{ij} + \delta_i - \delta_j\right) \tag{6.7}$$

where V_i, δ_i and V_j, δ_j are the voltage magnitude and angle at *bus-i* and *bus-j* respectively. Y_{ij} and θ_{ij} are the magnitude and angle of elements of bus-admittance matrix at row-*i* and column-*j*, and Y_c is a half of line charging admittance of the line connected between *bus-i* and *bus-j* .

For simplicity, only the sending end apparent power is considered due to the reason that in case of congestion the sending end always hits the limit before the receiving end as described in Chapter 5.

6.4 Congestion Relief Cost

The preferred transaction reveals the amount of power of each transaction expected to be dispatched in real time. In case the SO dispatches away from its preferred transaction, the owner of the requested transaction should have the right to receive reimbursement, according to all the concerned costs which can be described below.

6.4.1 Cost of Generation Re-dispatching

In this dissertation, the offered price of generation is assumed to be a quadratic function. This is a willingness to accept price in case of it is requested to increase its generation from the preferred value. On the other hand, if it is requested to decrease its generation, it will receive only the opportunity loss to make profit, which can be presented in percentage of the offered price [108]. To avoid generation gaming from receiving the reimbursement by over proposing, the SO has to verify the preferred transaction based on historical data of its forecasted load. To use the generation offer price with the Linear Programming Method, it must be revised in piecewise linear form as described in Appendix E.

6.4.2 Cost of Emergency Generating Units

For some situation, it is more economical to re-commit some generating units into the system [108]. These units are identified as ancillary services units, which can provide generation power within a short time. In general, costs of these ancillary services unit are composed of fuel cost and start up costs. For simplicity, both costs may be included in the willingness to accept price, which has the same characteristics with the offering price of those committed generations.

6.4.3 Cost of Reactive Power Sources

The reactive power sources considered in this paper are from synchronous generators and capacitors. There are some reasons encouraging trading reactive power from synchronous machines on a long term contract, which can be listed as below [109], [110].

- The lower production cost of reactive power compared to its real power.
- The difficulty of separating an excitation system from the whole machine parts.
- The continuous control nature of automatic voltage regulator (AVR).

Accordingly, the cost of reactive power injected from the synchronous machine may be neglected in an optimization problem even in congestion situation. In contrast, the costs of adjusting discrete control device, e.g. capacitor and on-load tap changer (OLTC), are of differences. The separation of investment cost and its expected life are incentives for short term procurement [111]. However, the cost of utilizing OLTC is not considered in this dissertation because, in general, the control signal to relief the congestion must be centralized, which generally excludes the OLTC switching. Therefore, it is left under local operator responsibility. Although, the exact cost of utilizing reactive resources can be calculated theoretically by taking various parameters into account i.e., investment, operation and maintenance cost, expected life, annual revenue return rate etc. However, these factors have a high degree of uncertainty. Consequently, in practice, it is offered by a fixed price per MVar.

6.4.4 Cost of Shedding Interruptible Load

The curtailment of interruptible load provides a flexible mean to relief congestion [112], [113]. It should be noted that, although we have a transaction contract made between a specified source and sink. However, curtailment can be performed by shedding only on the demand side. This is difference from a strictly curtailed power from both sides of a transaction as proposed by NERC in a TLR procedure [93], [94]. For selected interruptible loads it will receive reimbursement according to their willingness to accept price to allow for curtailment. The obtained result may satisfy all participants because it avoids a great amount of curtailment. In addition, it releases burden of the SO to re-arrange the trade [95].

6.5 Congestion Management Procedure

The congestion management can be categorized into congestion relief and congestion cost allocation procedures as described below.

6.5.1 Minimizing Congestion Relief Cost

In our proposed methodology, both real and reactive powers are taken into account. It is formulated in such a way that the congestion relief cost is minimized and all specified constraints are satisfied as follows:

$$Minimize \qquad [f]^T[X]$$

$$= \sum_{i\in G,S} C_{G_i}.\Delta P_{G_i} + \sum_{i\in L} C_{L_i}.\Delta P_{L_i} + \sum_{i\in R} C_{R_i}.\Delta Q_{R_i} \tag{6.8}$$

subject to

$$P_{sch_i} = \sum_{j=1}^{N} P_{ij} \tag{6.8a}$$

$$Q_{sch_i} = \sum_{j=1}^{N} Q_{ij} \tag{6.8b}$$

$$S_{ij}^{0} + \Delta S_{ij} \le S_{ij}^{max} \tag{6.8c}$$

$$\sum_{i \in G} \Delta P_{G_i} + \sum_{i \in L} \Delta P_{L_i} + \Delta P_{G_S} = 0 \tag{6.8d}$$

$$P_{G_i}^{min} \le P_{G_i}^{0} + \Delta P_{G_i} \le P_{G_i}^{max} \tag{6.8e}$$

$$Q_{G_i}^{min} \le Q_{G_i}^{0} + \Delta Q_{G_i} \le Q_{G_i}^{max} \tag{6.8f}$$

$$Q_{R_m}^{min} \le Q_{R_m}^{0} + \Delta Q_{R_m} \le Q_{R_m}^{max} \tag{6.8g}$$

$$V_{L}^{min} \le V_{L}^{0} + \Delta V_{L} \le V_{L}^{max} \tag{6.8h}$$

where

$[f]$ is a vector of willingness to accept prices of available means,

$[X]$ is a row vector of available means,

C_{G_i} is willingness to accept price of generation at *bus-i*,

C_{L_i} is willingness to accept to allow curtailment price of interruptible load at *bus-i*,

C_{R_i} is reactive power price of capacitor at *bus-i*,

ΔP_{G_i} is the change of generation at *bus-i*,

ΔP_{L_i} is the amount of load curtailment at *bus-i*,

ΔQ_{R_i} is the change of reactive power capacitor at *bus-i*,

ΔV_L is the change of voltage magnitude at load bus.

Subscripts *G*, *L* and *R* represent generation, load and reactive reserve buses respectively, where *N* represents the number of buses. The superscripts *0*, *min* and *max* represent current status, minimum and maximum values of available means respectively. The objective function of (6.8) is to minimize the congestion relief cost of available control variables/means as described in section 6.4. Equality constrains of (6.8a) and (6.8b) are nodal power flow balance of real and reactive power respectively. Inequality constraint of (6.8c) is an MVA line flow limit, whereas (6.8d) is necessary to activate the generation willingness to accept price of a slack bus. Inequalities (6.8e)-(6.8g) are traditionally included as acceptable capability limit of control apparatus, whereas voltage magnitude limit is reflected in (6.8h). Handling these constraints in LP has to employ sensitivity analysis, which is formulated in the Appendix B and D.

6.5.2 The Traditional Methods

The proposed transmission line thermal model is compared with two traditional models, which can be described below.

- Thermal limit is a MW power flow model. Thus, the effect of reactive power is neglected in re-scheduled process. We define this model as "MW model". Optimization problem in this model can be formulated in 6.5.2.1.
- Thermal limit is a MVA power flow model. However, reactive power is also neglected in re-scheduled process. We define this model as "MVA model". Optimization problem in this model can be formulated in 6.5.2.2.

6.5.2.1 The MW model

The MW model and its associated constraints can be expressed as follows:

$$Minimize \quad [f]^T [X]$$

$$= \sum_{i \in G,S} C_{G_i} . \Delta P_{G_i} + \sum_{i \in L} C_{L_i} . \Delta P_{L_i} \tag{6.9}$$

subject to

$$P_{sch_i} = \sum_{j=1}^{N} P_{ij} \tag{6.9a}$$

$$Q_{sch_i} = \sum_{j=1}^{N} Q_{ij} \tag{6.9b}$$

$$P_{ij}^{0} + \Delta P_{ij} \le P_{ij}^{max} \tag{6.9c}$$

$$\sum_{i \in G} \Delta P_{G_i} + \sum_{i \in L} \Delta P_{L_i} + \Delta P_{G_S} = 0 \tag{6.9d}$$

$$P_{G_i}^{min} \le P_{G_i}^{0} + \Delta P_{G_i} \le P_{G_i}^{max} \tag{6.9e}$$

$$V_L^{min} \le V_L^{0} + \Delta V_L \le V_L^{max} \tag{6.9f}$$

Distinctions between this model and the proposed model, (6.8)-(6.8h), are that the transmission thermal limit is presented in MW rather than MVA and the reactive power re-scheduled is performed in case voltage limit is violated.

6.5.2.2 The MVA model

The MVA model and its associated constraints can be expressed as follows:

$$Minimize \qquad [f]^T [X]$$

$$= \sum_{i \in G,S} C_{G_i}.\Delta P_{G_i} + \sum_{i \in L} C_{L_i}.\Delta P_{L_i} \tag{6.10}$$

subject to

$$P_{sch_i} = \sum_{j=1}^{N} P_{ij} \tag{6.10a}$$

$$Q_{sch_i} = \sum_{j=1}^{N} Q_{ij} \tag{6.10b}$$

$$S_{ij}^{0} + \Delta S_{ij} \le S_{ij}^{max} \tag{6.10c}$$

$$\sum_{i \in G} \Delta P_{G_i} + \sum_{i \in L} \Delta P_{L_i} + \Delta P_{G_S} = 0 \tag{6.10d}$$

$$P_{G_i}^{min} \le P_{G_i}^{0} + \Delta P_{G_i} \le P_{G_i}^{max} \tag{6.10e}$$

$$V_L^{min} \le V_L^{0} + \Delta V_L \le V_L^{max} \tag{6.10f}$$

The difference between this and the proposed models, (6.8)-(6.8h), is that the transmission line thermal limits is still presented in MVA, however problem of reactive power re-scheduling is adopted in case voltage limit is violated.

6.5.3 Congestion Cost Allocation

In general, we may say that congestion cost occurred from re-scheduling must be allocated fairly to all participants who have contribution to the flow excess beyond the thermal limit of congested lines [114]. For each transaction under bilateral markets, only real power is contracted, thereby we consider only the contribution of real power flow to the congested line as an index to distribute the additional cost in such fair sense. Although, reactive power is a part of the apparent power flow through a line, however its great valuation is mainly to maintain system security and voltage profiles. In addition reactive power is a local area problem, since it cannot be transmitted far from its injected source. The context of evaluating security cost in such aspect is an important issue debated under competitive environment so that implementation in a real system must be done carefully to avoid the reactive power gaming [130]. However, long term pricing, which reflects the capital cost as mentioned in section 6.4 is suitable for the consideration to convince the investor.

6.6 Numerical Results

The proposed method is tested with a 6-bus system as shown in Fig. 6.3 [2].

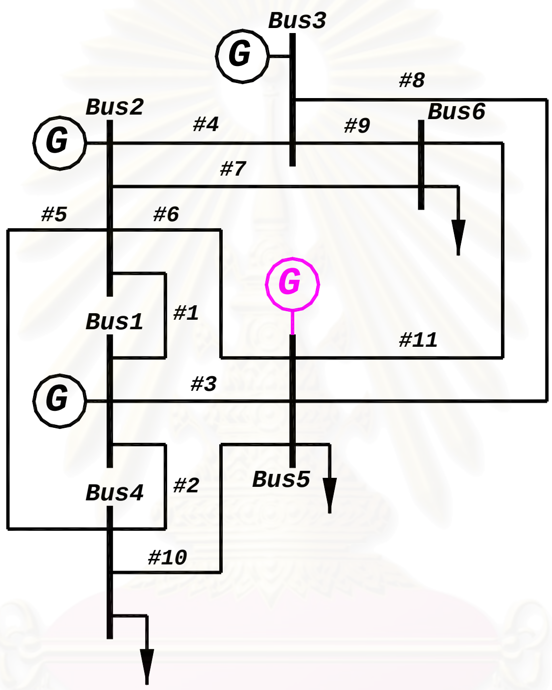

Figure 6.3 Network topology of a 6-bus system

In this system, buses 1, 2 and 3 are generator buses, whereas buses 4, 5 and 6 are load buses. In addition, bus 5 has a generation, which is not committed in the based case. All the required bus and line data are provided in the Appendix A.

The simulation is conducted in two cases to test the proposed method, i.e.

- line No. 2 connected between bus No. 1 and 4 is tripped, and
- lines No. 1, 6, 10 and 11 are tripped.

To relief the congestion, costs of various utilizing means, i.e. generation re-dispatch, interruptible loads and reactive power reserve costs are shown in Table 6.1. The means No. 1-4 are generation bidding prices; No. 1-3 are submitted in a quadratic format and No. 4 is a flat rate price of de-committed generating unit of bus 5. The interruptible load of buses 4-6 are means No. 5-7 respectively, which submit as flat rate prices. The means No. 8-10 are reactive power reserve from capacitor-bank of all load buses. In addition, their operating limits can be shown in Table 6.2.

Table 6.1 Costs of various utilized means

No.	Type	Costs (1000 Baht/(MW or MVar))
1	C_{G_1}	$213.1+11.669P_{G_1}+0.00533P_{G_1}^{\ 2}$
2	C_{G_2}	$200.0+10.333P_{G_2}+0.00889P_{G_2}^{\ 2}$
3	C_{G_3}	$240.0+10.833P_{G_3}+0.00741P_{G_3}^{\ 2}$
4	C_{G_5}	20
5	C_{L_4}	100
6	C_{L_5}	100
7	C_{L_6}	100
8	C_{R_4}	4
9	C_{R_5}	4
10	C_{R_6}	4

Table 6.2 Operating limit of various utilized means

No.	Type	Operating Limit (MW or MVar)	
		Min	Max
1	P_{G_1}	10	80
2	P_{G_2}	15	90
3	P_{G_3}	20	100
4	P_{G_5}	5	40
5	L_4	0	10
6	L_5	0	20
7	L_6	0	30
8	Q_{R_4}	0	20
9	Q_{R_5}	0	20
10	Q_{R_6}	0	20

We assume that reactive reserve installed at all load buses can continuously supply at a specified MVar value. Detail of the simulation of three cases can be described below.

6.6.1 Line No. 2 is outage

From a defined based case, if the line connected between bus 1 and 4 is tripped the line overloading will take place on the line No. 5, connected between bus 2 and 4, of which the line flow is 50.111 MVA, which is 10.111 MVA above its thermal limit. The power flow results of prior and after contingency are shown in Table 6 3.

Table 6.3 Power flow results of base case and contingency cases

Generation & Line	Based Case		L1-4 is outage	
	P (MW)	Q (MVar)	P (MW)	Q (MVar)
G1	42.734	15.435	43.801	-1.309
G2	50	40.549	50	60.023
G3	60	36.774	60	38.275
L1-2	6.534	-4.244	18.818	-9.929
L1-4	18.812	10.262	-	-
L1-5	17.388	9.418	24.982	8.62
L2-4	25.611	18.307	40.484	29.533
L2-5	12.979	10.063	11.594	11.272
L2-6	19.671	11.116	18.857	11.582
L3-2	1.779	-1.913	2.536	-2.059
L3-5	17.019	8.699	16.242	9.931
L3-6	41.202	29.987	41.223	30.403
L4-5	3.705	-0.303	0.739	-1.857
L5-6	0.003	-3.901	0.794	-4.768

After the proposed method has been executed, it is found that only reactive power re-scheduling can solve the congestion with its associated cost of 79,364 Bht. This is a minimum incurred costs corresponding to utilization of reactive reserve at bus 4 of 19.8409 MVar. The mismatch loss is compensated by generation at bus No.1 and is not included as congestion relief cost. Moreover, it is compared with the traditional method solved according to the objective function with their associated constraints in sections 6.5.2.1 and 6.5.2.2, of MW and MVA models. The power flow results of all models are shown in Table 6.4.

Table 6.4 Power flow results comparison

Generation & Line	Proposed Method		Method in section 6.5.2.1		Method in section 6.5.2.2	
	P (MW)	Q (MVar)	P (MW)	Q (MVar)	P (MW)	Q (MVar)
G1	43.97	8.81	43.77	-1.33	43.28	-1.71
G2	50.00	-20.00	49.45	59.60	41.02	53.30
G3	60.00	90.60	60.00	38.23	60.00	37.47
L1-2	19.30	1.03	18.81	-9.93	18.79	-9.92
L1-4	-	-	-	-	-	-
L1-5	24.67	7.05	24.95	8.59	24.49	8.21
L2-4	39.20	7.94	40.00	29.14	32.61	23.17
L2-5	11.26	2.10	11.56	11.25	11.10	10.91
L2-6	18.46	-5.34	18.48	11.58	18.52	11.54
L3-2	0.19	20.31	2.55	-2.06	2.84	-2.12
L3-5	18.14	19.60	16.22	9.90	15.89	9.49
L3-6	41.67	50.69	41.23	30.38	41.27	30.10
L5-4	1.61	-0.92	0.64	-1.94	0.80	-3.16
L5-6	0.95	-7.01	0.81	-4.75	1.07	-4.47

For the proposed method, it found that the higher the difference between regulated voltage values of bus No. 3 and 2 result in the lower of reactive power flow in the congested line. However, due to voltage constraint of generation bus No. 3, 1.05 p.u., and lower bound limit of reactive power of generation at bus No. 2, -20 MVar, results in the optimal solution of reactive power flow of the congested line 7.94 Mvar as shown in Table 6.4. Consequently, generation at bus No. 3 supplies reactive power of 90.60 MVar and voltage at bus No.2 is regulated at 0.9977 p.u. In the MW and MVA thermal model of section 6.5.2.1 and 6.5.2.2 respectively, load curtailment of 0.548 and 8.979 MW in associated with generation at bus No. 2 are selected to relief the congestion. Accordingly, the congestion relief costs of all cases are shown in Table 6.5.

Table 6.5 Utilized means with their associated relief costs

	Utilized Means			Congestion Relief Cost (Baht)		
	Proposed Method	Method in 6.5.2.1	Method in 6.5.2.2	Proposed Method	Method in 6.5.2.1	Method in 6.5.2.2
ΔP_{G_2} (MW)	-	-0.548	-8.9792	0	6,149	20,010
ΔQ_{R_4} (Mvar)	19.841	-	0	79,364	-	0
ΔP_{L_4} (MW)	-	0.548	8.9792	0	54,820	897,920
	Total Cost			79,364	60,969	917,930

It should be noted that, although using the method presented in 6.5.2.1 results in expense of 60,969 Baht, which is lower than of the proposed method. However, the MVA power flow is still higher than its thermal limit. Thus the thermal limit congestion still exists in the system.

The case examined in this section is the case which the congestion can be solved by performing only reactive power re-scheduling. The next example is the case where combining active and reactive power re-scheduling have to be combined to solve the congestion, which can be presented in section 6.6.2.

6.6.2 Lines No. 1, 6, 10 and 11 are Tripped

If lines No. 1, 6, 10 and 11 are tripped, the congestion occurred on line connected between buses No. 5 and 6, which is 163 % of its MVA rating, 25.620 + j20.306 MVA. The proposed method is performed to relief the congestion. Then it is compared with other methods presented in sections 6.5.2.1 and 6.5.2.2 in two aspects, i.e. with and without considering ancillary services of generation unit located at bus No. 5. Detailed results can be illustrated follow.

6.6.2.1 Considering Generation at Bus No. 5

In a based case, generation at bus No. 5 is not committed in the system. If this generation is considered as an ancillary service unit, comparison of power flow results between the proposed method and the methods formulated in section 6.5.2.1 and 6.5.2.2 can be shown in Table 6.6.

Table 6.6 Results comparison with unit at bus No. 5 as an ancillary service

Generation & Line	Proposed Method		Method in section		Method in section	
	P (MW)	Q (MVar)	P (MW)	Q (MVar)	P (MW)	Q (MVar)
G1	42.51	11.46	42.64	2.95	42.50	2.89
G2	50.00	26.09	50.00	26.02	50.00	26.10
G3	54.30	29.35	54.93	13.39	52.05	20.41
G5	5.70	35.99	5.07	54.73	7.95	53.35
L1-4	17.25	10.16	16.62	10.35	17.38	10.12
L1-5	25.26	1.30	26.02	-7.40	25.12	-7.24
L2-3	3.15	-2.18	2.79	-2.11	3.22	-2.19
L2-4	23.39	18.50	24.03	18.29	23.26	18.54
L2-6	23.46	9.77	23.18	9.84	23.51	9.75
L3-5	20.00	0.00	20.00	-9.82	17.87	-8.98
L3-6	37.44	37.27	37.72	30.20	37.09	30.29

For the proposed method, active and reactive power re-scheduling can solve the congestion. In this case all constraints are within their limits as shown in Table 6.6. As a result, voltage at all generation buses, i.e. No. 1, 2, 3 and 5 are regulated at 1.02, 1.02, 1.02 and 0.9944 p.u. respectively. In other methods, since it does not take into account reactive power re-scheduling, thus voltage of all generation buses are regulated at a specified value, 1.02 p.u. In addition, active power re-scheduling between generating units at buses No. 3 and 5 are selected to relief the congestion as shown in Table 6.6. As a consequence, the congestion relief costs of all cases can be shown in Table 6.7.

Table 6.7 Utilized means with their associated relief costs

	Utilized Means			Congestion Relief Cost (Baht)		
	Proposed Method	Method in 6.5.2.1	Method in 6.5.2.2	Proposed Method	Method in 6.5.2.1	Method in 6.5.2.2
ΔP_{G_3} (MW)	-5.7038	-5.07	-7.953	13,324	11,848	18,552
ΔP_{G_5} (MW)	5.7038	5.07	7.953	114,076	101,400	159,060
	Total Cost			127,380	113,248	177,612

6.6.2.2 Neglecting Generation at Bus No. 5

In this case, the comparison of power flow between the proposed and the methods formulated in sections 6.5.2.1 and 6.5.2.2 without taking generation at bus No. 5 as an ancillary service into account are shown in Table 6.8.

Table 6.8 Results of the proposed method and methods in section 6.5.2.1 and 6.5.2.2

Generation & Line	Proposed Method		Method in section		Method in section	
	P (MW)	Q (MVar)	P (MW)	Q (MVar)	P (MW)	Q (MVar)
G1	55.42	43.96	55.83	23.13	62.58	15.36
G2	50.00	-11.31	50.00	26.89	50.00	27.40
G3	48.15	56.12	47.66	48.09	40.69	43.19
L1-4	23.36	29.07	23.99	8.21	27.55	7.25
L1-5	32.06	14.89	31.84	14.92	35.03	8.11
L2-3	7.15	-13.22	6.93	-2.88	8.90	-3.24
L2-4	17.50	1.20	16.68	20.73	13.18	21.96
L2-6	25.35	0.71	26.40	9.05	27.93	8.68
L3-5	19.44	4.69	20.00	17.11	16.48	11.33
L3-6	35.75	40.54	34.57	31.10	33.07	31.54

For the proposed method, active and reactive power re-scheduling can solve the congestion. Voltage magnitude of generation buses No. 1, 2, and 3 are regulated at 1.02, 0.9607 and 0.9881 p.u. respectively while active power of buses No. 3 and 1 are re-dispatched to the value as shown in Table 6.8. In addition, reactive power at bus No. 5 is utilized 20 MVar to increase its voltage magnitude to a lower bound limit, 0.95 p.u.

For the method of section 6.5.2.1, active power of bus No. 3 and 1 are re-dispatched to the value shown in Table 6.8. Similarly, reactive power reserve at bus No. 5 is utilized 8.19 MVar to pull its voltage magnitude to 0.95 p.u.

For the method of section 6.5.2.2, the real power of buses No. 3 and 1 are re-dispatched more than other two cases as shown in Table 6.8. Moreover, reactive power reserve at bus No. 5 is utilized 20 MVar with its voltage magnitude of 0.9688 p.u. The congestion relief costs correspond to utilized means of all cases are shown in Table 6.9.

Table 6.9 Utilized means with their associated relief costs

	Utilized Means			Congestion Relief Cost (Baht)		
	Proposed Method	Method in 6.5.2.1	Proposed Method	Method in 6.5.2.1	Proposed Method	Method in 6.5.2.1
ΔP_{G_1} (MW)	11.8529	12.3379	19.3055	144,591	150,539	236,270
ΔP_{G_3} (MW)	-11.8529	-12.3379	-19.3055	27,580	28,700	44,708
ΔQ_{R_5} (Mvar)	20	8.1851	20	80,000	32,740	80,000
	Total Cost			252,171	211,979	360,978

สถาบันวิทยบริการ
จุฬาลงกรณ์มหาวิทยาลัย

The results of Tables 6.7 and 6.9 are then compared. it is obvious that generation at bus No. 5 has an impact to lower congestion relief cost. Additionally, the lower congestion relief costs of method presented in 6.5.2.1 compare to the proposed method is also found in both cases.

6.6.3 Congestion Cost Allocation

Congestion cost obtained in section 6.6.1 and 6.6.2 is allocated among transactions according to their flows along congested line. First, we assume that there are six bilateral contracts, which can be shown in Table 6.10.

Table 6.10 Transaction under bilateral markets

Transaction No.	Generation Bus No.	Load Bus No.	Quantity (MW)
1	1	4	20
2	1	5	20
3	2	4	20
4	2	6	30
5	3	5	30
6	3	6	30

Two types of PTDF, i.e. DC and AC PTDF will be compared. The formulation of both types can be found in Appendix B. The congestion cost in section 6.6.1 can be allocated as shown in Table 6.11.

Table 6.11 Allocation of congestion cost on the congested line No. 2

Transaction			Quantity (MW)	% PTDF		% of Contribution		Cost Allocation (Baht.)		% Error
No.	Source Bus No.	Sink Bus No.		DC	AC	DC PTDF	AC PTDF	DC PTDF	AC PTDF	
1	1	4	20	76.47	79.82	38.93	40.25	30,899	31,947	-3.28
2	1	5	20	10.60	10.00	5.40	5.04	4,283	4,002	7.01
3	2	4	20	83.53	83.62	42.53	42.17	33,751	33,467	0.85
4	2	6	30	7.62	6.64	5.82	5.02	4,618	3,986	15.86
5	3	5	30	9.59	9.93	7.32	7.51	5,812	5,961	-2.50
6	3	6	30	-0.46	-0.05	0.00	0.00	0	0	-

From Table 6.11, source and sink of transaction No. 6 are located at buses No. 3 and 6 respectively, which forms a counter flow to the congested line. Accordingly, it has no impact to the congested line and has no benefit from this action. In other word, only transaction, which has a positive PTDF is taken into account. In addition, percentage of contribution can be calculated from normalization of a PTDF times contracted power and the proposed method used this term to allocate congested cost.

For the case of example in section 6.6.2, considering generation at bus No. 5, congestion cost can be allocated to all transactions as shown in Table. 6.12.

Table 6.12 Congestion cost allocation based on DC and AC PTDF of the congested line No. 10 connected between bus No. 3 and 5 of example in section 6.6.2

Transaction			Quantity	% PTDF		% of Contribution		Cost Allocation (Baht.)		
No.	Source Bus No.	Sink Bus No.	(MW)	DC	AC	DC PTDF	AC PTDF	DC PTDF	AC PTDF	% Error
1	1	4	20	-20.07	-19.53	0.00	0.00	0	0	-
2	1	5	20	30.11	32.36	19.07	20.50	24,297	26,109	-6.94
3	2	4	20	10.04	10.21	6.36	6.47	8,102	8,238	-1.65
4	2	6	30	-9.12	-8.55	0.00	0.00	0	0	-
5	3	5	30	73.91	72.72	70.23	69.09	89,462	88,010	1.65
6	3	6	30	4.56	4.15	4.33	3.94	5,519	5,023	9.89

From Table 6.12, transactions No. 1 and 4 form a counter flow to the congested line. Accordingly, they have no contribution to the allocated congestion cost. We found from Tables 6.11 and 6.12 that error between DC and AC PTDF contributing to the congested cost is slightly difference.

6.7 Conclusions

In this chapter, we verify the proposed congestion management methodology. Some ancillary services, i.e. reactive power, interruptible loads and de-committed generation units are taken into account as means to relief the congestion. Various transmission line thermal limit models are examined and a comparison is conducted among them. In addition, an error analysis between DC and AC PTDF for congestion cost allocation purpose is found to be slightly difference.

สถาบันวิทยบริการ
จุฬาลงกรณ์มหาวิทยาลัย

CHAPTER 7

APPLICATION OF CONGESTION MANAGEMENT

7.1 Introduction

The proposed method presented in Chapter 6 is applied to a 28-bus of Thailand region 3 system with analysis of two circumstances, i.e. the co-existence between pool and bilateral trading in the same market, and the presence of multiple congested lines. The first situation normally exists in an actual market and differs from the case presented in Chapter 6, in which all trades are subjected to bilateral contracts. The latter situation may cause cross-subsidy among congested lines. Hence, allocating the congestion cost among participants is more complicated than the method proposed in Chapter 6. To cope with this problem, a methodology has been developed and presented in this Chapter. However, for simplicity, some assumptions are used to simplify the problems. For an example, cost of utilizing reactive power source for maintaining quality of system voltage profile is neglected in the base-case. In addition, reactive power re-scheduling cost is considered only in the case of reactive power reserve increase according to the request. Other concerned assumptions will be described later in the related section.

7.2 A 28-bus Thailand Region 3 System

A reduced actual network of the southern region power system in Thailand is selected for the test of the developed methodology. It comprises 28 buses with 5 generation buses, 22 load buses, and one interconnection bus (KNE) with Malaysia system via a HVDC link. For simplicity, the interconnected bus is assumed to be a generation bus. System generation information is shown in Table 7.1.

Table 7.1 Generating unit information

Bus No.	Size Description (unit x MW)	Type
1	3 x 600	Gas Turbine
15	3 x 70	Hydro Turbine
16	1 x 260	Steam Turbine
18	7 x 110	Combined Cycle
27	3 x 20	Hydro Turbine
28	1 x 300	HVDC Link

Details of the transactions according to bilateral contracts are assumed and shown in Table 7.2.

Table 7.2 Transactions under bilateral markets

Transaction No.	Generation Bus No.	Load Bus No.	Quantity (MW)
1	1	14	60
2	1	19	100
3	18	14	40
4	18	17	80
5	28	10	40
6	28	22	60

The single line diagram of the system is shown in Fig. 7.1.

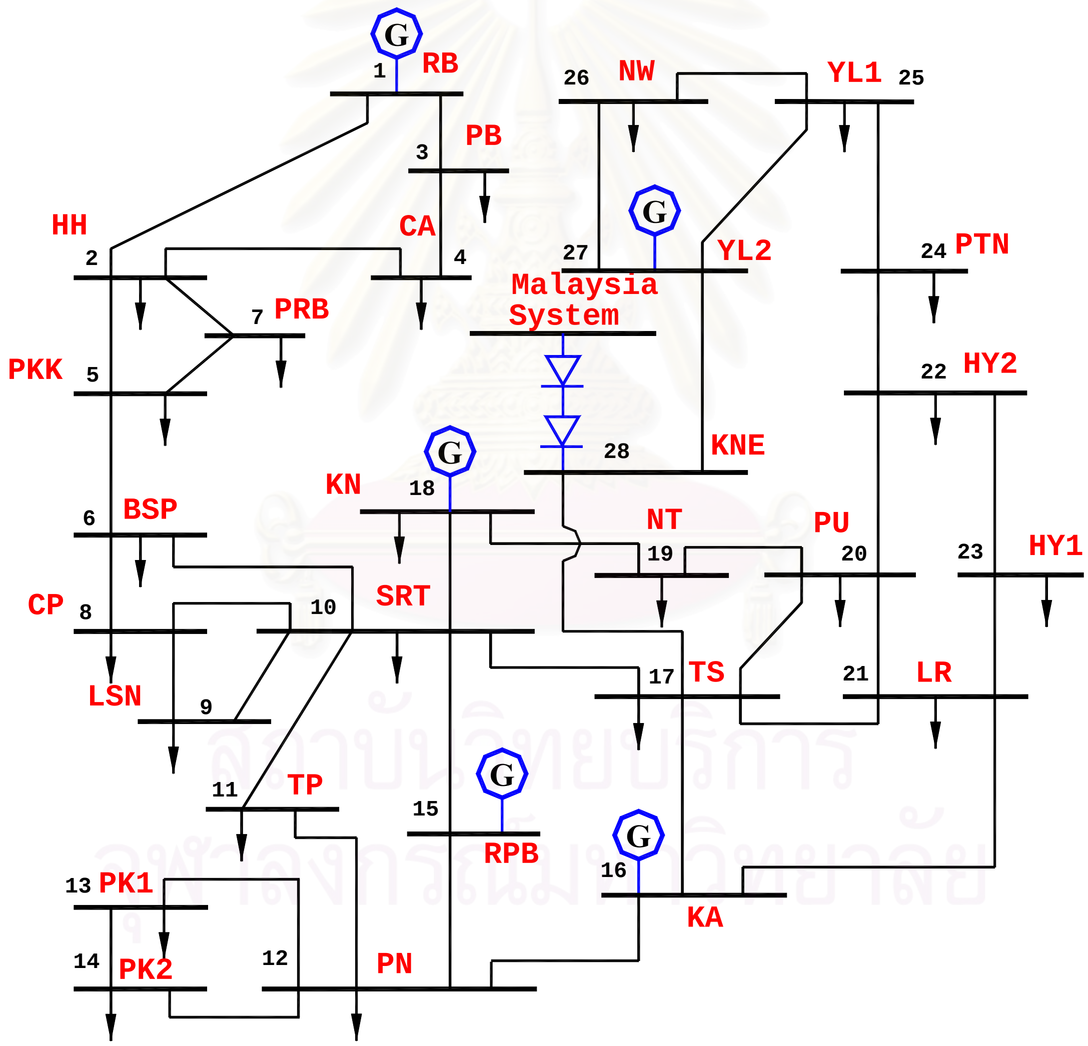

Figure 7.1 Network topology of the 28-bus system

There are two voltage levels of the transmission system, i.e. 115 and 230 kV. The southern region map of Thailand together with a transmission system topology of can be shown in Fig. 7.2.

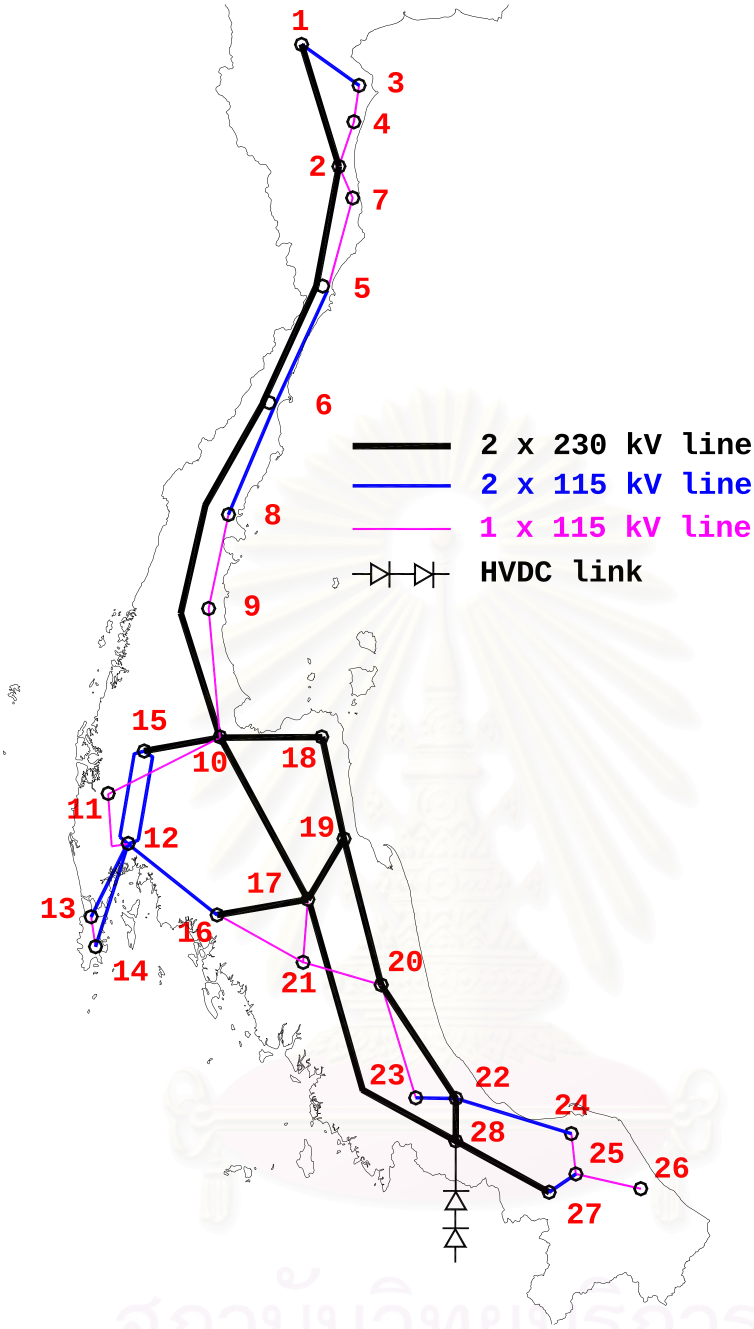

Figure 7.2 Transmission network of the 28-bus system

An actual peak demand of 1761.6 + j697.1 MVA occurred on the evening of Wednesday 5$^{th.}$ Jan. 2005 is used as a base-case in the analysis. All required information, i.e. generation, load and branch data are available in the Appendix A. The power flow results of this base-case can be shown also in the same Appendix. Two contingency cases, i.e. the outages of the double circuit line connected between buses No. 12 and 14 and the double circuit line connected between buses No. 16 and 17 are analyzed. The proposed congestion relief methodology is analyzed in section 7.3, whereas the congestion cost allocation is described in section 7.4.

7.3 Congestion Relief

There are two case studies in this section i.e., 1) tripping of the double circuit lines connected between buses No. 12 and 14 and 2) tripping double circuit lines connected between buses No.16 and 17. It is found in the first case that a single 115 kV line connected between buses No. 13 and 14 is congested, whereas in the second case there are two congested lines, i.e. line connected between buses No. 12 and 16, and the line connected between buses No. 16 and 21. The power flow results of all cases can be shown in Appendix F. To relieve the congestion, the objective function defined in (6.8) is used in association with the MVA thermal model. For simplicity, willingness to accept price of all available means assumed to be fixed in the unit of Baht per MW or MVar as shown in Table 7.3.

Table 7.3 Willingness to accept prices of various means

No.	Type	Location (Bus No.)	Costs (1000 Bht/(MW or MVar))
1	Gas Power Plant	1	8
2	Hydro Power Plant	15	4
3	Steam Power Plant	16	10
4	Combined Cycle Plant	18	6
5	Hydro Power Plant	27	6
6	HVDC Link	28	8
7	Reactive Power	All Buses	2
8	Interruptible Load	All Buses	40

Detail of analysis can be presented below.

7.3.1 Tripping of Lines Connected between Buses No. 12 and 14

With the tripping of the lines connected between buses No. 12 and 14, it is found that four constraints are violated. The line flow between buses No. 13 and 14 are 135.846 MVA (135.294 -j12.242 MVA), which is 4.5% above its thermal limit. Moreover, voltage magnitude of buses No. 11, 12, 13 and 14 are dropped to 0.910, 0.909, 0.833 and 0.816 p.u. respectively, which are less than the lower bound. Two means are applied to relieve the congestion, i.e. load curtailment at bus No. 14, and increase reactive power reserve at buses No. 13 and 14. The demand of bus No. 14 is curtailed to 119.2528 + j68.1706 MVA. In addition, reactive reserve of bus No. 13 and 14 are increased from 20 and 100 MVar to 46.38 and 120 MVar respectively. As a result, all the violated constraints are relieved within an acceptable range. The cost of congestion relief utilizing the three requested means can be summarized in Table 7.4.

Table 7.4 Utilized means with their associated congestion relief costs of case 1

Utilized Means	Quantity (MW or MVar)	Unit Prices (1000 Baht/(MW or MVar))	Prices (Baht)
$\Delta P_{L_{14}}$	11.2472	40	449,888
$\Delta Q_{R_{13}}$	26.3800	2	52,760
$\Delta Q_{R_{14}}$	20	2	40,000
Total			542,648

7.3.2 Tripping of Lines Connected between Buses No. 16 and 17

In this case, it is found that two lines, i.e. the line connected between buses No. 12 and 16 and the line connected between buses No. 16 and 21 are congested. For convenience, we denote the line connected between buses No. 12 and 16 and the line connected between buses No. 16 and 21 are denoted as lines No. 22 and 25 corresponding to the data provided in Appendix A. The power flow of the former and the latter lines are 105.045 (103.621 -j17.238 MVA) and 98.644 (96.379 -j21.020 MVA) MVA respectively, which are 19.4 and 12.1 % over their thermal limit respectively. Moreover, voltage magnitude of buses No. 11, 12, 13 and 14 are dropped to 0.944, 0.948, 0.948 and 0.946 p.u. respectively. To relieve the congestion, it is found that generation at buses No. 15, 16 and 18 have to be re-dispatched to form counter flows. Accordingly, generation at buses No. 15 and 18 should increase their power output from 200 to 210 MW and from 660 to 683.927 MW. respectively, whereas generation at bus No. 16 should decrease its power output from 200 to 166.073 MW. In addition, the voltage magnitude of generation at bus No. 16 has to be set to its upper bound at 1.05 p.u. As a result, the power flow of the lines No. 22 and 25 are 88.000 and 79.561 MW respectively. Additionally, voltage magnitude of buses No. 11, 12, 13 and 14 are restored to be within acceptable range, i.e. 0.957, 0.963, 0.963 and 0.962 p.u. respectively. Congestion relief cost of re-dispatching the three generation buses can be summarized in Table 7.5.

Table 7.5 Utilized means with their associated congestion relief costs of case 2

Utilized Means	Quantity (MW or MVar)	Unit Prices (1000 Baht/(MW or MVar))	Prices (Baht)
$\Delta P_{G_{15}}$	10	4	40,000
$\Delta P_{G_{16}}$	-33.927	-2*	67,854
$\Delta P_{G_{18}}$	23.927	6	143,562
Total			251,416

* It should be noted that the generation receives only 20% of the willingness to accept price.

7.4 Congestion Cost Allocation Methodology

Normally, the power trading volume in both pool and bilateral markets may contribute to the congested lines. Thus, degree of the contribution between these two markets to any congested lines must be firstly calculated. This can be described in section 7.4.1. Then, the congestion cost, which should be responsible by participants in the market can be allocated by the method presented in Chapter 6. However, multiple congested lines may exist. This situation requires a methodology to estimate correlation of the congestion relief cost among congested lines, which can be presented in section 7.4.2. To overcome nonlinear characteristics of the network and operating conditions, a DC power flow is adopted instead of an AC method.

7.4.1 Contributory Degree of Bilateral Transactions to the Congested Lines

In this section we attempt to calculate the contributory degree of bilateral transactions to the congested lines. Theoretically, for trading in market having both pool and bilateral schemes, contribution of trading volume in a pool market can be found by moving all transactions in bilateral market out from the network and vice versa contribution of transactions in bilateral market can be found by neglecting volume of trade in pool market. However, due to nonlinear characteristics of the network ordering of moving transactions in and out may result in different impact to the line flow. To overcome the effect of ordering, we adopt a DC power flow method and the overall procedures can be described as below.

For a congested line *k*, we assume that a power flow through this line may come from both pool and bilateral markets, which can be expressed in (7.1).

$$PF^k = PFPo^k + PFBi^k \tag{7.1}$$

where

PF^k is the power flow through line *k*

$PFPo^k$ is the amount of power flow through line *k* from pool market

$PFBi^k$ is the amount of power flow through line *k* from bilateral markets

The term PF^k can be obtained without considering trading arrangement. The terms $PFPo^k$ and $PFBi^k$ can be obtained by treating the trade under bilateral and pool markets independently. The ratio between $PFPo^k$ and $PFBi^k$ to the actual power flow through line k, PF^k, can be defined as a contributory degree of trading under pool and bilateral markets to the congested line respectively. We use these indices to separate the net congestion relief cost from pool and bilateral markets. Since trading in pool market is centralized in practice, the allocated congestion relief cost among participants is normally reflected as the shadow of the nodal price and this issue is out of the scope of this dissertation. On the other hand, the term $PFBi^k$ can be decomposed to reveal the degree of contribution of each transaction under bilateral markets as shown in (7.2).

$$PFBi^k = \sum\left(PTDF_{i,j}^k\right)\left(t_{i,j}\right) \quad \forall \quad i \in So, j \in Si \tag{7.2}$$

where

$PTDF_{i,j}^k$ is the PTDF of line *k* for the source at *bus-i* and the sink at *bus-j*, and

$t_{i,j}$ is the amount of power contracted from source at *bus-i* and sink at *bus-j*,

The terms *So* and *Si* are used to represent source and sink buses in the transaction matrix presented in Chapter 4.

Detail of the procedure to allocate the congestion relief cost among transactions in bilateral markets can be found in Chapter 6.

It should be noted that power flow results obtained from DC an AC method may vary considerably. However, using a DC method, ordering of the trades between pool and bilateral markets and ordering among transactions in bilateral market are trivial. In addition, we use the proposed method just for congestion cost allocation purpose.

In a single congested line case, undoubtedly that utilized means are requested to relieve this congestion. However, cross subsidy may be occurred if the multiple congested lines exist. The methodology to define correlation among multiple congested lines will be described in section 7.4.2.

7.4.2 Congestion Cost Allocated Among Multiple Congested Lines

For a single congested line, the congestion relief cost obtained from section 7.4.1 can be allocated among transactions in a bilateral market as presented in Chapter 6. However, the allocation procedure differs from those procedures in case of the presence of multiple congested lines. In this situation, the correlation among all congested lines may be existed. In another word, relieving some of the congested lines may release system congestion. Thus, cross subsidy of the congestion relief costs should be considered carefully, and allocated in an equitable manner. Accordingly, a methodology has been proposed to find correlation and to allocate congestion relief cost among congested lines, which can be described below.

Step 1: For the defined base-case, counting a number of congested lines.

Step 2: For the congested line k, calculate the minimum relief cost, denoted as CC^k, that can be relieved overloading of this line without considering others lines. This can be achieved using objective function defined in (6.8) with relaxing the constraint (6.8c).

Step 3: Repeat step 2 for others lines listed in step 1.

Step 4: Calculate CCI^k by normalize CC^k obtained in step 2 using (7.3).

$$CCI^k = \frac{CC^k}{\sum CC^k} \quad \forall\ k \in \ congested\ lines \tag{7.3}$$

Step 5: Calculate the minimum congestion relief cost, denoted as MCC, using objective function defined in (6.8) while satisfying the constraints (6.8a)-(6.8h).

Step 6: For the congested line k, calculate the allocated congestion relief cost, denoted as ACC^k, using (7.4).

$$ACC^k = CCI^k * MCC \tag{7.4}$$

Step 7: From the allocated congestion relief cost of the line k obtained in (7.4), employ the congestion cost allocation method present in 6.6.3 to find cost that each transaction has responsible for.

7.5 Numerical Results

We employ the method proposed in section 7.4 to allocate the congestion relief cost of the two cases of section 7.3 i.e., lines connected between buses No. 12 and 14 and lines connected between buses No. 16 and 17 are tripped. Detail of analysis can be described below.

7.5.1 Tripping of Lines Connected between Buses No. 12 and 14

As described in section 7.3, these contingency results in congestion of the lines connected between buses No. 13 and 14. From a DC power flow results, real power of 130.5 MW flows through lines. Use (7.1) and (7.2), we found that $PFPo^k$ and $PFBi^k$ of the congested lines are 30.5 and 100 MW respectively. Additionally, contribution of transactions under bilateral markets to the congested lines can be calculated and shown in Table 7.6.

Table 7.6 Contribution of transactions to the congested lines

Transaction No.	Generation Bus No.	Load Bus No.	Quantity (MW)	% PTDF	Contribution (MW)
1	1	14	60	100	60
2	1	19	100	0	0
3	18	14	40	100	40
4	18	17	80	0	0
5	28	10	40	0	0
6	28	22	60	0	0

From Table 7.6, transactions No. 1 and 3 have impact to the congested lines. This is due to the load of bus No. 14 receives only power from bus No. 13 so that only the transactions, which their generation have contract with this load have contribution to the congested lines with PTDF 100%. The congestion relief cost of this case is 542,648 Baht which can be allocated among pool market and bilateral transactions as shown in Table 7.7.

Table 7.7 Allocated congestion relief cost among participants

Trading Arrangement	Contribution (MW)	Contributory Degree	Responsible Congestion Relief Cost (Baht.)
Pool Market	30.5	0.2337	126,826
Transaction No. 1	60	0.4598	249,493
Transaction No. 3	40	0.3065	166,329

7.5.2 Tripping of Lines Connected between Buses No. 16 and 17

From section 7.3.2, the lines No. 22 and 25 are overloaded 19.4 and 12.1 % over their thermal limits. However, from a DC power flow results, the power flow of the former and the latter congested lines are 100.202 and 99.798 MW respectively, which are 16.1 and 13.4 % overloading respectively. To evaluate correlation and to allocate congestion relief cost among these two congested lines, the method proposed in section 7.4.2 is performed. The results show that relieving overloading of the line No. 22 only can also relieve congestion of the system. Thus, CC^{22} in this case is 251,416 Baht, which is the same cost found in section 7.3.2. However, relieving overloading of the line No. 25 only cannot relief the system congestion. In this case, power flow through line No. 22 is 96.698 (96.038 - j11.275 MVA), which is still 9.9 % overloading. Utilized means with their associated congestion relief costs on this case can be shown in Table 7.8.

Table 7.8 Utilized means and congestion relief costs of considering line No. 25

Utilized Means	Quantity (MW or MVar)	Unit Prices (1000 Bht/(MW or MVar))	Prices (Baht)
$\Delta P_{G_{16}}$	-17.0055	-2*	34,011
$\Delta P_{G_{27}}$	17.0055	6	102,033
Total			136,044

The terms proposed in section 7.4.2 can be summarized and shown in Table 7.9.

Table 7.9 Correlations cost between the congested lines No. 22 and 25

Congested Line No. (k)	CC^k (Baht)	CCI^k	ACC^k (Baht)
22	251,416	0.6489	163,139
25	136,044	0.3511	88,277

To obtain $PFPo^k$ and $PFBi^k$, we first calculate contribution of bilateral transactions of the congested lines, which can be shown in Table 7.10.

Table 7.10 Contribution of bilateral transactions to the congested lines No. 22 and 25

Transaction No.	Generation Bus No.	Load Bus No.	Quantity (MW)	% PTDF		Contribution (MW)	
				Line No. 22	Line No. 25	Line No. 22	Line No. 25
1	1	14	60	12.49	-12.49	7.4943	-7.4943
2	1	19	100	-2.52	2.52	-2.5239	2.5239
3	18	14	40	13.6	-13.6	5.4398	-5.4398
4	18	17	80	-1.45	1.45	-1.1603	1.1603
5	28	10	40	3.26	-3.26	1.3026	-1.3026
6	28	22	60	-0.10	0.10	-0.0599	0.0599

From the last column of Table 7.10, $PFBi^{22}$ and $PFBi^{25}$ is the sum of all values in the last two columns which are 10.493 and -10.493 MW respectively. Since $PFBi^{25}$ is a negative value, it means that transactions under bilateral markets form a counter flow to the congestion. Accordingly, these transactions have no responsibility for the cost of 88,275 Baht corresponds to congestion of the line No. 25. It should be noted that, from the proposed method any benefits are not be paid to these transactions. In contrast, these transactions contribute to the congestion of line No. 22 of 10.493 MW thus $PFPo^{22}$ is 89.529 MW (100.022-10.493). As a result, responsible congestion cost allocated between pool and bilateral markets can be shown in Table 7.11. Then, congestion cost allocation among transactions under bilateral markets can be shown in Table. 12.

Table 7.11 Responsible congestion cost between pool and bilateral markets

Market	Contribution (MW)		Contributory Degree		Responsible Cost (Bht.)	
	Line No. 22	Line No. 25	Line No. 22	Line No. 25	Line No. 22	Line No. 25
Pool	89.529	110.291	0.8951	1	146,025	88,277
Bilateral	10.493	-10.493	0.1049	0	17,114	0

Table 7.12 Congestion cost allocation among bilateral transactions

Transaction No.	Contribution (MW)	Contributory Degree	Responsible Congestion Relief Cost (Bht.)
1	7.4943	0.5264	9,009
3	5.4398	0.3821	6,539
5	1.3026	0.0915	1,566

7.6 Conclusions

In this chapter, we have extended our developed methodology from Chapter 6 to a real 28-bus Thailand region 3 system. A transmission line MVA thermal limit model associated with the proposed objective function of section 6.5.1 is used in a study. In addition, two situations, i.e. the co-existence between pool and bilateral trading in the same electricity markets and the presence of multiple congested lines are described. Accordingly, an allocating methodology of the congestion cost to cope with these circumstances has been developed and proposed.

CHAPTER 8

CONCLUSIONS AND FUTURE WORKS

This chapter provides conclusions and contributions of this dissertation, including suggestions for related future works.

8.1 Conclusions

This dissertation emphasizes on congestion management for transactions under a bilateral based market. The highlighted topics in this dissertation can be summarized below.

- The thermal constraint generally limits transfer capability of a system. An MVA thermal limit model is used in stead of a MW model to obtain a more accurate result of zonal congestion management.
- The proposed methodology can be applied for an on-line voltage security assessment. Formulation of the proposed method is based on a feasible operating region on a P-Q plane, which is convenient to visualize and can be applied to verify a transmission line loading margin. Moreover, two-transmission line performance indices are proposed, i.e. the line loading and the line severity indices, and can also be adopted for transmission system expansion.
- Regarding transmission services, a slack bus independence concept has been developed to analyze the transmission loss and the congestion cost allocation, taking into account a pair of source and sink nodes under each bilateral contract. Consequently the contributory degree of each node to transmission loss and congestion cost can be obtained.
- The congestion management proposed in this dissertation can be classified into two procedures, i.e. congestion relief and congestion cost allocation. A congestion relief procedure is defined as a methodology to utilize existing means to relieve the congestion, with an objective to minimize the congestion cost. Besides generation re-dispatch and load shedding, we take into account reactive power re-scheduling and de-committed generation units as means to relieve the congestion. For

congestion cost allocation, we employ a power transfer distribution factor (PTDF) as an index to verify contributory degree of each transaction to the congested line.

- Analysis of trading under bilateral markets has been examined in details using a 3-bus system. A comparison of several loss allocation methods is conducted under a feasible transaction. In case of congestion, various objective functions are used and compared. It is found that the proposed method results in the least congestion relief cost which satisfies all participants who contribute to the congestion.
- For practical purposes, the congestion management of the co-existence trading in both pool and bilateral-based markets has also been analyzed. In addition, a methodology to cope with multiple congestions has also been developed.

8.2 Future Works

To analyze the congestion management of a power system in more datails, some further research described below may be of interest.

8.2.1 Transmission Loss Allocation

Since transmission loss is a nonlinear function, it cannot be explicitly identified how much of the contribution from each participant is. Suggestions for research in this regards can be presented as follows:

- In a real market, the co-existence of different trading arrangements requires methodology for separating the total loss for each part of the system. For example, charge on transmission loss may be included in either nodal or zonal prices, whereas the proposed method presented in Chapter 4 can be used to allocate loss among participants under bilateral based markets.
- As presented in Chapter 4, the markets can manage loss in two different ways. Firstly, loss may be treated as the responsibility from each participant. If we treat loss as a commodity, some participants may acquire the service of loss from generation entities more than in the past. Although, this approach is hard to achieve in practice, however, it may be justified. Another way to manage loss is to treat it as a commodity so that the SO may compensate it and charge among all participants according to their contributions in an ex-post time.

- For responsibility-based loss management approach as presented above, it can be formulated as an optimization problem with the objective of minimizing cost of transmission loss services. Then, the obtained cost may be allocated to participants later.

8.2.2 Transmission Line Loading Margin

The loading margin evaluation method proposed in Chapter 5 is inspired by the fact that the system loading capability is limited by a hard constraint on a transmission system. However, some points are still left unclear and needed further research, which can be described below.

- The proposed transmission line performance indices formulated for transmission planning has to apply with a real system e.g. a 28-bus of Thailand region-2 system. The obtained results can then be compared with the recent plan from EGAT Power Development Plan (PDP). However, due to longitudinal characters of this system, the author expects that none transmission line flow located close to an infeasible boundary at the collapsing point. This situation reveals drawback of the proposed method.
- To cope with this drawback, transmission flow path is used instead of considering only on a particular line. The concept is to decompose the system power flow into a few radial flow paths, which can be investigated its loading margin. If this successes, it exposes the fact that voltage instability may be initiated from transfer capability limit on some transmission paths.

8.2.3 On-line Voltage Security Assessment

Although the transmission line loading margin, presented in Chapter 5, may be used for planning purposes, however it cannot cope with voltage collapse phenomenon, which requires real-time voltage security assessment. The cause of this phenomenon, generally initiated by cascade tripping, is normally based on classical contingency screening methodology. However, it neglects the influence of system protection and therefore is not sufficient to analyze. A new version of contingency screening method should take into account the consequences from the first tripping event. As a result, system protection model must be taken into account, so that the SO can identify which contingency is the root cause of the cascading tripping. Consequently, a preventive or corrective measures, e.g. load shedding scheme can be performed in time.

8.2.4 Generation and Transmission Planning

Besides the procurement of some ancillary service and transmission service charges during a short-run period, a long-term planning under competitive environment is a challenge issue. This planning is generally to verify adequacy of generation and transmission systems. From this study the SO can promote some incentive strategies to encourage investment in new infrastructures. Although evaluation techniques should be performed in a long-term simulation however trading in a spot market via power pool is necessary. Therefore, some factors reflecting correct/in-correct market signals of a short run competition should be taken into account. This can be described below.

- For nodal/zonal prices concept, it should be noted that the incremental transmission loss reflects a short run operation cost, which depend significantly on participants bidding strategies. In contrast, the incremental real power flow of the congested line contained a signal reflects to lacking of generations and transmission systems of some regions. Moreover, a methodology to select a slack bus should be questionable.
- Sine generation entities attempt to maximize their profits thereby generation in-adequacy opens the door of gaming so that price spike may be un-avoided. This price spike may or may not reflect generation in-adequacy.
- The existing transmission pricing methodology e.g. MW-Mile, cannot encourage transmission investment in some regions, which always import power from neighborhood area due to the product of MW and Mile is constant.

8.2.5 A Hybrid Pool and Bilateral Market

A bilateral based market may be satisfied in some countries as mentioned in Chapter 1. However, trading in a spot market via power pool is necessary for a balancing mechanism. Thus the future works should be conducted under a hybrid pool and bilateral market.

REFERENCES

[1] Athay, T. M. Generation Scheduling and Control. *Proceeding of the IEEE*, vol. 75, No. 12, Dec. 1987, pp. 1592-1606.

[2] Wood, A. J. and Wollenberg, B. F. *Power Generation Operation and Control*. 2nd. edition, Copyright 1996, John Wiley & Sons Inc.

[3] Kunder, P. *Power System Stability and Control*. McGraw-Hill 1994.

[4] Toshida, N.; Uesugi, M.; Nakata, Y.; Nomoto M.; and Uchida, T. Open Distributed EMS/SCADA System. *Hitachi Review*, vol. 47, No.5, 1998, pp. 208-213.

[5] Wu, F. F.; Moslahi K.; and Bose, A. Power System Control Centers: Past, Present, and the Future. *Proceeding of the IEEE*, vol. 93, No. 11, Nov. 2005, pp. 1890-1908.

[6] Gaushell, D. J.; and Darlington, H. T. Supervisory Control and Data Acquisition. *Proceeding of the IEEE*, vol. 75, No. 12, Dec. 1987, pp. 1645-1658.

[7] *Resource for Understanding the Blackout of 2003* [Online], Available: http://www.pserc.wisc.edu/Resources.htm.

[8] Andersson, G.; Donalek, P.; Farmer, R; Hatziargyriou, N.; Kamwa, I.; Kundur, P.; Martins, N.; Paserba, J.; Pourbeik, P.; Sanchez-Gasca, J.; Schulz, R.; Stankovic, A.; Taylor C. W.; and Vittal, V. Causes of the 2003 major grid blackouts in North America and Europe, and recommended means to improve system dynamic performance. *IEEE Transactions on Power Systems*, vol. 20, No. 4, Nov. 2005, pp. 1922-1928.

[9] Makarov, Y. V.; Reshetov, V. I.; Stroev, V. A.; and Voropai, N. I. Blackout Prevention in United States, Europe and Russia. *Proceeding of the IEEE*, vol. 93, No. 11, Nov. 2005, pp. 1942-1955.

[10] *Network Control System EMS/SCADA/OTS Introduction* [Online], Available: http://www.toshiba.co.jp.

[11] Momoh, J. A. *Electric Power System Application of optimization*. Copyright 2001, Marcel Dekker Inc.

[12] Fink, L. H. *et al.*, Emergency control practices. *IEEE Transactions on Power Apparatus and Systems*, vol. 104, No. 9, Sep. 1985, pp. 2336-2441.

[13] Balu, N. *et al.*, On-Line Power System Security Analysis. *Proceeding of the IEEE*, vol. 80, No. 12, Feb. 1992, pp. 262-280.

[14] Nirenberg, S. A.; Mcinnis, D. S.; and Sparks, K. D. Fast acting load shedding. *IEEE Transactions on Power Systems*, vol. 7, No. 2, May 1992, pp. 873-877.

[15] Crespo, J. M.; Usaola, J.; and Fernandez, J. L. Security-Constrained Optimal Generation Scheduling in Large-Scale Power Systems. *IEEE Transactions on Power Systems*, vol. 21, No. 1, Feb. 2006, pp. 321-332.

[16] Capitanescu, F. and Custem, T .V. Preventive Control of Voltage Security Margins: A Multicontingency Sensitivity-Based Approach. *IEEE Transactions on Power Systems*, vol. 17, No. 2, May 2002, pp. 358-364.

[17] Schlueter, R. A.; Alemadi, S.; and Liu, N. Preventive and Corrective Open Access Dispatch Based on the Voltage Security Stability Assessment and Diagnosis. *Electric Power System Research*, vol. 60, No. 1, Nov. 2001, pp. 17-28.

[18] Vega, D. R. and Pavella, M. A. Comprehensive Approach to Transient Stability Control: Part I-Near Optimal Preventive Control, *IEEE Transactions on Power Systems*, vol. 18, No. 8, Nov. 2003, pp. 1446-1453.

[19] Vu, H.; Pruvot, P. Launay, C.; and Harmand, Y. An Improved Voltage Control on Large-Scale Power System. *IEEE Transactions on Power Systems*, vol. 11, No. 3, Aug. 1996, pp. 1295-1303.

[20] Taylor, C. W. *Power System Voltage Stability*. McGraw-Hill 1994.

[21] Custem, T. V. *Voltage Stability of Electric Power Systems*. Kluwer Academic Publishers 1998.

[22] Salcha, J. L.; Fernandez, J. L.; Cortes A.; and Abarca, J. T. Secondary Voltage Control: Analysis, Solutions and Simulation Results for the Spanish Transmission Systems. *IEEE Transactions on Power Systems*, vol. 11, No. 2, May 1996, pp. 630-638.

[23] Conejo, A. and Aguilar, M. J. Secondary Voltage Control: Nonlinear Selection of Pilot Buses, Design of an Optimal Control Law, and Simulation Results. *IEE Proceedings-Generation, Transmission and Distribution,* vol. 145, No. 1, Jan.1998, pp. 77-81.

[24] Ilic, M. D.; Liu, X.; Leung G.; and Athans, M. Improved Secondary and New Tertiary Voltage Control. *IEEE Transactions on Power Systems*, vol. 10, No. 4, Nov. 1995, pp. 1851-1862.

[25] Shahidehpour, M.; Yamin H.; and Li, Z. *Market Operations in Electric Power Systems*. Copyright 2002, John Wiley & Sons Inc.

[26] Lai, L. L. P*ower System Restructuring and Deregulation*. Copyright 2001, John Wiley & Sons Inc.

[27] Varaiya, P. and Wu, F. MinISO: A Minimal Independent System Operator. *System Sciences 1997, Proceeding on the thirteenth Hawaii International Conference on*, vol. 5, 7-10 Jan. 2001, pp. 602-607.

[28] Wu F. F.**,** and Varaiya, P. *Coordinated Multilateral Trades for Electric Power Networks: Theory and Implementation* [Online]. Ph. D.' Thesis, Jun. 1995, Available: http://www.eecs.berkeley.edu/-varaiya.

[29] Brendan Kirby and John Kueck, *Consortium for Electric Reliability Technology Solutions Grid of the Future White Paper on Review of the Structure of Bulk Power Markets* [Online]. Dec. 1999, Available: http://certs.lbl.gov/pdf/certs-bulkpower.pdf

[30] Li Y. and Flynn, P. C. Deregulated Power Prices: Changes Over Time. *IEEE Transactions on Power Systems*, vol. 20, No. 2, May 2005, pp. 565-572.

[31] Hesmondhalgh, S. Is NETA the Blueprint for Wholesale Electricity Trading Arrangements of the Future. *IEEE Transactions on Power Systems*, vol. 18, No. 2, May 2003, pp. 548-554.

[32] Lamoureux, M. A. Evolution of Electric Utility Restructuring in the UK. *IEEE Power Engineering Review*, vol. 21, No. 6, Jun. 2001, pp. 6-9.

[33] Woo, C. K.; Lloyd, D.; and Tishler, A. Electricity Market Reform Failures: UK, Norway, Alberta and California. *Energy Policy*, vol. 31, No. 11, Sep. 2003, pp. 1103-1115.

[34] Budhraja, V. S. California's Electricity Crisis. *IEEE Power Engineering Review*, vol. 22, No. 8, Aug. 2002, pp. 6-7.

[35] Shreffins, A. California Power Crisis: Failure of Market Design or Regulation. *IEEE Power Engineering Review*, vol. 22, No. 8, Aug. 2002, pp. 8-11.

[36] Oren, F.; Alvarado, F.; Gross G.; and Mount, T. Market Redesign: *Incorporating the Lessons Learned for Enhancing Market Design; The Final Report* [Online], Available: http://www.pserc.org.

[37] Dehdashti, E. and Developing S. Countries Restructuring with Benefits from Competition (or not). *IEEE Power and Energy magazine,* vol. 2, No., Sep.-Oct. 2004, pp. 16-23.

[38] Ruff, L. E. The Proposed New Electricity Trading Arrangement for England and Wales: A Setback for Competition, Consumers, and Logic. *The Electricity Journal,* vol. 13, No. 1, Jan.-Feb. 2000, pp. 69-72.

[39] Rudnick, H. California Crisis Influences Further Reforms in Latin America. *IEEE Power Engineering Review,* vol. 22, No. 8, Aug. 2002, pp. 12-14.

[40] Rivier, M.; Perez Arriaga I. J.; and Vazquez, C. Will the California Crisis Perturb Spain's Liberalization Process. *IEEE Power Engineering Review,* vol. 22, No. 8, Aug. 2002, pp. 15-16.

[41] Chirarattananon, S and Nirukkanaporn, S. Deregulation of ESI and Privatization of State Electric Utilities in Thailand. *Energy Policy*, vol 31, No. 16, Nov. 2006, pp. 2521-2531.

[42] E. Caruso, M. Discorato, A. Minoia; and M. Ilic, The Impact of Physical Bilateral Agreements on the Wholesale Electricity Price, *Bulk Power System Dynamics and Control VI,* Cortina d'Ampazzo Italy, Aug. 22-27 2004, pp. 554-559.

[43] Andersen, A.; Dunn Barker; Rossi, D. McKenna; and Shandwick, P. *Thailand Power Pool and Electric Supply Reform Study-Phase 1, Energy Policy and Planning Office, Thailand,* [Online]. Available: http://www.eppo.go.th.

[44] Lui, Y. and Wu, F.F. Impacts of Network Constraints on Electricity Market Equibrium. *IEEE Transactions on Power Systems*, vol. 22, No. 1, Feb. 2007, pp. 126-135.

[45] Gil, H. A.; Galiana F. D. and da Silva E. L. Nodal Price Control: A Mechanism for Transmission Network Cost Allocation. *IEEE Transactions on Power Systems*, vol. 21, No. 1, Feb. 2006, pp. 3-10.

[46] Schweppe, F. C.; Caramanis, M. C.; Tabors R. D.; and R. E. Bohn, Spot Pricing of Electricity (Book), Copyright 1988, Kluwer Acadamic Publishers.

[47] Chen, L.; Suzuki, H.; Wachi, T.; and Shimura, Y. Components of Nodal Prices for Electric Power Systems. *IEEE Transactions on Power Systems*, vol. 17, No. 1, Feb. 2002, pp. 41-49.

[48] Mateus, J. C. and Franco, P. C. Transmission Loss Allocation Through Equivalent Bilateral Exchanges and Economical Analysis. *IEEE Transactions on Power Systems*, vol. 20, No. 4, Nov. 2005, pp. 1799-1807.

[49] Galiana, F. D. and Phelan, M. Allocation of Transmission Loss to Bilateral Contracts in a Competitive Environment. *IEEE Transactions on Power Systems*, vol. 15, no. 1, Feb. 2000, pp. 143-150.

[50] Gross, G. and Tao, S. Transmission Loss Compensation in Multiple Transaction Networks. *IEEE Transactions on Power Systems*, vol. 15, Aug. 2000, pp. 909-915.

[51] Gubina, F.; Grgic D.; and Banic, I. A Method for Determining the Generators Share in a Consumer Load. *IEEE Transactions on Power Systems*, vol. 15, no. 4, Nov. 2000, pp. 1376-1381.

[52] Kirschen, D.; Allan R. and Strbac, G. Contributions of Individual Generators to Load and Flows. *IEEE Transactions on Power Systems*, vol. 12, Feb. 1997, pp. 52-60.

[53] Bialek, J. Topological Generation and Load Distribution Factors for Supplement Charge Allocation in Transmission Open Access. *IEEE Transactions on Power Systems*, Vol. 12, No.3, Aug.1997, pp. 1185-1193.

[54] Wu, Z. Q. and Chen, G. Z. MVA Power Flow and Loss Analysis for electricity Market. *IEE Proceedings-Generation, Transmission and Distribution*, vol. 148, no. 2, March. 2001, pp. 153-158.

[55] Wei, P.; Yuan, B.; Ni, Y.; and Wu, F. F. Power Flow Tracing for Transmission Open Access. *Electric Utility Deregulation and Restructuring and Power Technologies* 2000, pp. 476 -481.

[56] Rosado, S. P.; Abdel-Rahman K.; and HadjSaid, N. Tracing the Path of Electric Power Flow - A Study for Deregulated Power System. *Power Engineering Society Winter Meeting*, 2001, vol. 3, 28 Jan.-1 Feb. 2001, pp. 1479-1484.

[57] Conejo, A.; Galiana, F. D. and Kockar, I. Z-bus loss allocation. *IEEE Transactions on Power Systems*, vol. 16, Feb. 2001, pp. 105-110.

[58] Tuglie, E. D. and Francesco Torelli. Nondiscriminatory System Losses Dispatching Policy in a Bilateral Transaction-Based Market. *IEEE Transactions on Power Systems*, vol. 17, No. 4, Nov. 2002, pp. 992-1000.

[59] Galiana, F. D.; Conejo, A. J.; and Kockar, I. Incremental Transmission Loss Allocation Under Pool Dispatch. *IEEE Transactions on Power Systems*, vol. 17, No.1, Feb. 2002, pp. 26-33.

[60] *Principles for Transmission Loss Methodology* [Online], Available: http://128.242.83.219/Doc/loss_principles.PDF.

[61] Conejo, A. J.; Arroyo, J. M.; Alguacil, N. and Guijarro, A. L. Transmission Loss Allocation: A Comparison of Different Practical Algorithms. *IEEE Transactions on Power Systems*, vol. 17, No. 3, Aug. 2002, pp. 571-576.

[62] Daroj, K. and Eua-arporn, B. On the Investigation of Transmission System Limit: A Two Buses Equivalent Model. *EECON-27 Thailand*.

[63] Keshavarzian, M. and Priebe, C. H Sag and Tension Calculations for Overhead Transmission Lines at High Temperatures-Modified Ruling Span Method. *IEEE Transactions on Power Delivery*, vol. 15, No. 2, Apr. 2000, pp. 777-783.

[64] Seppa, T. O. Accurate Ampacity Determination: Temperature-Sag Model for Operational Real Time Ratings. *IEEE Transactions on Power Delivery*, vol. 10, No.3, Jul. 1995, pp. 1460-1470.

[65] Seppa, T. O. Factors Influencing the Accuracy of High Temperature Sag Calculations. *IEEE Transactions on Power Delivery*, vol. 9, No. 2, Apr. 1994, pp. 1079-1089.

[66] Grijalva, S.; Sauer, P. W. and Weber, J. D. Enhancement of Linear ATC Calculations by the Incorporation of Reactive Power Flows. *IEEE Transactions on Power Systems,* vol. 18, No. 2, May 2003, pp. 619-624.

[67] Haque, M. H. Use of V–I Characteristic as a Tool to Assess the Static Voltage Stability Limit of a Power System. *IEE Proceedings-Generation, Transmission and Distribution,* vol. 151, No. 1, Jan. 2004, pp. 1-7.

[68] Vu, K.; Begovic, M. M.; Novosel D.; and Saha, M. M. Use of Local Measurements to Estimate Voltage Stability–Margin. *IEEE Transactions on Power Systems,* vol. 14, No. 3, Aug. 1999, pp. 1029-1035.

[69] Soliman, S. A.; Temraz H. K. and El-Kohdary, S. M. Power System Voltage Stability Margin Identification Using Local Measurements. *Power Engineering Conference on Large Engineering System*, May 2003, pp. 100-104.

[70] Haque, M. H. On-Line Monitoring of Maximum Permissible Loading of a Power System within Voltage Stability Limit. *IEE Proceedings–Generation, Transmission and Distribution*, vol. 150, No. 1, Jan. 2003, pp. 107-112.

[71] Haque, M. H. Determination of Steady-State Voltage Stability Limit Using P-Q Curve. *IEEE Power Engineering Review*, Apr. 2002, pp. 71-72.

[72] Cannella, M. A.; E. O. Disher; and Gagliardi, R. T. Beyond the Contract Path: A Realistic Approach to Transmission Pricing. *The Electricity Journal*, vol. 9, No.9, Nov. 1996, pp. 26-33.

[73] Shirmohammadi, D.; Rajagopalan, C.; Alward E. R.; and Thomas, C. L. Cost of Transmission Transactions: An introduction. *IEEE Transactions on Power Systems*, vol. 6, No. 3, Aug. 1991, pp. 1006-1016.

[74] Shirmohammadi, D.; Filho, X. V.; Gorenstin B.; and Pereira, M. V. P. Some Fundamental, Technical Concepts about Cost Based Transmission Pricing. *IEEE Transactions on Power Systems*, vol. 11, No. 2, May 1996, pp. 1002-1008.

[75] Rotoras, R. E.; Lefevre T.; and Pacudan, R. B. Marginal Transmission Pricing and Supplemental Cost Allocation Method: A Case of Philippines. *Electric Power Systems Research*, vol. 63, No. 3, 28 Oct. 2002, pp 213-227.

[76] Shirmoharnnadi, D.; Gribik, P. R.; Law, E. T. K.; Malinowski, J. H. and O 'Donnell, R. E. Evaluation of Transmission Network Capacity Use for Wheeling Transactions. *IEEE Transactions on Power Systems*, vol. 4, No. 4, Oct. 1989, pp. 1405-1413.

[77] Happ, H. Transmission Access Raised Unsolved Economic Issues, *IEEE Power Engineering Review*. vol. 14, No. 8, Aug. 1994, pp. 11-13.

[78] Maragon Lima, J. W. Allocation of Transmission Fixed Charges: An Overview, *IEEE Transactions on Power Systems*. vol. 11, No. 3, Aug. 1996, pp. 1409-1418.

[79] Yu, C. W. Long-run Marginal Cost Based Pricing of Interconnected System Wheeling. *Electric Power Systems Research*, vol. 50, No. 3, Jun. 1999, pp. 205-212.

[80] Galiana F. D. and Ilic, M. A Mathematical Framework for the Analysis and Management of Power Transactions Under Open Access. *IEEE Transactions on Power Systems*, vol. 13, No. 2, May 1998, pp. 681-687.

[81] Cheng, J. W.; McGillis M. D. T.; and Galiana, F. D. Bilateral Transactions Considered as Interconnections in a Deregulated Environment under Open Access. *IEEE Canadian Conference on Electrical & Computer Engineering*, vol. 2, May 1998, pp. 497-500.

[82] Saadat, H. *Power System Analysis*. Copyright 1999, McGraw-Hill Publishers.

[83] Ajjarapu, V. and Lee, B. Bibliography on Voltage Stability, *IEEE Transactions on Power Systems*. vol. 13, No. 1, Feb. 1998, pp. 115-125.

[84] Ajjarapu, V. and Christy, C. Continuation Power Flow: A Tool for Steady State Voltage Analysis. *IEEE Transactions on Power Systems*, vol. 7, No. 1, Feb.1992, pp. 416-423.

[85] Li Zarate, L. A. and Castro, C. A. Fast Method for Computing Power System Security Margins to Voltage Collapse. *IEE Proceedings-Generation, Transmission and Distribution*, vol. 151, No. 1, Jan. 2004, pp. 19-26.

[86] Tare R. S. and Bijwe, P. R. Look-Ahead Approach to Power System Loadability Enhancement. *IEE Proceedings-Generation, Transmission and Distribution*, vol. 144, No. 4, Jul. 1997, pp. 357-262.

[87] Alves, D. A.; da Silva, L. C. P.; Castro, C. A.; and da Costa, V. F. Continuation Fast Decoupled Power Flow With Secant Predictor. *IEEE Transactions on Power Systems*, vol. 18, No. 3, Aug. 2003, pp. 1078-1085.

[88] Dobson, I. and Lu, L. Computing an Optimum Direction in Control Space to Avoid Saddle Node Bifurcation and Voltage Collapse in Electric Power Systems. *IEEE Transaction on Automatic Control*, vol. 37, No. 10, Oct. 1992, pp. 1616-1620.

[89] Dobson I. and Lu, L. New Method for Computing a Closest Saddle Node Bifurcation and Worst Case Load Power Margin for Voltage Collapse. *IEEE Transactions on Power Systems*, vol. 8, No. 3, Aug. 1993, pp. 905-913.

[90] Alverado, F.; Dobson, I. and Hu, Y. Computation of Closest Bifurcations in Power Systems. *IEEE Transactions on Power Systems*, vol. 9, No. 2, May 1994, pp. 918-928.

[91] Canizares, C. A. Calculating Optimal System Parameters to Maximize the Distance to Saddle-Node Bifurcations. *IEEE Transactions on Circuits and Systems I: Fundamental Theory and Applications*, vol. 45, No.3, Mar. 1998, pp. 225-236.

[92] Canizares, C. A.; de Souza A. C. Z.; and Quintana, V. H. Comparison of Performance Indices for Detection Proximity to Voltage Collapse. *IEEE Transactions on Power Systems,* vol. 11, No. 3, Aug. 1996, pp. 1441-1450

[93] *NERC Operating Manual, Appendix 9C1-Transmission Loading Relief Procedure, Version 2* [Online]. Available : http://www.nerc.com

[94] *North American Electric Reliability Council (September 1999), Transmission Loading Relief: Possible Improvements and Long-term Solutions* [Online]. Available: http://www.nerc.com.

[95] Rajaraman; R. and Alvarado, F. L. Inefficiencies of NERC's Transmission Loading Relief Procedures. *The Electricity Journal,* vol. 11, No. 8, Oct. 1998, pp. 47-54.

[96] Bialek, J. W.; Germond, A.; and Cherkaoui**,** R. Improving NERC Transmission Loading Relief Procedures. *The Electricity Journal*, vol. 13, No. 5, Jun. 2000, pp.11-19

[97] Fang, R. S. and David, A. K. Optimal Dispatch under Transmission Contracts. *IEEE Transactions on Power Systems*, vol. 14, No. 2, May 1999, pp. 732-737.

[98] David, A. K. Dispatch Methodologies for Open Transmission Systems. *IEEE Transactions on Power Systems,* vol. 13, No. 1, Feb. 1998, pp. 46-53.

[99] Alomoush M. I. and Shahidehpour, S. M. Contingency-Constrained Congestion Management with a Minimum Number of Adjustments in Preferred Schedules. *International Journal of Electrical Power & Energy Systems,* vol. 22, No. 4, May 2000, pp. 277-290.

[100] Kumar, A.; Srivastava, S. C.; and Singh, S. N. A Zonal Congestion Management Approach Using Real and Reactive Power Rescheduling. *IEEE Transactions on Power Systems*, vol. 19, No. 1, Feb. 2004 pp. 554-562.

[101] Wang, Xing; Song, Yong-Hua; and Qiang, Lu. A Coordinated Real-Time Optimal Dispatch Method for Unbundled Electricity Markets. *IEEE Transactions on Power Systems*, vol. 17, No. 2, May 2002, pp. 482-490.

[102] Alvarado, F. L. Converting System Limits to Market Signals. *IEEE Transactions on Power Systems*, vol. 18, No. 2, May 2003, pp. 422-427.

[103] Kumar, A. and Srivastava, S. C. AC Power Transfer Distribution Factors for Allocating Power Transactions in a Deregulated Market. *IEEE Power Engineering Review*, vol. 22, No. 7, Jul. 2002, pp. 42-43

[104] Fradi, A.; Brignone, S. and Wollenberg, B. F. Calculation of Energy Transaction Allocation Factors. *IEEE Transactions on Power Systems*, vol. 16, No. 2, May 2001, pp. 266-272.

[105] Liu, M. and Gross, G. Role of Distribution Factors in Congestion Revenue Rights Applications. *IEEE Transactions on Power Systems*, vol.19, No. 2, May 2004, pp. 802-810.

[106] Yan, H. H. PTDF and TLR from a power marketer's perspective. *IEEE Power Engineering Summer Meeting 1999*, vol. 1, 18-22 Jul., pp.156-161.

[107] Cheng X. and Overbye, T. J. PTDF-based power system equivalents. *IEEE Transactions on Power Systems*, vol. 20, No. 4, Nov. 2005, pp.1868-1876.

[108] Deqiang, G. and Litvinov, E. Energy and Reserve Market Designs with Explicit Consideration to Lost Opportunity Costs. *IEEE Transactions on Power Systems*, vol. 18, No. 1, Feb. 2003, pp.53-59.

[109] Bhattacharya, K. and Zhong, J. Reactive Power as an Ancillary Service, *IEEE Transactions on Power Systems*. vol. 16, No. 2, May 2001, pp. 294-300.

[110] Lamont, J. W. and Fu, J. Cost analysis of reactive power support. *IEEE Transactions on Power Systems*, vol. 14, No. 3, Aug. 1999, pp. 890-898.

[111] Gross, G.; Tao, S.; Bompard E. and Chicco, G. Unbundled Reactive Support Service: Key Characteristics and Dominant Cost Component. *IEEE Transactions on Power Systems*, vol. 17, No. 2, May 2002, pp. 283-289.

[112] Jian, F. and Lamont, J. W. A Combined Framework for Service Identification and Congestion Management. *IEEE Transactions on Power Systems,* vol. 16, No. 1, Feb. 2001, pp. 56-61.

[113] Kockar I. and Galiana, F. D. Combined Pool/Bilateral Dispatch. II. Curtailment of Firm and Nonfirm Contracts. *IEEE Transactions on Power Systems,* vol.17, No. 4, Nov. 2002, pp. 1184-1190.

[114] Rau, N. S. Transmission Loss and Congestion Cost Allocation-An Approach Based on Responsibility. *IEEE Transactions on Power Systems,* vol. 15, No. 4, Nov. 2000, pp. 1401-1409.

APPENDICES

APPENDIX A

A1: A Modified 6-Bus System

A1.1 Bus Data for Loss Allocation (Chapter 4)

Bus		Voltage	Pgen	Pload	Qload
No.	Type	(p.u.)	(MW)	(MW)	(MVAr)
1	PV	1.05	100	-	-
2	PV	1.05	80	-	-
3	PV	1.05	120	-	-
4	PQ	-	-	80	40
5	PQ	-	-	100	50
6	PQ	-	-	120	60

A1.2 Bus Data for Transmission Line Loading Margin Evaluation (Chapter 5)

Bus		Voltage	Pgen	Pload	Qload
No.	Type	(p.u.)	(MW)	(MW)	(MVAr)
1	PV	1.00	90	-	-
2	PV	1.00	80	-	-
3	Slack	1.00	Not Specified	-	-
4	PQ	-	-	180	90
5	PQ	-	-	135	67.5
6	PQ	-	-	90	45

A1.3 Bus Data for Congestion Management in Bilateral Markets (Chapter 6)

Bus		Voltage	Pgen	Pload	Qload
No.	Type	(p.u.)	(MW)	(MW)	(MVAr)
1	Slack	1.02	Not Specified	-	-
2	PV	1.02	50	-	-
3	PV	1.02	60	-	-
4	PQ	-	-	40	30
5	PQ	-	-	50	40
6	PQ	-	-	60	40

A1.4 Transmission Line Data

Bus		R	X	(1/2)B	Limit
From	To	(p.u.)	(p.u.)	(p.u.)	(MVA)
1	2	0.10	0.20	0.01	30
1	4	0.05	0.20	0.01	50
1	5	0.08	0.30	0.015	40
2	3	0.05	0.25	0.015	30
2	4	0.05	0.10	0.005	40
2	5	0.10	0.30	0.01	20
2	6	0.07	0.20	0.0125	30
3	5	0.12	0.26	0.0125	20
3	6	0.02	0.10	0.005	70
4	5	0.20	0.40	0.02	20
5	6	0.10	0.30	0.015	20

* Generation power and reactive power of all units are assumed to be no limited for all cases.

A1.5 NETWORK TOPOLOGY

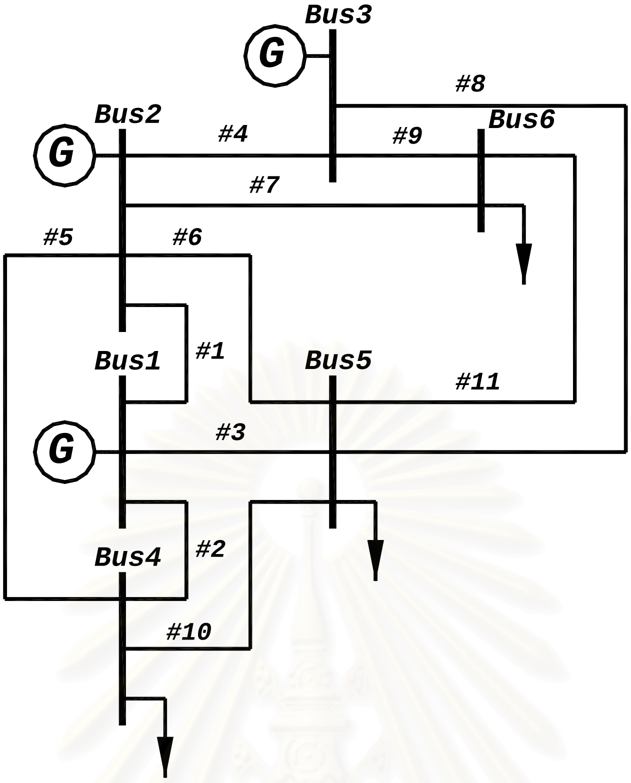

A2: IEEE 30-BUS SYSTEM

A2.1 BUS DATA

Bus		Voltage	Pgen	Pload	Qload	Capacitor
No.	Type	(pu)	(MW)	(MW)	(MVAr)	(MVAr)
1	Slack	1.06	Not Specified	0	0	0
2	PV	1.043	40	21.7	12.7	0
3	PQ	-	-	2.4	1.2	0
4	PQ	-	-	7.6	1.6	0
5	PV	1.01	0	94.2	19	0
6	PQ	-	-	0	0	0
7	PQ	-	-	22.8	10.9	0
8	PV	1.01	0	30	30	0
9	PQ	-	-	0	0	0
10	PQ	-	-	5.8	2	19
11	PV	1.082	0	0	0	0
12	PQ	-	-	11.2	7.5	0
13	PV	1.071	0	0	0	0
14	PQ	-	-	6.2	1.6	0
15	PQ	-	-	8.2	2.5	0
16	PQ	-	-	3.5	1.8	0
17	PQ	-	-	9	5.8	0
18	PQ	-	-	3.2	0.9	0
19	PQ	-	-	9.5	3.4	0
20	PQ	-	-	2.2	0.7	0
21	PQ	-	-	17.5	11.2	0
22	PQ	-	-	0	0	0
23	PQ	-	-	3.2	1.6	0
24	PQ	-	-	8.7	6.7	4.3
25	PQ	-	-	0	0	0
26	PQ	-	-	3.5	2.3	0
27	PQ	-	-	0	0	0
28	PQ	-	-	0	0	0
29	PQ	-	-	2.4	0.9	0
30	PQ	-	-	10.6	1.9	0

A2.2 Transmission Line Data

Bus		R	X	(1/2)B	Transformer
From	To	(p.u.)	(p.u.)	(p.u.)	Tap
1	2	0.0192	0.0575	0.0264	-
1	3	0.0452	0.1852	0.0204	-
2	4	0.0570	0.1737	0.0184	-
3	4	0.0132	0.0379	0.0042	-
2	5	0.0472	0.1983	0.0209	-
2	6	0.0581	0.1763	0.0187	-
4	6	0.0119	0.0414	0.0045	-
5	7	0.0460	0.1160	0.0102	-
6	7	0.0267	0.0820	0.0085	-
6	8	0.0120	0.0420	0.0045	-
6	9	0	0.2080	0	0.978
6	10	0	0.5560	0	0.969
9	11	0	0.2080	0	-
9	10	0	0.1100	0	-
4	12	0	0.2560	0	0.932
12	13	0	0.1400	0	-
12	14	0.1231	0.2559	0	-
12	15	0.0662	0.1304	0	-
12	16	0.0945	0.1987	0	-
14	15	0.2210	0.1997	0	-
16	17	0.0824	0.1923	0	-
15	18	0.1073	0.2185	0	-
18	19	0.0639	0.1292	0	-
19	20	0.0340	0.0680	0	-
10	20	0.0936	0.2090	0	-
10	17	0.0324	0.0845	0	-
10	21	0.0348	0.0749	0	-
10	22	0.0727	0.1499	0	-
21	22	0.0116	0.0236	0	-
15	23	0.1000	0.2020	0	-
22	24	0.1150	0.1790	0	-
23	24	0.1320	0.2700	0	-
24	25	0.1885	0.3292	0	-
25	26	0.2544	0.3800	0	-
25	27	0.1093	0.2087	0	-
28	27	0.0000	0.3960	0	0.968
27	29	0.2198	0.4153	0	-
27	30	0.3202	0.6027	0	-
29	30	0.2399	0.4533	0	-
8	28	0.0636	0.2000	0.0214	-
6	28	0.0169	0.0599	0.0650	-

*Generation power and reactive power limits are neglected for IEEE 30-bus system.

A3: A 28-Bus Thailand Region 2 System

A3.1 Bus Data

Bus		Voltage	Pgen	Pload	Qload	Capacitor
No.	Type	(pu)	(MW)	(MW)	(MVAr)	(MVAr)
1	Slack	1.04	Not Specified	0.0	0.0	-
2	PQ	-	-	101.0	10.0	-
3	PQ	-	-	51.4	25.1	10
4	PV	1.04	-	52.0	25.2	10
5	PQ	-	-	62.2	8.2	-
6	PQ	-	-	108.0	46.0	20
7	PQ	-	-	17.5	6.8	10
8	PQ	-	-	52.7	10.1	10
9	PQ	-	-	23.4	9.8	10
10	PQ	-	-	163.4	75.1	40
11	PQ	-	-	48.6	14.9	10
12	PQ	-	-	35.4	13.9	10
13	PQ	-	-	48.7	18.3	20
14	PQ	-	-	130.5	74.6	60

Bus		Voltage	Pgen	Pload	Qload	Capacitor
No.	Type	(pu)	(MW)	(MW)	(MVAr)	(MVAr)
15	PV	1.04	200	0.0	0.0	-
16	PV	1.04	200	0.0	0.0	-
17	PQ	-	-	118.3	53.8	20
18	PV	1.04	660	0.0	0.0	-
19	PQ	-	-	132.3	59.8	20
20	PQ	-	-	45.5	15.2	10
21	PQ	-	-	83.3	37.3	20
22	PQ	-	-	279.1	108.9	80
23	PQ	-	-	50.3	19.0	10
24	PQ	-	-	47.1	20.6	20
25	PQ	-	-	56.9	25.2	20
26	PQ	-	-	54.0	19.3	10
27	PV	1.04	40	0.0	0.0	-
28	PV	1.04	100	0.0	0.0	-

A3.2 TRANSMISSION LINE DATA

Bus		R	X	(1/2)B	Limit
From	To	(p.u.)	(p.u.)	(p.u.)	(MVA)
1	2	0.0056	0.0434	0.1634	950
1	3	0.0083	0.0555	0.0285	700
2	4	0.0291	0.0856	0.0111	130
2	5	0.0043	0.0389	0.1278	950
2	7	0.0259	0.0761	0.0099	130
3	4	0.0162	0.0482	0.0060	130
5	6	0.0031	0.0184	0.1098	950
5	7	0.0634	0.1865	0.0243	130
6	8	0.0560	0.1800	0.0456	260
6	10	0.0144	0.1129	0.4256	950
8	9	0.0528	0.1552	0.0202	130
8	10	0.1787	0.5253	0.0684	130
9	10	0.1285	0.0378	0.0492	130
10	11	0.2161	0.3762	0.0394	78
9	10	0.1285	0.0378	0.0492	130
10	11	0.2161	0.3762	0.0394	78
10	15	0.0021	0.0201	0.0759	950
10	17	0.0030	0.0294	0.2852	1900
10	18	0.0038	0.0300	0.1132	950
11	12	0.0427	0.0728	0.0079	88
12	13	0.0385	0.1145	0.0292	260
12	14	0.0189	0.1265	0.0355	300
12	15	0.0308	0.1099	0.0608	360
12	16	0.1849	0.3187	0.0170	88
13	14	0.0180	0.0530	0.0069	130
16	17	0.0039	0.0281	0.0128	950
16	21	0.1607	0.2770	0.0295	88
17	19	0.0021	0.0202	0.0763	950
17	21	0.0502	0.1475	0.0192	130
17	28	0.0051	0.0529	0.4471	1900
18	19	0.0050	0.0383	0.1444	950
19	20	0.0045	0.0352	0.1326	950
20	21	0.1207	0.2057	0.0224	88
20	22	0.0044	0.0346	0.1304	950
20	23	0.1553	0.2649	0.0288	88
22	23	0.0057	0.0122	0.0030	200
22	24	0.0482	0.1417	0.0369	260
22	28	0.0008	0.0078	0.0658	1900
24	25	0.0399	0.1187	0.0151	130
25	26	0.0874	0.1883	0.0227	100
25	27	0.0004	0.0026	0.0014	700
26	27	0.0550	0.1800	0.0280	100
27	28	0.0031	0.0305	0.2953	950

APPENDIX B

B1: DC PTDF

For a DC power flow approximation, the power flow from *bus-i* to *bus-j* can be expressed as (B1), which can be shown in a matrix form as (B2).

$$P_{ij} = \frac{\delta_i - \delta_j}{x_{ij}} \tag{B1}$$

$$[\theta] = [X][P] \tag{B2}$$

where

P_{ij}	is a real power flow from *bus-i* to *bus-j*,
δ_i and δ_j	are voltage angle of *bus-i* and *bus-j* respectively,
x_{ij}	is a reactance of line connected between *bus-i* and *bus-j*,
$[\theta]$	is a system voltage angle matrix,
$[X]$	is a system reactance matrix,
$[P]$	is a system scheduled power matrix.

To obtain DC PTDF, we first calculate a Generation Shift Factor ($GSF_{l,g}$), which can be defined as an incremental change of power flow through line *l*, connected between *bus-i* and *bus-j* to injected power at *bus-g* as below.

$$GSF_{l,g} = \frac{\partial P_{ij}}{\partial P_g} \tag{B3}$$

Using (B1), (B3) can be written as (B4), which can be simplified to (B5)

$$GSF_{l,g} = \frac{\Delta\left[\frac{1}{x_{ij}}\left(\delta_i - \delta_j\right)\right]}{\Delta P_g} \tag{B4}$$

$$GSF_{l,g} = \frac{1}{x_{ij}}\left[\frac{\Delta\delta_i - \Delta\delta_j}{\Delta P_g}\right] \tag{B5}$$

The terms in bracket of (B5) can be replaced with elements of $[X]$ as shown in (B6).

$$GSF_{l,g} = \frac{1}{x_{ij}}\left[X_{ig} - X_{jg} \right] \tag{B6}$$

From the above derivations, a DC PTDF of transaction between source at *bus-g* and sink at *bus-d* contributed to a real power flow through line *l*, which is denoted as $PTDF_{g,d}^{l}$, can be expressed as below.

$$PTDF_{g,d}^{l} = GSF_{l,g} - GSF_{l,d} \tag{B7}$$

Substitute *GSF* of (B7) from (B6) result in (B8) and can be simplified to (B9).

$$PTDF_{g,d}^{l} = \frac{1}{x_{ij}}\left[X_{ig} - X_{jg} \right] - \frac{1}{x_{ij}}\left[X_{id} - X_{jd} \right] \tag{B8}$$

$$PTDF_{g,d}^{l} = \frac{1}{x_{ij}}\left[\left(X_{ig} + X_{id} \right) - \left(X_{jg} + X_{jd} \right) \right] \tag{B9}$$

B2: AC PTDF

In AC power flow, real power flow from *bus-i* to *bus-j* can be expressed by (B10)

$$P_{ij} = V_i V_j Y_{ij} \cos\left(\theta_{ij} - \delta_i + \delta_j \right) - V_i^2 Y_{ij} \cos\theta_{ij} \tag{B10}$$

where

V_i	is the voltage magnitude at *bus-i*,
V_j	is the voltage magnitude at *bus-j*,
Y_{ij}	is the magnitude of bus-admittance matrix elements at *row-i* and *column-j*,
θ_{ij}	is the angle of Y_{ij},
δ_i	is the angle of V_i, and
δ_j	is the angle of V_j.

To obtain an incremental change of real power flow defined by (B10) to an injected power at each bus, denoted as $\partial P_{ij} / \partial P_m$, we first calculate $\partial P_{ij} / \partial \delta_m$ and $\partial P_{ij} / \partial V_k$, which can be calculated from (B11) and (B12) respectively.

$$\frac{\partial P_{ij}}{\partial \delta_m} = \sum_{u \in m}\left[\frac{\partial P_{ij}}{\partial P_u} \cdot \frac{\partial P_u}{\partial \delta_m} \right] + \sum_{w \in k}\left[\frac{\partial P_{ij}}{\partial Q_w} \cdot \frac{\partial Q_w}{\partial \delta_m} \right] \tag{B11}$$

$$\frac{\partial P_{ij}}{\partial V_k} = \sum_{u \in m}\left[\frac{\partial P_{ij}}{\partial P_u}\cdot\frac{\partial P_u}{\partial V_k}\right] + \sum_{w \in k}\left[\frac{\partial P_{ij}}{\partial Q_w}\cdot\frac{\partial Q_w}{\partial V_k}\right]. \tag{B12}$$

Subscript m represents all buses except the slack bus and k represents all the load buses.

The relationships of (B11) and (B12) can be presented in a matrix form as (B13)

$$\begin{bmatrix} \dfrac{\partial P_{ij}}{\partial \delta_m} \\ \dfrac{\partial P_{ij}}{\partial V_k} \end{bmatrix} = \left[J\right]^T \begin{bmatrix} \dfrac{\partial P_{ij}}{\partial P_m} \\ \dfrac{\partial P_{ij}}{\partial Q_k} \end{bmatrix}. \tag{B13}$$

$\left[J\right]$ is a conventional Jacobian matrix, which can be divided into J_1, J_2, J_3 and J_4. The terms $\partial P_{ij} / \partial \delta_m$ and $\partial P_{ij} / \partial V_k$ are zero everywhere excepted where the index of bus m and k are either i or j, which provides non-zero values and can be calculated from (B14) to (B17) respectively.

$$\frac{\partial P_{ij}}{\partial \delta_i} = V_i V_j Y_{ij}\, sin\left(\theta_{ij} - \delta_i + \delta_j\right) \tag{B14}$$

$$\frac{\partial P_{ij}}{\partial \delta_j} = -V_i V_j Y_{ij}\, sin\left(\theta_{ij} - \delta_i + \delta_j\right) \tag{B15}$$

$$\frac{\partial P_{ij}}{\partial V_i} = V_j Y_{ij}\, cos\left(\theta_{ij} - \delta_i + \delta_j\right) - 2V_i Y_{ij}\, cos\,\theta_{ij} \tag{B16}$$

$$\frac{\partial P_{ij}}{\partial V_j} = V_i Y_{ij}\, cos\left(\theta_{ij} - \delta_i + \delta_j\right) \tag{B17}$$

To obtain the term $\partial P_{ij} / \partial P_m$, we can rearrange (B13) into (B18).

$$\begin{bmatrix} \dfrac{\partial P_{ij}}{\partial P_m} \\ \dfrac{\partial P_{ij}}{\partial Q_k} \end{bmatrix} = \left[J^T\right]^{-1} \begin{bmatrix} \dfrac{\partial P_{ij}}{\partial \delta_m} \\ \dfrac{\partial P_{ij}}{\partial V_k} \end{bmatrix} \tag{B18}$$

The obtained results of $\partial P_{ij} / \partial P_m$ of all buses m except a slack bus can be used to defined an AC PTDF. Eventually, for a transaction between source at *bus-g* and sink at *bus-d* that contributed to a real power flow through line *l*, which is denoted as $PTDF_{g,d}^{l}$, can be expressed as (B19).

$$PTDF_{g,d}^{l} = \frac{\partial P_{ij}}{\partial P_g} - \frac{\partial P_{ij}}{\partial P_d} \tag{B19}$$

It should be noted that the term $\partial P_{ij} / \partial Q_k$ is a by product that can be used to handle MVA flow limit of line, which can be presented in Appendix C. In addition, $PTDF_{g,d}^{l}$ obtained from (B9) and (B18) have slightly differences. The former is independent from the operating condition and a selected slack bus. In contrast, both operating condition and a selected slack have impact to the latter one.

APPENDIX C

C1: THE PREDICTED GRADIENT VECTOR

To calculate the gradient vector of each receiving end line flow from a specified loading scenario, we define the set of buses as $\mathbb{N} = \{s, G, L\}$, where *s* refers to a slack bus, *G* is a set of generation buses, and *L* is a set of load buses.

From Fig.1, the real and reactive power flow into the receiving end bus can be expressed in (C1) and (C2) respectively.

$$P_{ijr} = V_j^{\,2} Y_{ij} \cos\theta_{ij} - V_i V_j Y_{ij} \cos\left(\theta_{ij} + \delta_i - \delta_j\right) \quad \text{(C1)}$$

$$Q_{ijr} = V_i V_j Y_{ij} \sin\left(\theta_{ij} + \delta_i - \delta_j\right) - V_j^{\,2}\left(Y_{ij} \sin\theta_{ij} - Yc\right) \quad \text{(C2)}$$

$Y_{ij}\angle\theta_{ij}$ represents elements of the bus admittance matrix.

First we need to calculate sensitivity factors of the real and reactive power flowing into the receiving end bus compared to the real and reactive power injected into the generation and load buses, i.e. $\partial P_{ijr} / \partial P_m$, $\partial Q_{ijr} / \partial P_m$, $\partial P_{ijr} / \partial Q_k$ and $\partial Q_{ijr} / \partial Q_k$, where *m* and *k* represent all buses except the slack bus and all the load buses respectively. All the sensitivity factors can be expressed as shown in (C3)–(C6).

$$\frac{\partial P_{ijr}}{\partial \delta_m} = \sum_{u,m \in G \cup L} \left[\frac{\partial P_{ijr}}{\partial P_u} \cdot \frac{\partial P_u}{\partial \delta_m} \right] + \sum_{m \in G \cup L, w \in L} \left[\frac{\partial P_{ijr}}{\partial Q_w} \cdot \frac{\partial Q_w}{\partial \delta_m} \right] \quad \text{(C3)}$$

$$\frac{\partial P_{ijr}}{\partial V_k} = \sum_{u \in G \cup L, k \in L} \left[\frac{\partial P_{ijr}}{\partial P_u} \cdot \frac{\partial P_u}{\partial V_k} \right] + \sum_{w,k \in L} \left[\frac{\partial P_{ijr}}{\partial Q_w} \cdot \frac{\partial Q_w}{\partial V_k} \right] \quad \text{(C4)}$$

$$\frac{\partial Q_{ijr}}{\partial \delta_m} = \sum_{u,m \in G \cup L} \left[\frac{\partial Q_{ijr}}{\partial P_u} \cdot \frac{\partial P_u}{\partial \delta_m} \right] + \sum_{m \in G \cup L, w \in L} \left[\frac{\partial Q_{ijr}}{\partial Q_w} \cdot \frac{\partial Q_w}{\partial \delta_m} \right] \quad \text{(C5)}$$

$$\frac{\partial Q_{ijr}}{\partial V_k} = \sum_{u \in G \cup L, k \in L} \left[\frac{\partial Q_{ijr}}{\partial P_u} \cdot \frac{\partial P_u}{\partial V_k} \right] + \sum_{w,k \in L} \left[\frac{\partial Q_{ijr}}{\partial Q_w} \cdot \frac{\partial Q_w}{\partial V_k} \right] \quad \text{(C6)}$$

(C3) and (C4) can be represented by (C7),

$$\begin{bmatrix} \dfrac{\partial P_{ijr}}{\partial \delta_m} \\ \dfrac{\partial P_{ijr}}{\partial V_k} \end{bmatrix} = \left[J \right]^T \begin{bmatrix} \dfrac{\partial P_{ijr}}{\partial P_m} \\ \dfrac{\partial P_{ijr}}{\partial Q_k} \end{bmatrix} \tag{C7}$$

whereas (C5) and (C6) can be represented by (C8).

$$\begin{bmatrix} \dfrac{\partial Q_{ijr}}{\partial \delta_m} \\ \dfrac{\partial Q_{ijr}}{\partial V_k} \end{bmatrix} = \left[J \right]^T \begin{bmatrix} \dfrac{\partial Q_{ijr}}{\partial P_m} \\ \dfrac{\partial Q_{ijr}}{\partial Q_k} \end{bmatrix} \tag{C8}$$

The terms $\partial P_{ijr} / \partial \delta_m$, $\partial P_{ijr} / \partial V_k$, $\partial Q_{ijr} / \partial \delta_m$ and $\partial Q_{ijr} / \partial V_k$ are zero for every bus except *bus–i* and *bus–j*, of which the values can be obtained from (C9)–(C14).

$$\frac{\partial P_{ijr}}{\partial \delta_i} = -\frac{\partial P_{ijr}}{\partial \delta_j} = V_i V_j Y_{ij}\, sin\left(\theta_{ij} + \delta_i - \delta_j\right) \tag{C9}$$

$$\frac{\partial P_{ijr}}{\partial V_i} = -V_j Y_{ij}\, cos\left(\theta_{ij} + \delta_i - \delta_j\right) \tag{C10}$$

$$\frac{\partial P_{ijr}}{\partial V_j} = 2V_j Y_{ij}\, cos\left(\theta_{ij}\right) - V_i Y_{ij}\, cos\left(\theta_{ij} + \delta_i - \delta_j\right) \tag{C11}$$

$$\frac{\partial Q_{ijr}}{\partial \delta_i} = -\frac{\partial Q_{ijr}}{\partial \delta_j} = V_i V_j Y_{ij}\, cos\left(\theta_{ij} + \delta_i - \delta_j\right) \tag{C12}$$

$$\frac{\partial Q_{ijr}}{\partial V_i} = V_j Y_{ij}\, sin\left(\theta_{ij} + \delta_i - \delta_j\right) \tag{C13}$$

$$\frac{\partial Q_{ijr}}{\partial V_j} = V_i Y_{ij}\, sin\left(\theta_{ij} + \delta_i - \delta_j\right) - 2V_j\left(Y_{ij}\, sin\left(\theta_{ij}\right) - Yc\right) \tag{C14}$$

$\left[J \right]$ is a conventional Jacobian matrix, which can be divided into J_1, J_2, J_3 and J_4. J_1 is an *m x m* matrix, of which the diagonal and off–diagonal elements are presented in (C15) and (C16).

$$\frac{\partial P_i}{\partial \delta_i} = \sum_{j=1,\neq i}^{n} V_i V_j Y_{ij}\, sin(\theta_{ij} - \delta_i + \delta_j),\ i \in G \cup L \tag{C15}$$

$$\frac{\partial P_i}{\partial \delta_j} = -V_i V_j Y_{ij}\, sin(\theta_{ij} - \delta_i + \delta_j), j \neq i\,, \tag{C16}$$

J_2 is a *m x k* matrix, of which the diagonal and off–diagonal elements are shown in (C17) and (C18) respectively.

$$\frac{\partial P_i}{\partial V_i} = 2V_i Y_{ii}\, cos(\theta_{ii}) + \sum_{j=1,\neq i}^{n} V_j Y_{ij}\, cos(\theta_{ij} - \delta_i + \delta_j),\ i \in L \tag{C17}$$

$$\frac{\partial P_i}{\partial V_j} = V_i Y_{ij}\, cos(\theta_{ij} - \delta_i + \delta_j), j \neq i\,, \tag{C18}$$

J_3 is a *k x m* matrix, of which the diagonal and off–diagonal elements are shown by (C19) and (C20) respectively.

$$\frac{\partial Q_i}{\partial \delta_i} = \sum_{j=1,\neq i}^{n} V_i V_j Y_{ij}\, cos(\theta_{ij} - \delta_i + \delta_j),\ i \in G \cup L \tag{C19}$$

$$\frac{\partial Q_i}{\partial \delta_j} = -V_i V_j Y_{ij}\, cos(\theta_{ij} - \delta_i + \delta_j), j \neq i \tag{C20}$$

J_4 is a *k x k* matrix whose diagonal and off–diagonal elements are expressed by (C21) and (C22).

$$\frac{\partial P_i}{\partial V_i} = -2V_i Y_{ij}\, sin(\theta_{ii}) - \sum_{j=1,\neq i}^{n} V_j Y_{ij}\, sin(\theta_{ij} - \delta_i + \delta_j),\ i \in L \tag{C21}$$

$$\frac{\partial Q_i}{\partial V_j} = -V_i Y_{ij}\, sin(\theta_{ij} - \delta_i + \delta_j), j \neq i \tag{C22}$$

Using (C15)–(C22), we can rewrite (C7) and (C8) as (C23) and (C24) respectively.

$$\begin{bmatrix} \dfrac{\partial P_{ijr}}{\partial P_m} \\ \dfrac{\partial P_{ijr}}{\partial Q_k} \end{bmatrix} = \begin{bmatrix} J_1 & J_3 \\ J_2 & J_4 \end{bmatrix}^{-1} \begin{bmatrix} \dfrac{\partial P_{ijr}}{\partial \delta_m} \\ \dfrac{\partial P_{ijr}}{\partial V_k} \end{bmatrix} \tag{C23}$$

สถาบันวิทยบริการ
จุฬาลงกรณ์มหาวิทยาลัย

$$\begin{bmatrix} \dfrac{\partial Q_{ijr}}{\partial P_m} \\ \dfrac{\partial Q_{ijr}}{\partial Q_k} \end{bmatrix} = \begin{bmatrix} J_1 & J_3 \\ J_2 & J_4 \end{bmatrix}^{-1} \begin{bmatrix} \dfrac{\partial Q_{ijr}}{\partial \delta_m} \\ \dfrac{\partial Q_{ijr}}{\partial V_k} \end{bmatrix} \tag{C24}$$

We can solve (C23) and (C24) to obtain $\partial P_{ijr} / \partial P_m$, $\partial Q_{ijr} / \partial P_m$, $\partial P_{ijr} / \partial Q_k$ and $\partial Q_{ijr} / \partial Q_k$, which can be used to calculate the gradient vector of each receiving end line flow, denoted as $\Delta P_{ijr} + j\Delta Q_{ijr}$. Equations (C25) and (C26) are used to calculate such gradient vectors.

$$\Delta P_{ijr} = \sum_{m \in G \cup L} \left[\frac{\partial P_{ijr}}{\partial P_m} . \Delta P_m \right] + \sum_{k \in L} \left[\frac{\partial P_{ijr}}{\partial Q_k} . \Delta Q_k \right] \tag{C25}$$

$$\Delta Q_{ijr} = \sum_{m \in G \cup L} \left[\frac{\partial Q_{ijr}}{\partial P_m} . \Delta P_m \right] + \sum_{k \in L} \left[\frac{\partial Q_{ijr}}{\partial Q_k} . \Delta Q_k \right] \tag{C26}$$

The terms ΔP_m and ΔQ_k in (C25) and (C26) are referred to an incremental change of the real and reactive power at buses *m* and *k* respectively.

สถาบันวิทยบริการ
จุฬาลงกรณ์มหาวิทยาลัย

APPENDIX D

D1: LINEARLIZE TRANSMISSION LINE THERMAL LIMIT

To handle the transmission line thermal limit, we considered both real and reactive power flow. In Appendix B, we derived the terms $\partial P_{ij} / \partial P_m$ and $\partial P_{ij} / \partial Q_k$. In this section, we extend our previous formulation to obtain the terms $\partial Q_{ij} / \partial P_m$ and $\partial Q_{ij} / \partial Q_k$ which can be described as follow.

In AC power flow, reactive power flow from *bus-i* to *bus-j*, Q_{ij} can be expressed by (D1)

$$Q_{ij} = V_i^2 Y_{ij} \sin\theta_{ij} - V_i^2 Y_c - V_i V_j Y_{ij} \sin\left(\theta_{ij} - \delta_i + \delta_j\right) \qquad \text{(D1)}$$

where the term Y_c represent a half of line charging admittance.

To obtain an incremental change of reactive power flow of (B10) to an injected real and reactive power at each bus, denoted as $\partial Q_{ij} / \partial P_m$ and $\partial Q_{ij} / \partial Q_k$, we first calculate $\partial Q_{ij} / \partial \delta_m$ and $\partial Q_{ij} / \partial V_k$, which can be calculated from (D2) and (D3) respectively.

$$\frac{\partial Q_{ij}}{\partial \delta_m} = \sum_{u \in m} \left[\frac{\partial Q_{ij}}{\partial P_u} . \frac{\partial P_u}{\partial \delta_m} \right] + \sum_{w \in k} \left[\frac{\partial Q_{ij}}{\partial Q_w} . \frac{\partial Q_w}{\partial \delta_m} \right] \qquad \text{(D2)}$$

$$\frac{\partial Q_{ij}}{\partial V_k} = \sum_{u \in m} \left[\frac{\partial Q_{ij}}{\partial P_u} . \frac{\partial P_u}{\partial V_k} \right] + \sum_{w \in k} \left[\frac{\partial Q_{ij}}{\partial Q_w} . \frac{\partial Q_w}{\partial V_k} \right]. \qquad \text{(D3)}$$

The relationships of (D2) and (D3) can be presented in a matrix form as (C4)

$$\begin{bmatrix} \dfrac{\partial Q_{ij}}{\partial \delta_m} \\ \dfrac{\partial Q_{ij}}{\partial V_k} \end{bmatrix} = \left[J \right]^T \begin{bmatrix} \dfrac{\partial Q_{ij}}{\partial P_m} \\ \dfrac{\partial Q_{ij}}{\partial Q_k} \end{bmatrix}. \qquad \text{(D4)}$$

Likewise, the terms $\partial Q_{ij} / \partial \delta_m$ and $\partial Q_{ij} / \partial V_k$ are zero everywhere excepted where the index of bus *m* and *k* are either *i* or *j*, which provides non-zero values and can be calculated from (D5) to (D8).

$$\frac{\partial Q_{ij}}{\partial \delta_i} = -V_i V_j Y_{ij} \cos\left(\theta_{ij} - \delta_i + \delta_j\right) \qquad \text{(D5)}$$

$$\frac{\partial Q_{ij}}{\partial \delta_j} = V_i V_j Y_{ij}\, cos\left(\theta_{ij} - \delta_i + \delta_j\right) \tag{D6}$$

$$\frac{\partial Q_{ij}}{\partial V_i} = 2V_i Y_{ij}\, sin\,\theta_{ij} - 2V_i Y_c - V_j Y_{ij}\, sin\left(\theta_{ij} - \delta_i + \delta_j\right) \tag{D7}$$

$$\frac{\partial Q_{ij}}{\partial V_j} = -V_i Y_{ij}\, sin\left(\theta_{ij} - \delta_i + \delta_j\right) \tag{D8}$$

To obtain the terms $\partial Q_{ij} / \partial P_m$ and $\partial Q_{ij} / \partial Q_k$, rearrange (D4) into (D9).

$$\begin{bmatrix} \dfrac{\partial Q_{ij}}{\partial P_m} \\ \dfrac{\partial Q_{ij}}{\partial Q_k} \end{bmatrix} = \left[J^T \right]^{-1} \begin{bmatrix} \dfrac{\partial Q_{ij}}{\partial \delta_m} \\ \dfrac{\partial Q_{ij}}{\partial V_k} \end{bmatrix} \tag{D9}$$

The relationships between active, reactive and apparent power flow from *bus-i* to *bus-j* can be expressed as (D10).

$$P_{ij0}^2 + Q_{ij0}^2 = S_{ij0}^2 \tag{D10}$$

Linearlize (D10) results in (D11)

$$\Delta S_{ij0} = \frac{P_{ij0}.\Delta P_{ij0} + Q_{ij0}.\Delta Q_{ij0}}{S_{ij0}} \tag{D11}$$

where the additional subscript *0* represent the current status of based case and the prefix Δ is used to denote an incremental change. The incremental changes of real and reactive power flow from *bus-i* to *bus-j* can be shown in (D12) and (D13) respectively.

$$\Delta P_{ij0} = \sum_{u\in m} \frac{\partial P_{ij0}}{\partial P_u}.\Delta P_u + \sum_{w\in k} \frac{\partial P_{ij0}}{\partial Q_w}.\Delta Q_w \tag{D12}$$

$$\Delta Q_{ij0} = \sum_{u\in m} \frac{\partial Q_{ij0}}{\partial P_u}.\Delta P_u + \sum_{w\in k} \frac{\partial Q_{ij0}}{\partial Q_w}.\Delta Q_w \tag{D13}$$

Substitute ΔP_{ij0} and ΔQ_{ij0} of (D11) by (D12) and (D13) respectively results in (D14) as shown.

$$\Delta S_{ij0} = \frac{P_{ij0}\cdot\left(\sum_{u\in m}\frac{\partial P_{ij0}}{\partial P_u}.\Delta P_u + \sum_{w\in k}\frac{\partial P_{ij0}}{\partial Q_w}.\Delta Q_w\right) + Q_{ij0}\cdot\left(\sum_{u\in m}\frac{\partial Q_{ij0}}{\partial P_u}.\Delta P_u + \sum_{w\in k}\frac{\partial Q_{ij0}}{\partial Q_w}.\Delta Q_w\right)}{S_{ij0}} \quad \text{(D14)}$$

Rearrange (D14) can be expressed in (D15).

$$\Delta S_{ij0} = \frac{\sum_{u\in m}\left(P_{ij0}\frac{\partial P_{ij0}}{\partial P_u} + Q_{ij0}\frac{\partial Q_{ij0}}{\partial P_u}\right).\Delta P_u + \sum_{w\in k}\left(P_{ij0}\frac{\partial P_{ij0}}{\partial Q_w} + Q_{ij0}\frac{\partial Q_{ij0}}{\partial Q_w}\right).\Delta Q_w}{S_{ij0}} \quad \text{(D15)}$$

The terms $\partial P_{ij0} / \partial P_u$, $\partial P_{ij0} / \partial Q_k$, $\partial Q_{ij0} / \partial P_u$ and $\partial Q_{ij0} / \partial Q_k$ are the sensitivity factors represented the changes of active and reactive power flow through line due to the changes in injected active and reactive power into bus, which can be calculated from (B18) and (D9) respectively. To keep the apparent power flow of the overloaded lines within their thermal limit, (D15) is included as one of inequality constraints for an objective function of minimizing congestion relief cost. Then, optimization tool in MATLAB e.g., Linear Programming (LP) or Interior Point (IP) methods can be employed to solve this problem. Details to handle this constrains using MATLAB will be described in Appendix D.

D2: LINEARLIZE BUS VOLTAGE LIMIT

An AC power flow equation can be shown in a matrix form as (D16)

$$\begin{bmatrix}\Delta P_m \\ \Delta Q_k\end{bmatrix} = \begin{bmatrix}J_1 & J_2 \\ J_3 & J_4\end{bmatrix}\begin{bmatrix}\Delta\delta_m \\ \Delta V_k\end{bmatrix} \quad \text{(D16)}$$

The J_1, J_2, J_3 and J_4 are sub-matrices of m x m, m x k, k x m and k x k dimensions respectively. These sub-matrices are a part of a Jacobian matrix, its details of can be found in Chapter 4. Subscript m represents all buses except the slack bus and k represents all the load buses.

We can decompose (D16) into (D17) and (D18).

$$\Delta P_m = J_1\Delta\delta_m + J_2\Delta V_k \quad \text{(D17)}$$

$$\Delta Q_k = J_3\Delta\delta_m + J_4\Delta V_k \quad \text{(D18)}$$

Rearrange (D17) into (D19).

$$\Delta\delta_m = \left(J_1\right)^{-1}\left(\Delta P_m - J_2\Delta V_k\right) \tag{D19}$$

Substitute δ_m of (D19) into (D18), then (D18) can be rewritten as (D20).

$$\Delta Q_k = J_3\left(\left(J_1\right)^{-1}\left(\Delta P_m - J_2\Delta V_k\right)\right) + J_4\Delta V_k \tag{D20}$$

We can rewrite (D20) as shown in (D21).

$$\Delta V_k = \left(J_3\left(J_1\right)^{-1}J_2 - J_4\right)^{-1}\left(J_3\left(J_1\right)^{-1}\right)\Delta P_m - \left(J_3\left(J_1\right)^{-1}J_2 - J_4\right)^{-1}\Delta Q_k \tag{D21}$$

The term $\left(J_3\left(J_1\right)^{-1}J_2 - J_4\right)^{-1}\left(J_3\left(J_1\right)^{-1}\right)$ and $\left(J_3\left(J_1\right)^{-1}J_2 - J_4\right)^{-1}$ are matrices with dimension of *k x m* and *k x k* respectively. The equation (D21) may be included as one of inequality constraints to handle with bus voltage limit, which will be described in Appendix D. It should be noted that both in equality constraints of (D15) and (D21) are derived with variables of injected real and reactive power, which are suitable to use with optimization toolbox.

สถาบันวิทยบริการ
จุฬาลงกรณ์มหาวิทยาลัย

APPENDIX E

E1: LINEAR PROGRAMMING WITH MATLAB

We solve optimization problem in this dissertation using “**linprog**” function, which is used for solving a large linear programming problem that can be wrote in a set of equations shown in (E1)

$$\begin{aligned} &\min_x \ f^T x \\ &subject \quad to \\ &A.x \le b \\ &A_{eq}.x = b_{eq} \\ &lb \le x \le ub \end{aligned} \tag{E1}$$

where f, x, b, b_{eq}, lb, and ub are vectors and A and A_{eq} are matrices. The function expressed in (E1) is used for minimizing $f^T x$ so while satisfying inequality constraints $A.x \le b$ and equality constraints $A_{eq}.x = b_{eq}$. In addition, all values of x must be within an acceptable range of lower and upper bound. Syntax of a function *“linprog”* employed in the dissertation can be expressed in (E2).

$$x = linprog(f, A, b, A_{eq}, b_{eq}, lb, ub) \tag{E2}$$

The $f^T x$ is a congestion relief cost where a vector f and x is a cost and a change of utilized means described in section 6.4 respectively. Inequality constraint $A.x \le b$ is activated whenever some line flow or bus voltage are violated. A matrix A is a sensitivity matrix obtained from coefficient of injected real and reactive power expressed in (D15) and (D21). A vector b represents either transmission line or voltage constraints. The equality constraints $A_{eq}.x = b_{eq}$ can be neglected by setting A_{eq} and b_{eq} as null set. However, a power flow must be re-executed after solving optimization problem. The lb and ub are required as lower and upper bound of utilized means of each iteration.

BIOGRAPHY

Komson Daroj received the B. E. and M. E. degrees in electrical engineering from Chulalongkorn University, Bangkok, Thailand, in 1993 and 1999 respectively. During 1993-1996, he worked for private sectors. He joined the Department of Electric Engineering at Sripatum and Ubonratchathani University in 1998 and 2000 respectively. He pursued the Ph.D. degree at Chulalongkorn University in 2002. His interested researches are in the areas of power system operation & control, power system deregulation, distribution reliability and planning and power quality. During study the doctoral degree, he has 10 publications as list below.

Conference Papers

1. Voltage Correction Based Power Flow for Radial Distribution Systems.
2. On the Investigations of Transmission System Limit: A Two-bus Equivalent Model.
3. Understanding a Static Voltage Stability Limit Part 1: Transmission Line Loading Margin Evaluation.
4. Understanding a Static Voltage Stability Limit Part 2.
5. Slack Bus Independent Incremental Real Power Loss Allocation in Bilateral Markets.
6. Transmission Line Performance Indices Calculation Based on Voltage Stability Criterion, [Best Paper Award].
7. Real Power Loss Allocation for Transactions in Bilateral Markets.
8. On-Line Voltage Security Assessment (VSA) for Cross-Border Trade.

International Journal Papers

9. Transmission Line Performance Indices Calculation Based on Voltage Stability Criterion. ECTI Transactions on Electrical Eng., Electronics, and Communications Vol. 5, No. 1, Feb. 2007, pp. 70-78.
10. Transmission Line Loading Margin Evaluation”, International Journal on Power and Energy Systems; [Submitted in Partial Fulfillment of the Requirements for the Degree of Doctor].

สถาบันวิทยบริการ
จุฬาลงกรณ์มหาวิทยาลัย